

UNIVERSITY OF SALERNO



DEPARTMENT OF INDUSTRIAL ENGINEERING

*Ph.D. Course in Industrial Engineering
Curriculum in Chemical Engineering
XXXIII Cycle*

Moderate Electric Field (MEF) heating of heterogeneous food systems

Supervisor

Prof. Francesco Marra

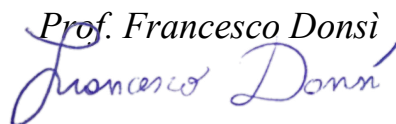

Ph.D. student

Oriana Casaburi


Scientific Referees

*Prof. James G. Lyng
Prof. Fabrizio Sarghini*

Ph.D. Course Coordinator

Prof. Francesco Donsì


Academic Year 2021/2022

UNIVERSITY OF SALERNO



DEPARTMENT OF INDUSTRIAL ENGINEERING

*Ph.D. Course in Industrial Engineering
Curriculum in Chemical Engineering
XXXIII Cycle*

Moderate Electric Field (MEF) heating of heterogeneous food systems

Supervisor

Prof. Francesco Marra


Ph.D. student

Oriana Casaburi


Scientific Referees

*Prof. James G. Lyng
Prof. Fabrizio Sarghini*

Ph.D. Course Coordinator

Prof. Francesco Donsì


Academic Year 2021/2022

Acknowledgements

Undertaking this PhD journey has been an important opportunity for my academic and personal growth.

I would like to express my gratitude to my supervisor Prof. Francesco Marra, who expertly guided me in all time of the research. Without his guidance and persistent help this dissertation would not have been possible.

I wish to thank Prof. James Lyng (University College Dublin, Ireland) for hosting me to conduct experiments at UCD laboratories during my international mobility.

I exhibit my gratitude and appreciation to my colleagues Aldo, Cosimo and Francesco. I also acknowledge Sara for her help and her valuable advices.

I also thank the research group of University College Dublin for their support and friendship.

I would also like to acknowledge COST Action and Erasmus program for their supports.

Last but not least, I would like to thank my parents, my aunt and Gianfranco for their support that has accompanied me constantly.

List of publications

Journal articles

- Casaburi, O., Orrico, D., Bedane, T. F., Lyng, J.G. and Marra, F. *The feasibility of Moderate Electric Field processing applied to a heterogeneous food system.* (under preparation).
- Casaburi, O., Petrosino, F. and Marra, F., 2021. *Modeling aspects in simulation of MEF processing of solid behaving foods.* Chemical Engineering Transactions, **87**, pp. 223-228.
- Casaburi, O., Brondi, C., Romano, A. and Marra, F., 2021. *Ohmic heating of basil-based sauces: Influence of the electric field strength on the electrical conductivity.* Chemical Engineering Transactions, **87**, pp. 343-348.

Conference proceedings

- Casaburi O., Romano A., Brondi C., Marra F., 2022. *Electrical conductivity of basil based sauces for MEF processing.* (Submitted to GRICU 2022, Ischia 3-6 luglio 2022).
-
- Casaburi, O., Orrico D., Marra. F., Bedane, T.F., Lyng, J.G. (2019) *Analysis of Moderate Electric Field processing in a heterogeneous system.* Proceedings of 3rd World Congress on Electroporation, Toulouse, France, 3-6 September 2019.
- Casaburi, O., Orrico D., Marra. F., Bedane, T.F., Lyng, J.G. (2019) *Riscaldamento mediante MEF applicati a sistemi eterogenei.* Convegno GRICU 2019 Palermo, Italy, 30 June – 3 July 2019.

Book Chapters

- Marra F., Bedane T.F., Casaburi O., Altin O., Uyar R., Erdogdu F. (2018). *Computational modeling of radio frequency thawing of frozen food products.* Computational Fluid Dynamics in Food Processing. CRC Press Taylor & Francis Group, 487-508. <https://doi.org/10.1201/9781351263481-22>.

Table of contents

LIST OF FIGURES	V
LIST OF TABLES	IX
ABSTRACT	XIII
1 INTRODUCTION.....	1
1.1 OVERVIEW ON FOOD PROCESSING DEVELOPMENTS AND DECLARATION OF THE PROBLEM.....	1
1.2 AIM OF THE STUDY	3
1.3 OUTLINE OF THE DISSERTATION	4
2 MODERATE ELECTRIC FIELD HEATING.....	5
2.1 BASIC PRINCIPLE OF MEF HEATING	5
2.2 MEF EQUIPMENT	7
2.3 MEF HEATING PROPERTIES AND PARAMETER	10
2.3.1 <i>Food properties affecting MEF heating</i>	10
2.3.2 <i>Process parameters</i>	13
2.3.3 <i>MEF heating control parameters</i>	14
2.4 FOOD PROCESSING APPLICATIONS OF MEF HEATING.....	14
2.5 BUBBLING PHENOMENA DURING MEF HEATING	19
2.6 OTHER INDUSTRIAL APPLICATIONS OF MEF HEATING	20
2.7 SUMMARY.....	20
3 ELECTRICAL PROPERTIES: ELECTRICAL CONDUCTIVITY	22
3.1 LIQUID FOODS.....	22
3.1.1 <i>Effect of temperature</i>	22
3.1.2 <i>Effect of electric field strength</i>	22
3.1.3 <i>Effect of ingredients</i>	23
3.2 SOLID FOODS	29
3.2.1 <i>Effect of temperature and electric field strength</i>	29
3.3 MEASUREMENT METHODS OF ELECTRICAL CONDUCTIVITY	32
3.4 SUMMARY.....	35
4 PRELIMINARY TRIALS ON MEF HEATING	36
4.1 RAW MATERIALS FOR MEF HEATING TEST	36
4.1.1 <i>Meatballs</i>	36
4.1.2 <i>Reconstituted flakes potatoes</i>	37
4.2 SAMPLES PREPARATION	38
4.3 MEATBALLS CONFIGURATION	39
4.4 MEF HEATING EQUIPMENT.....	43

Table of contents

4.4.1	<i>MEF heating equipment at University College Dublin</i>	43
4.4.2	<i>MEF heating equipment at University of Salerno</i>	45
4.5	MEF HEATING PROCEDURE	51
4.6	ELECTRICAL CONDUCTIVITY MEASUREMENTS.....	52
4.7	ELECTRICAL CONDUCTIVITY TREATMENT CELLS CALIBRATION	54
4.7.1	<i>Cylindrical cell calibration (UCD)</i>	54
4.7.2	<i>Rectangular cell calibration (UNISA)</i>	55
4.7.3	<i>Cylindrical cell calibration (UNISA)</i>	56
4.8	STATISTICAL ANALYSIS	57
4.9	SUMMARY	57
5	MEF HEATING: RESULTS AND DISCUSSIONS	59
5.1	ELECTRICAL CONDUCTIVITY OF CHICKEN MEATBALLS AND RPF	59
5.2	TEMPERATURE-TIME PROFILE OF MEF HEATING.....	60
	IN HOMOGENEOUS SYSTEM.....	60
5.3	TEMPERATURE EVOLUTION FOR HETEROGENEOUS SYSTEM WITH DIFFERENT CONFIGURATIONS	62
5.4	EFFECT OF DIFFERENT APPLIED VOLTAGES ON TEMPERATURE- TIME EVOLUTION IN HETEROGENEOUS SYSTEM	68
5.5	POWER DENSITY GENERATED IN MEF HEATING	72
5.6	SUMMARY.....	73
6	MEF HEATING: COMPARISON OF HOMOGENEOUS AND HETEROGENEOUS FOOD SYSTEMS	75
6.1	MEF HEATING OF HOMOGENEOUS FOOD SYSTEM.....	75
6.1.1	<i>MEF heating of homogeneous system RPFNB</i>	75
6.1.2	<i>Reconstituted potato flakes with butter (RPFNB)</i>	81
6.1.3	<i>Temperature- time evolution comparison.....</i>	86
	<i>between homogeneous food systems</i>	86
6.2	MEF HEATING APPLIED TO HETEROGENEOUS FOOD SYSTEM	88
6.2.1	<i>Temperature- time evolution of MEF heating applied to heterogeneous food system</i>	88
6.2.2	<i>Effect of applied voltage on temperature- time distribution for heterogeneous system with configuration 2PSiRP</i>	90
6.2.3	<i>Effect of applied voltage on temperature- time distribution for heterogeneous system with configuration 2PAiRP</i>	95
6.2.4	<i>Effect of applied voltage on temperature- time distribution for heterogeneous system with configuration 3PIRP</i>	99
6.3	SUMMARY.....	102
7	SIMULATION OF MEF HEATING	105
7.1	MEF HEATING MODELLING	105
7.1.1	<i>Measurement of physical properties</i>	105
7.1.2	<i>Modeling implementation</i>	106
7.1.3	<i>Initial and boundary conditions</i>	107
7.1.4	<i>Numerical solution solver implementation</i>	108

Table of contents

7.2	RESULTS AND DISCUSSION	109
7.2.1	<i>Model 3D plots analysis</i>	109
7.2.2	<i>MEF profiles experimental comparison</i>	112
7.3	SUMMARY.....	113
	CONCLUSIONS	115
	BIBLIOGRAPHY	117
	NOMENCLATURE	128
	APPENDIX A.....	131
	APPENDIX B.....	139
	APPENDIX C.....	147
	POSTER AND ORAL CONTRIBUTIONS.....	147

List of figures

Figure 2.1 MEF system.	5
Figure 2.2 Electrodes polarization (Chassagne, Dubois, Jiménez, van der Ploeg, & Turnhout, 2016).	6
Figure 2.3 Electrodes configurations in MEF heating (Sakr & Liu, 2014).	9
Figure 3.1 Electrical conductivity of orange juice subjected to different electric field strengths. Electrical conductivity decreases at around 100 °C could be due to boiling phenomena (Palaniappan & Sastry, 1991a).....	23
Figure 3.4 Electrical conductivity of strawberry jelly at different electric field strengths (Castro et al., 2003).	29
Figure 3.5 Electrical conductivity of vegetable tissue (carrot, potato and yam) conventionally heated (elaborated from Palaniappan & Sastry, 1991b).	30
For carrots, for example, increasing the electric field strength, as shown in Figure 3.6 , the change in electrical conductivity became less sharp and, at sufficiently high electric field strengths, the electrical conductivity-temperature trend assumed a linear evolution. Therefore, this means that a sample subjected to MEF undergone to cellular structure breakdown at lower temperatures than when is conventionally heated.	30
Figure 3.6 Electrical conductivity of carrot tissue subjected to various electric field strength (elaborated from Palaniappan & Sastry, 1991b).	31
Figure 3.7 Effect of salt infusion at different concentrations on the electrical conductivity (Wang & Sastry, 1993b).	32
Figure 3.8 Classic system used to measure electrical conductivity.	32
Figure 3.9 Electrical conductivity measurement method for particularly delicate sample	34
Figure 4.1 Reconstituted potato flakes storage in wrap plastic film.	39
Figure 4.2 Top and front view of the different configurations analyzed . White big circles represent chicken meatballs. Black points represent temperature measurement points. Grey sections represent the portions of space occupied by reconstituted potato flakes (RPF).....	40
Figure 4.3 Top and front view of the different configurations analyzed. Black points represent temperature measurement points. Grey sections represent the portions of space occupied by reconstituted potato flakes (RPFNB).	41
Figure 4.4 Top and front view of the different configurations analyzed. White big circles represent chicken meatballs. Black points represent	

List of figures

temperature measurement points. Grey sections represent the portions of space occupied by reconstituted potato flakes (RPFB).	42
Figure 4.5 MEF heating equipment.....	43
Figure 4.6 Top view of MEF heating treatment cell.	44
Figure 4.7 MEF heating cell with three thermocouples inserted in positions P1, P2 and P3.	44
Figure 4.8 Schematic diagram of MEF heating setup.	45
Figure 4.9 Rectangular treatment cell.	46
Figure 4.10 Cylindrical treatment cell.....	47
Figure 4.11 (a) rectangular cell electrodes. (b) cylindrical cell electrodes	48
Figure 4.12 Voltage regulator, VAM20F-1N (K-Factor srl).....	50
Figure 4.13 FEP coated thermocouples (TC- direct, Torino, Italy)	51
Figure 4.14 Experimental setup used to carry out electrical conductivity measurements.	52
Figure 4.15 Electrical conductivity treatment cell.	53
Figure 4.16 Front view of the treatment cell for electrical conductivity measurements.	53
Figure 5.1 Electrical conductivity of chicken meatballs and RPF at 5.7% and 10.9% salt content (20 V, 50 Hz).	59
Figure 5.3 Temperature- time evolutions in key points (P1, P2 and P3) of the system 2PSiRP at 5.7% salt content (30 V, 50 Hz).	63
Figure 5.5 Temperature- time evolutions in key points (P1, P2 and P3) of the system 2PAiRP at 5.7 % salt content (30 V, 50 Hz).	64
Figure 5.6 Temperature- time evolutions in key points (P1, P2 and P3) of the system 2PAiRP at 10.9 % salt content (30 V, 50 Hz).	65
Figure 5.7 Temperature- time evolutions in key points (P1, P2 and P3) of the system 3PiRP at 5.7 % salt content (30 V, 50 Hz).	66
Figure 5.8 Temperature- time evolutions in key points (P1, P2 and P3) of the system 3PiRP at 10.9 % salt content (30 V, 50 Hz).	66
Figure 5.9 Temperature-time evolution in meatball core (P3) of the system 2PSiRP at 20 V, 30 V, 40 V and 5.7% salt content.....	69
Figure 5.10 Temperature-time evolution in RPF (P2) of the system 2PSiRP at 20 V, 30 V, 40 V and 5.7% salt content.....	69
Figure 5.11 Temperature-time evolution on the surface of meatball in key point P1 of the system 2PSiRP in RPF containing 5.7% and 10.9% salt content (30 V, 50 Hz).	71
Figure 6.1 Electrical conductivity of RPFNB at 0.37%, 0.74%, 1.39%, 2.75% salt content (30 V, 50 Hz).	76
Figure 6.2 Temperature- time evolution in key point P2 of the homogeneous system RPFNB at 0.37%, 0.74%, 1.39%, 2.75% salt content (30 V, 50 Hz).....	77

Figure 6.5 Temperature time evolution in key point P2 of the system RPFNB at 30 V, 40 V, 50 V and 0.74% salt content. 80

Figure 6.6 Temperature time evolution in key point P2 of the system RPFNB at 30 V, 40 V, 50 V and 0.37% salt content. 80

Figure 6.9 Temperature- time evolution in key points P1, P2, P3 of the system RPFB at 30 V, 40 V, 50 V and 0% salt content. 84

Figure 6.10 Temperature- time evolution in key points P1, P2, P3 of the system RPFB at 30 V, 40 V, 50 V and 2.9% salt content. 85

Figure 6.11 Temperature- time evolution in key points P1, P2, P3 of the system RPFB at 30 V, 40 V, 50 V and 5.7% salt content. 85

Figure 6.16 Temperature- time evolution in key points P1, P2, P3 of the heterogeneous system RPFB and meatballs (2PSiRP) at 40 V and 2.9% salt content. 91

Figure 6.17 Temperature- time evolution in key points P1, P2, P3 of the heterogeneous system RPFB and meatballs (2PSiRP) at 50 V and 5.7% salt content. 91

Figure 6.18 Temperature- time evolution in key points P1, P2, P3 of the heterogeneous system RPFB and meatballs (2PSiRP) at 40 V and 5.7% salt content. 92

Figure 6.19 Temperature- time evolution in key points P1, P2, P3 of the heterogeneous system RPFB with meatballs, using 2PAiRP configuration, at 2.9% salt content (30 V, 50 Hz). 93

Figure 6.20 Temperature- time evolution in key points P1, P2, P3 of the heterogeneous system RPFB with meatballs, using 2PAiRP configuration, at 5.7% salt content (30 V, 50 Hz). 94

Figure 6.21 Temperature- time evolution in key points P1, P2, P3 of the heterogeneous system RPFB and meatballs (2PAiRP) at 50 V and 2.9% salt content. 95

Figure 6.22 Temperature- time evolution in key points P1, P2, P3 of the heterogeneous system RPFB and meatballs (2PAiRP) at 40 V and 2.9% salt content. 96

Figure 6.23 Temperature- time evolution in key points P1, P2, P3 of the heterogeneous system RPFB and meatballs (2PAiRP) at 50 V and 5.7% salt content. 96

Figure 6.24 Temperature- time evolution in key points P1, P2, P3 of the heterogeneous system RPFB and meatballs (2PAiRP) at 40 V and 5.7% salt content. 97

Figure 6.25 Temperature- time evolution in key points P1, P2, P3 of the heterogeneous system RPFB with meatballs, using 3PiRP configuration, at 2.9% salt content (30 V, 50 Hz). 98

Figure 6.26 Temperature- time evolution in key points P1, P2, P3 of the heterogeneous system RPFB with meatballs, using 3PiRP configuration, at 5.7% salt content (30 V, 50 Hz). 98

Figure 6.27 Temperature- time evolution in key points P1, P2, P3 of the heterogeneous system RPFB and meatballs (3PiRP) at 50 V and 2.9% salt content. 100

Figure 6.28 Temperature- time evolution in key points P1, P2, P3 of the heterogeneous system RPFB and meatballs (3PiRP) at 40 V and 2.9% salt content. 100

Figure 6.29 Temperature- time evolution in key points P1, P2, P3 of the heterogeneous system RPFB and meatballs (3PiRP) at 50 V and 5.7% salt content. 101

Figure 6.30 Temperature- time evolution in key points P1, P2, P3 of the heterogeneous system RPFB and meatballs (3PiRP) at 40 V and 5.7% salt content. 101

At high voltages, especially at 5.7% salt content, differences between dimensionless temperature reached at P1, P2 and P3 could be linked to the beginning of physical- chemical phenomena. 102

Figure 7.1 Mesh structure of the analyzed system. 109

Figure 7.2 Slice plot of temperature within the considered system after 4min with an applied voltage of 30 V and reconstituted potato flakes (RPFB) at 2.9% salt content. (a) $h=5 \text{ W/(m}^2 \text{ K)}$, (b) $h=25 \text{ W/(m}^2 \text{ K)}$, (c) $h=50 \text{ W/(m}^2 \text{ K)}$ and (d) $h=100 \text{ W/(m}^2 \text{ K)}$ 110

Figure 7.3 Electric field plot after 4min with Applied voltages equal to 30V (a, c) and 40V (b, d), reconstituted potato flakes (RPFB) at 2.9% (a, b) and 5.7% (c, d), $h=5 \text{ W/(m}^2 \text{ K)}$ 110

Figure 7.4 Electric potential slice plot after 4 minutes of MEF heating. Reconstituted potato flakes at 2.9% salt content, $h=5 \text{ W/(m}^2 \text{ K)}$, applied voltage of 40 V, $h_c (\text{MP29MB})=800 \text{ S/m}^2$. (a) $h_c (\text{MP29steel})=180 \text{ S/m}^2$, (b) $h_c (\text{MP29steel})=300 \text{ S/m}^2$, (c) $h_c (\text{MP29steel})=1000 \text{ S/m}^2$ 111

Figure 7.5 Comparison between experimentally measured and model predicted temperature evolution for an applied voltage of 30 V (a) and 40 V (b), mashed potato salt concentration A (2.9%) and B (5.7%). A concentration model profiles are solid blue for P1, dotted dark red for P2, short-dashed grey for T3. B concentration model profiles are dashed brown for T1, point&dash blue for T2, long dashed green for T3. 113

List of Tables

Table 2.1 Electrical conductivity values of different food products.	11
Table 2.2 Inactivation of microorganisms comparing..... conventional heating treatment and MEF heating..... (Jaeger et al., 2016).....	16
Table 2.3 “Cooking loss” comparison between MEF heating and conventional heating for meat products (Pathare & Roskilly, 2016; Yildiz- Turp, Sengun, Kendirci, & Icier, 2013).	18
Table 3.1 Parameters for electrical conductivity relationships (eqs. (3-4) and (3-5)). $K_{C,25}$ is the concentration parameter at 25 °C; K_T is the temperature parameter; K_{TC} is the interaction parameter between (T-25) and C.....	25
Table 3.2 Relationship parameters of eq. 3-6 at different salt contents for the various analyzed hydrocolloids (Marcotte, Trigui, Ramaswamy, 2000).	26
Table 4.1 Nutritional values for 100 g of Alemansrätten chicken meatballs.	37
Table 4.2 Nutritional values for 100 g of Huvudroll chicken meatballs.	37
Table 4.3 Samples composition used at UCD and UNISA.	38
Table 4.4 Technical specifications of MEF heating rectangular treatment cell.....	46
Table 4.5 Technical specification of MEF heating..... cylindrical cell.....	47
Table 4.6 Meat- based sauce composition.....	48
Table 4.7 Electrical conductivities for beef and tomato (Palaniappan & Sastry, 1991a,b).....	49
Table 4.8 Electrical conductivities of meat-based sauce compounds. ..	49
Table 4.9 Values obtained for the equipment.....	50
Table 4.10 Voltage regulator, technical specifications.....	50
Table 4.11 Electrical conductivity and K values of KCl aqueous solutions.	55
Table 4.12 Comparison between experimental and literature electrical conductivity values of NaCl aqueous solution.	55
Table 4.13 Comparison between experimental and literature electrical conductivity values for rectangular treatment cell calibration.	56
Table 4.14 Comparison between experimental and literature electrical conductivity values for cylindrical treatment cell calibration.	56
Table 5.1 Linear regression of electrical conductivity (S/m) in function of temperature (°C).	60

List of tables

Table 5.2 Processing time to reach 72°C in meatballs core 67 for the different configurations surrounded by RPF at 5.7% 67 or 10.9% salt content..... 67	67
Table 5.3 Processing time to reach target temperature in P1, P2, P3 for the different configurations at 5.7% and 10.9% salt content..... 68	68
Table 5.4 Specific power source in RPF and meatballs 70 core of the system 2PSiRP at 20 V, 30 V, 40 V and 70 5.7% salt content. 70	70
Table 5.5 Specific power source generated inside meatballs for the different configurations in 5.7% and 10.9% salt content. 72	72
Table 5.6 Specific power source in meatballs core and RPF, at 5.7% salt content, of the systems 2PSiRP and 2PAiRP. 72 73	72
Table 6.1 Linear regression of electrical conductivity 76 [S/m] as function of temperature [°C] for the homogeneous system RPFNB. 76	76
Table 6.2 Comparison of T_{red} reached at target time of 4 minutes for RPFNB at 0.37%, 0.74%, 1.39% and 2.75% salt content. 78	78
Table 6.3 Linear regressions of T_{red} as function of time [min] for the homogeneous system RPFNB. 78	78
Table 6.4 Dimensionless temperature reached at target 81 time of 4 minutes for RPFNB homogeneous system at 81 0.37%, 0.74%, 1.39%; 2.75 % salt content and 30 V, 40 V, 50 V..... 81	81
Table 6.5 Linear regression of electrical conductivity [S/m] 82 as function of temperature [°C] for the homogeneous system RPFNB. ... 82	82
Table 6.6 Dimensionless temperature reached at target time for the homogeneous system RPFNB at 0%, 2.9% and 5.7% salt content (30 V, 50 Hz)..... 83	83
Table 6.7 Linear trend of Θ as function of time [min] for the homogeneous system RPF..... 84	84
Table 6.8 Dimensionless temperature reached at target time for RPFNB homogeneous system at 30 V, 40 V, 50 V and 0%, 2.9%, 5.7% salt content. 86	86
Table 6.9 Distance between the electrodes and electric field strengths applied for the two homogeneous system RPFNB and RPF at 5.7% salt content (30 V, 50 Hz). 87	87
Table 6.10 Linear functions of T_{red} in function of time [min] for homogeneous systems RPFNB and RPF at 5.7% salt content (30 V, 50 Hz). 87	87
Table 6.11 T_{red} reached at target time for RPFNB heterogeneous system at 30 V, 40 V, 50 V and 2.9%, 5.7% salt content..... 92	92
Table 6.12 Dimensionless temperature reached at target time for heterogeneous system using 2PSiRP and 2PAiRP configurations at 2.9% and 5.7% salt content (30 V, 50 Hz). 94	94

List of tables

Table 6.13 T_{red} reached at target time for RPFB heterogeneous (2PAiRP) system at 30 V, 40 V, 50 V and 2.9%, 5.7% salt content.....	97
Table 6.14 Comparison between T_{red} at target time for 2PSiRP, 2PAiRP, 3PiRP configurations at 2.9% and 5.7% salt content and 30 V.	99
Table 6.15 T_{red} reached at target time for RPFB heterogeneous (3PiRP) system at 30 V, 40 V, 50 V and 2.9%, 5.7% salt content.....	102
Table 7.1 Physical properties best fitting as function of temperature of mashed potatoes RPFNB 2.9% salt. The temperature T is in °C.	106
Table 7.2 Physical properties best fitting as function of temperature of mashed potatoes RPFNB 5.7%. The temperature T is in °C.....	106
Table 7.3 Physical properties best fitting as function of temperature of meatball. The temperature T is in °C.	106
Table 7.4 Electric conductance for mashed.....	112
potato 2.9% (MP29) and 5.7% (MP57) - steel.....	112
and mashed potato (MPXX) – meatball (MB).....	112
interfaces.....	112

Abstract

In recent years, consumers' focus to healthy lifestyle is increasing significantly. Therefore, on food market the demand for safe, minimally processed and healthy food products is growing exponentially.

Food industries, consequently, started redesigning their market strategy and production in favour of healthy and nutritious food products.

In the context of processes related to the food industry, thermal treatments, such as heating, drying, sterilization, pasteurization, are a set of processes able to guarantee shelf-life enhancement of the treated product and improvement of the food safety. Conventional heating methods are characterized by high temperatures gradients and long-time lasting processes due to slow heating regions within the processed food. To prevent the possibility that in the slowest heating regions of the food products there is an insufficient thermal inactivation of pathogen microorganisms, in conventional heating methods foods are often over processed. This brings to the degradation of important food components, such as vitamins, proteins and other desirable food compounds. In addition, they can influence the organoleptic properties and quality of the treated food products, bringing to a loss of nutrients, texture and colour. To address these problems, novel thermal technologies, based on electro-heating, such as Moderate Electric Field (MEF), have been developed. MEF heating process is based on the passage of an electric current through a conductive material. This method allows to reduce energy consumption and processing time, compared to conventional heating methods, due to its volumetric heating nature.

MEF has the potential to heat homogenous food materials rapidly and uniformly. However, the heating uniformity of heterogeneous food products, with components, and thus properties, of different nature, represents a challenge for MEF heating applications. There is, indeed, a lack of information regarding MEF heating of heterogeneous systems.

For this reason, this PhD work focused on the investigation and analysis on the MEF heating feasibility to heterogeneous food systems.

Being based on the passage of electric current in a food item, MEF requires food product having a certain electrical conductivity (and thus a certain ionic content) to be effective. So, a first part of the work was devoted to analyze how the different ionic content influenced the heating of a heterogeneous food system (meatballs in reconstituted potato puree), regardless of the taste of the food.

The first part of the work consisted in the study of the relevant aspects of this process, also in order to be able to design and build a MEF unit at

University of Salerno, Italy. Then, a first experimental campaign was developed at University College Dublin (Dublin, Ireland) including a training on a MEF system already available among the facilities of the School of Life Sciences. First of all, MEF heating of a homogeneous food system, composed by reconstituted potato flakes puree at 5.7% and 10.9% ionic content, was investigated. Obtained results showed a good uniform heating in the three key points analyzed.

Subsequently, a heterogeneous food system composed by reconstituted potato flakes puree (RPF), at 5.7% and 10.9% ionic content, and meatballs was investigated. Meatballs were heated in reconstituted potato flakes considering different system configurations (2PSiRP, 2PAiRP, 3PiRP). Results showed that, even if the components are characterized by different electrical conductivities (5.60 S/m for RPF at 5.7%, 9.75 S/m for RPF at 10.9% and 1.46 S/m for meatballs), a heterogeneous system can be evenly heated by MEF, with the right choice of ingredients. Particularly, meatballs in reconstituted potato flakes puree with 5.7% ionic content showed a heating dynamic similar to the reconstituted potato flakes in which they were dispersed, while a further increase of the ionic content (10.9%) shortened the time required to reach a target temperature, but it also increased the difference in heating between meatballs and potatoes, producing a less even heating. Meatballs' heating did not depend on their relative position, but it was affected by the number of meatballs in the system. Moreover, results showed that spherical geometry gives to the meatballs a different and higher local potential variation than reconstituted potato flakes in which they were heated. Furthermore, for a symmetric heterogeneous system (2PSiRP) the effect of different applied voltages (20 V, 30 V, 40 V) was investigated: it was proven that, both for meatball and potatoes, the heating time to target increased as the applied voltage decreased.

In the second year at University of Salerno, to carry out further experimental tests and studies a MEF heating system was designed and developed.

A first set of MEF heating experimental tests was carried out, at different applied voltages (30 V, 40 V, 50 V, in order to test the behaviour of the system at different electric field strengths), on two homogeneous food system, composed, respectively, by only reconstituted potato flakes, one with butter among the ingredients (RPFb) and one not (RPFNB), at different salt compositions (RPFb at 0%, 2.9% and 5.7% salt content; RPFNB at 0.37%, 0.74%, 1.39% and 2.75% salt content). For both analyzed homogeneous system, a good uniform heating was obtained in the three investigated points. Obviously, higher the salt content, higher the electrical conductivity and higher the temperature reached from the different analyzed homogeneous system at the target time.

Obtained results of the homogeneous system RPFb were compared with the ones obtained from the system RPF: the two homogeneous systems were

Abstract

affected from the different applied electric field strength. RPF system was subjected to an electric field strength higher (0.43 V/cm) than RPF (0.30 V/cm). RPF reached at the same target time a higher temperature than RPF. Therefore, it was proved that higher the electric field strength applied and greater the heating.

Another set of experimental tests was carried out on a heterogeneous food system composed by reconstituted potato flakes (RPF) at different salt contents (0%, 2.9% and 5.7%) and meatballs. Chicken meatballs were heated in RPF using different configurations (2PSiRP, 2PAiRP, 3PiRP). For configuration 2PSiRP, results showed that meatballs reached, at target time, a higher temperature than reconstituted potato flakes. This was linked to the proximity to the electrodes and to the fact that, due to the spherical geometry, meatballs were more affected from electrical field strength than reconstituted potato flakes.

Finally, a mathematical modeling of MEF assisted heating of foods, has been embedded in a simulation tool able to explore further MEF heating scenarios and to propose the design of more efficient MEF treatment cells

1 Introduction

In chapter 1, an overview on the food processing, developments and innovation challenges, is presented. In addition, the aim of this work is declared and the outline of the dissertation is summarized.

1.1 Overview on food processing developments and declaration

of the problem

Over the last decades, consumers demand in food market for healthy and nutritious food products has increased exponentially. The NOVA (a name, not an acronym) classification system, developed by Center for Epidemiological Studies in Health and Nutrition (School of Public Health, University of Sao Paulo, Brazil), divides food products depending on the type of process to which they are subjected. In particular, NOVA classification characterizes foods into four groups, according to the processing level (Monteiro et al., 2016). Group 1 regards unprocessed or minimally processed foods (for example, vegetables, grains, legumes, fruits, eggs and milk). The first ones are not subjected to any type of process remaining in their natural state; the second ones, instead, are products subjected to treatments such as cleaning, fractioning, drying and pasteurization but no sugar, fats, oils and salt are added. Group 2, also called Processed Culinary Ingredients (such as oils, honey and syrup), concerns products obtained from natural foods subjected to pressing, grinding, crushing and refining. They are used in homes and restaurants to season and cook foods. Group 3 regards processed foods, that are products manufactured by industries using salt, sugar and oils (group 2) added to unprocessed or minimally processed foods (group 1). For example, bread, canned legumes or vegetables in brine, bacon and cheese. Group 4 concerns ultra-processed foods, which are products with a high energy value, they contain many added ingredients and they are highly manipulated. Examples are chocolate, carbonated soft drinks, hotdogs, fries, ice-cream and candy.

Fardet (2016), showed that the level of food processing is linked to the satiety index and to the glycaemic response. In particular, when the food is over processed the satiety resulted from it is lower and the glycaemic load assimilated by the consumption of that product is higher. It is easy to guess that processed foods are considered less healthy than unprocessed or minimally processed

ones and they are often considered the cause of numerous diseases, such as, for example, heart diseases and diabetes. Consequently, the development of minimal treatment techniques capable of guaranteeing maintenance the microbial safety of food, together with its nutritional and sensory properties, has increasingly interested scientific, institutional and industrial fields.

Thermal treatments are a set of processes (such as heating, curing, drying, etc) able to guarantee shelf life enhancement of the treated product and improvement of the food safety but, on the other hand, they are able to destroy food components, such as vitamins and other health beneficial compounds (Bansal, Sharma, Ghanshyam, & Singla, 2014).

In conventional heating methods, once the heat arrives to the external surface of the food, it is transferred inside the treated product by conduction (in solid products, such as meat) or convection (in liquid products, such as milk). In products with interrupted heating curves (such as starch- containing soups) conduction and convection may alternatively prevail in different periods during the treatment. Between these two heat transfer mechanisms, the second one is certainly much faster than the first one. In solid foods to guarantee that the internal of the product is heated to suited temperatures, the sample needs to be heated for much longer times than a liquid product. This over processing can lead to overheated regions on the outer surface of the product (Marra, Zhang, & Lyng, 2009).

Products subjected to conventional heating methods (such as pasteurization, sterilization, cooking, etc), therefore, are subjected to high temperatures and long-time processes. This leads to affect organoleptic properties and quality of the treated products through loss of nutrients such as, for example, vitamins and minerals, proteins denaturation (as in case of meat cooking) and loss of texture and colour.

Conventional thermal treatments, therefore, can bring to the presence of over- heated regions or to the so-called “cold- spots”, i.e. the presence of untreated areas in the food. Obviously, the presence of underheated regions in the food product can conduce to an insufficient inactivation of microorganisms. To overcome the limits linked to conventional thermal treatments, novel thermal technologies, mainly based on electro- heating, have been developed. Electro-heating processes can be divided in indirect electro-heating (Microwave, MW, and Radio Frequency, RF) in which the electrical energy is transformed in electromagnetic radiation which, in turn, generates heat within the food product; and direct electro- heating (Moderate Electric Field, MEF), in which the electrical current is transferred directly to the food and generate heat inside it.

MW heating involves the application of electromagnetic waves. For heating or power MW applications, frequencies designated for ISM (Industrial, Scientific and Medical) purposes are 915 MHz and 2.45 GHz (Barron & Nordh, 2020). It is used as a heat source in food treatments, such as heating, drying, sterilization and thawing. It is based on the application of

electromagnetic waves directed to the food product through waveguides. Microwave systems, although very rapid, are limited by thermal instability problems, in particular, parts of the treated food product, absorbing energy preferentially, can be overheated, while other parts remain untreated. For this reason, in order to improve the efficiency of the process, in the last few years, attention is being paid to new technologies, such as solid- state microwave. Więckowski et al. (2014) studied a solid- state microwave generators system, as alternative option to the conventional magnetron. This technology allowed to better control the frequency and the phase of the electromagnetic field generated. Authors carried out that the efficiency of the process was rather improved and, therefore, a better and more uniform energy transfer from the source to the food was obtained, compared to the use of conventional microwave.

RF systems, as established by the Federal Communication Commission (FCC, USA), for ISM applications are used at frequencies of 13.56 MHz, 27.12 MHz and 40.68 MHz (Marra, Zhang & Lyng, 2009). When a food product is subjected to radio frequency, its molecules tend to re-align themselves. Due to the friction that occurs between the molecules, heating occurs within the treated product (Jojo & Mahendran, 2013). One of the major limits linked to RF is the runaway heating. This phenomenon is mainly linked to the nature of the food product and it is most likely in food products rich in fat (Farag, Lyng, Morgan, & Cronin, 2011).

MEF heating is based on the passage of an electric current through a conductive material, in particular a food product, with frequencies ranging between 50 Hz and 25 kHz and electric field strength between 1-1000 V/cm (Sastry, 2008). This technology is growing of interest for the treatment of food products and it is often classified as “green method”. The sustainability of MEF is justified for two reasons: first of all, compared to conventional heating methods, it is a very fast process and, therefore, the time available for heat losses is significantly reduced. Secondly, it concerns a direct application of electrical current to the product and, consequently, the possibility of energy losses is minimized. It has been applied to a wide range of applications regarding homogeneous food systems; further studies, instead, are required for MEF heating regarding experimental analysis, design of process models, influence of physicochemical product properties and parameters that can affect the process and estimation of cold-spots and over-heated regions for heterogeneous food systems.

1.2 *Aim of the study*

The general aim of this study was to assess the feasibility of MEF heating to heterogeneous food systems.

Chapter 1

In particular, the main objectives were:

- Experimental studies to evaluate the practicability of MEF heating to heterogeneous food systems.
- Characterization of the electrical conductivity of the foods constituting the heterogeneous food system analyzed.
- Design and development at the University of Salerno of a MEF heating system.
- Development of a mathematical model using a simulation tool to analyze modelling and virtual aspects related the MEF heating.

1.3 Outline of the dissertation

The PhD dissertation is organized in 8 chapters.

Chapter 1 leads the current trends in food processing, the problem statement and the overall aim of the research.

Chapter 2 concerns the basic principle and mechanism of MEF heating, the main factors affecting it and an overview on its food processing and industrial applications.

Chapter 3 shows the effects and consequences that different parameters have on electrical conductivity on solid and liquid foods. Electrical conductivity measurement methods are discussed too.

Chapter 4 deals the materials and methods used to perform experimental work at University College Dublin, during the international mobility, and materials and methods utilized at University of Salerno to carry out experimental tests on heterogeneous food systems. The design of MEF heating apparatus realized at University of Salerno is reported and discussed too.

Chapter 5 shows experimental results obtained from the experimental work carried out at University College Dublin on a heterogeneous food system, composed by meatballs and reconstituted potato flakes at different salt content and system configurations.

Chapter 6 concerns experimental results obtained from experimental work performed at University of Salerno carried out on two different heterogeneous food systems, composed by meatballs and reconstituted potato flakes at different salt content, system configurations and applied voltages.

Chapter 7 deals the development of a mathematical model using COMSOL Multiphysics to analyze modelling aspects related to the simulation of MEF processing applied to a heterogeneous system. A direct comparison between experimental results and heating trends obtained from the developed model are discussed too

2 Moderate Electric Field heating

This chapter discusses the principle, working mechanism and the most important parameters and properties affecting the MEF heating. In addition, the main applications of MEF heating are discussed.

2.1 Basic principle of MEF heating

MEF heating is a process in which heat is generated volumetrically into the food product by the passage of an AC electric current, with an electric field strength ranging between 1- 1000 V/cm and frequencies between 50 Hz and 25 kHz. A simplified scheme of a MEF heating system is shown in [Figure 2.1](#). L'origine riferimento non è stata trovata.: a power supply provides an AC voltage that is applied to a pair of electrodes placed at both ends of the sample. The sample to be treated is placed in a treatment cell.

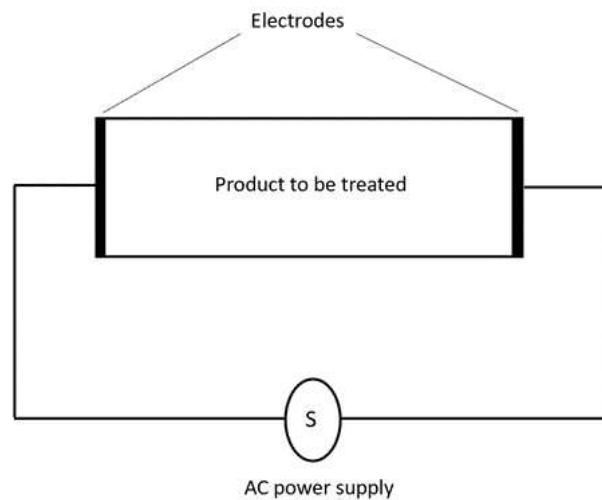


Figure 2.1 MEF system.

If scheme in [Figure 2.1](#). L'origine riferimento non è stata trovata. is looked at as an electrical circuit, the voltage is the electrical driving force that provides a

flow of electric current which pass through a conductive food product that acts like a resistance. MEF heating, therefore, is based on Ohm's law which is known as the relation between current, voltage and resistance (eq. (2-1))

$$I = \frac{V}{R} \tag{2-1}$$

where V [V] is the voltage, I [A] is the current and R [Ω] is the resistance.

In MEF heating, heat is generated volumetrically by Joule heating by the passage of electric current through the resistance. The result is a generation of energy causing a rise in temperature. According to Joule's first law the heat generated is given by:

$$Q = RI^2t \tag{2-2}$$

where I [A] is the current, R [Ω] is the resistance, t [s] is the time and Q [J] is the thermal energy generated by the passage of the current.

It is a common idea to consider metals the best conductors of electric current. Many food products, however, are not very different from metals and are able to conduct electricity: if they contain enough water and dissolved salts they can act like ionic conductor. An ionic conductor includes positive and negative charges, also known as charged ions, able to move freely when they get in touch with a driving force (in the specific case, a voltage). The simplest example is a solution of salt dissolved in water. When this type of solution is subjected to an electric field and put in contact with the electrodes, positive ions (in this case, Na^+) move towards the negative electrode and, vice versa, negative ions (Cl^-) move towards the positive electrode. At the negative electrode, the positive ions take the electrons, reducing themselves. At the positive electrode, negative ions liberate electrons, oxidizing themselves. The aggregation of reduced or oxidized ions causes the so-called electrodes polarization (Errore. L'origine riferimento non è stata trovata.).

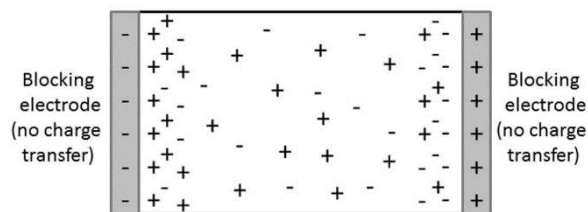


Figure 2.2 *Electrodes polarization (Chassagne, Dubois, Jiménez, van der Ploeg, & Turnhout, 2016).*

If DC current is used, this phenomenon could quickly occur, and the current flow could stop. For this reason, in MEF treatment AC current is

used: the cyclical variation of current direction does not give sufficient time for a polarization to take place.

2.2 *MEF equipment*

As discussed in the previous section, the simplest set-up of a MEF system for food treatment is composed by:

- **AC power supplier;**
- **an electrical circuit;**
- **treatment cell:** for its construction, different types of materials have been used in literature (Marra, Zell, Lyng, Morgan, Cronin, 2009; Zareifard, Ramaswamy, Trigui, & Marcotte, 2003; Bozkurt & İçier, 2012, Engchuan, Jittanit, & Garnjanagoonchorn, 2014) . Principally, it must be of insulating material, should not confer unpleasant flavours to the treated product and should withstand to high temperatures;
- **electrodes:** they are connected to the power supply and put in direct contact with the sample. Their geometry and distance can vary according to the shape and size of treatment cell. They must be smooth, not corrosives and do not soak up odours or materials. It is essential that they are made of conductive material such as carbon (Moses, 1938), aluminium (Mizrahi, Kopelman, & Perlman, 1975), titanium (Amatore, Berthou, & Hébert, 1998) and stainless-steel (Assiry, Sastry, & Samaranayake, 2003), chosen on the base of price, degree of corrosion and type of treatment. In case MEF used for waste treatment, carbon electrodes – which are not particularly resistant to corrosion - can be used. Vice versa, when the quality of the treated product is a main aspect, the choice goes toward materials better resistant to corrosion, such as stainless steel or titanium. Obviously, material and thickness of the electrode influence the efficiency of the process. Samaranayake & Sastry (2005), analyzed four different types of electrode materials (titanium, stainless steel, platinized- titanium and graphite) at pH 3.5, 5.0, 6.5, to better understand their electrochemical behaviour. Obviously, all types of electrodes showed more severe corrosion at pH of 3.5 than the other pH values. Stainless- steel electrodes showed to be the most active in electrochemical behaviour at the investigated pH values. Authors demonstrated that the migration of functional groups and oxides, as for example organic compounds, were the cause of graphite electrodes corrosion. Platinized-titanium electrodes, obviously, resulted the better choice because of their inert electrochemical performance.

Of course, ancillary systems for process control and monitoring can be implemented too, such as systems for temperature measurement, systems for online colour detection, systems for data logging and I/O communication.

Generally, in continuous MEF heating systems, different electrode configurations (**Figure 2.3**) are used to optimize the process (Sakr & Liu, 2014):

- **Parallel plate configuration:** it is well used for fluids with low electrical conductivity (< 5 S/m). In this configuration, the uniformity of the electric field is enhanced, resulting in a good uniform heating. This arrangement can work at standard voltages, such as 240 V or 415 V.
- **Parallel rod design:** it is cheaper than parallel plate configuration or collinear design. This arrangement is suitable when cost considerations are not negligible but, on the other hand, it results less efficient in heating uniformity of the product.
- **Collinear design:** it is the best option for materials with high electrical conductivity. This arrangement requires applied voltage higher than the parallel plate. The current distribution is less uniform. At the edges of the electrodes, there is a high current density and, then, boiling can be produced.
- **Staggered rod arrangement:** it is an economical solution, but it is more efficient, in terms of heating uniformity, than parallel rod design.

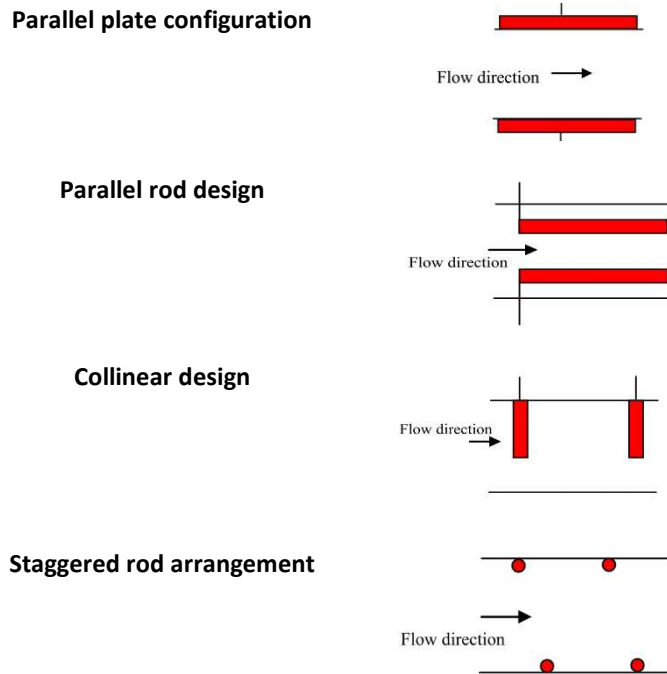


Figure 2.3 *Electrodes configurations in MEF heating (Sakr & Liu, 2014).*

Configurations mentioned above are well used for MEF treatment of liquid or solid- liquid systems.

In batch configuration, instead, the flow of the sample is not to be considered and, therefore, the medium is defined static.

Static ohmic heaters can have two or more parallel electrodes, placed within a treatment cell. Different types of materials are used to realize treatment cells but the most used are teflon, very easy to clean, or glass, more delicate but allows to view phenomena occurring inside the cell during MEF treatment. Among the most used geometries for treatment cells, there are the rectangular and cylindrical one. Many studies have been carried out to better understand the limits of the different cell treatment geometries and many researches are still necessary to reach their optimization. Jun & Sastry (2007), for example, simulated MEF heating of tomato soup in a pouch system. Obtained results, showed that bottom corners of the pouch were an area with low current density, consequently their temperature resulted very low (about 53.3 °C) even when the rest of the pouch reached a temperature of 139 °C. Marra, Zell, Lyng, Morgan, Cronin (2009) developed a mathematical model simulating MEF heating of reconstituted potato in a cylindrical cell treatment. Results demonstrated that there were no cold spots inside the food product but slightly cold regions were present near the

electrodes and cell surfaces. Choi, Kim, Park, Ahn, & Kang (2020) developed a mathematical model to simulate the temperature distribution and inactivation of *E. coli O157:H7* in orange juice pasteurization. A rectangular treatment cell was used for the scope. Obtained results showed the presence of a cold point in the bottom corner that led to apply longer time treatment to ensure a 5-log reduction of *E. coli O157:H7*.

Static ohmic heaters are mostly utilized in small scale applications, such as water heaters and laboratory scale, while flow ohmic heaters are generally employed in industrial applications.

2.3 MEF heating properties and parameter

MEF heating is affected by food properties and process and control parameters. In this section, the main crucial food properties and parameters are discussed.

2.3.1 Food properties affecting MEF heating

- **Electrical properties**

Electrical conductivity

Electrical conductivity (EC) is the capability of a material, such as a food, to conduct electricity. EC affects MEF heating rate and it is a critical property. In MEF heating an appropriate balance between voltage and current is crucial to obtain the correct and desired temperature rise in the treated product. In particular, in conductive materials, such as metals or foods containing significant amounts of water and dissolved salts, a considerable current will flow with a limited voltage gradient. Instead, for insulator materials, such as foods containing significant amount of fat, also applying high voltage gradient values, the flow of current will result very low.

Moreover, the design of MEF heating equipment and the product safety are closely related to electrical conductivity. Indeed, the design and development of MEF equipment require good knowledges on EC property. On the other hand, for an existing equipment, very important are considerations related to the electrical conductivity of the product to be treated.

Several papers reported measured values of foods electrical conductivity (σ), as shown in **Table 2.1**.

Table 2.1 *Electrical conductivity values of different food products.*

Food	State	Temperature [K]	σ [S/m]	References
Apple	Solid	298.15- 413.15	0.067- 0.571	Sarang, Sastry, & Knipe, 2008
Peach	Solid	298.15- 413.15	0.170- 1.299	Sarang, Sastry, & Knipe, 2008
Pear	Solid	298.15- 413.15	0.084- 0.642	Sarang, Sastry, & Knipe, 2008
Pineapple	Solid	298.15- 413.15	0.037- 0.575	Sarang, Sastry, & Knipe, 2008
Strawberry	Solid	298.15- 413.15	0.186- 1.276	Sarang, Sastry, & Knipe, 2008
Chicken (breast)	Solid	298.15- 413.15	0.665- 2.212	Sarang, Sastry, & Knipe, 2008
Pork (Top loin)	Solid	298.15- 413.15	0.560- 1.751	Sarang, Sastry, & Knipe, 2008
Beef (Bottom round)	Solid	298.15- 413.15	0.489- 1.608	Sarang, Sastry, & Knipe, 2008
Pickles and chutneys	Solid	298.15	2.0- 3.0	Varghese et al., 2012
Soups, various	Solid-liquid	298.15	1.4- 1.8	Varghese et al., 2012
Full-cream milk	Liquid	298.15	0.52	Varghese et al., 2012
Syrup	Liquid	298.15	0.001	Varghese et al., 2012
Margarine	Solid	298.15	0.027	Varghese et al., 2012
Tomato juice (0 % solids)	Liquid	298.15- 358.15	0.87-1.58	Palaniappan & Sastry, 1991a
Tomato juice (16.7 % solids)	Solid-liquid	298.15- 358.15	0.69- 1.29	Palaniappan & Sastry, 1991a
Orange juice (0% solids)	Liquid	298.15- 358.15	0.57- 1.27	Palaniappan & Sastry, 1991a
Orange juice (21% solids)	Solid-liquid	298.15- 358.15	0.52- 1.03	Palaniappan & Sastry, 1991a

As shown in **Table 2.1**, Sarang, Sastry, & Knipe (2008) evaluated electrical conductivity of different types of fruit (apple, peach, pear, pineapple and strawberry) and meats (chicken, pork, beef) in a range of temperatures between 25 °C- 140 °C. Electrical conductivities of fruit, were found ranging between 0.037 S/m and 1.299 S/m. Electrical conductivities of meats were between 0.489 S/m and 2.212 S/m. Varghese, Pandey, Radhakrishna & Bawa, (2012) reported electrical conductivities of different food product at 25 °C.

Palaniappan & Sastry (1991a) evaluated electrical conductivity values of orange and tomato juices at different solid contents in a temperature range of 25 °C- 85 °C. Authors stated that electrical conductivity values, for both considered juices, decreased with solid contents. Tomato juice at 0% of solids had electrical conductivity values ranging between 0.87 S/m and 1.58 S/m. At 16.7% solids content electrical conductivity values of tomato juice

was between 0.69 and 1.29 S/m. Orange juice, instead, at 0% solids content ranging between 0.57 S/m and 1.27 S/m. At 21% solids content electrical conductivity values of orange juice were between 0.52 S/m and 1.03 S/m.

As shown in **Table 2.1**, electrical conductivity of a food product can vary according its composition, its structure, and of course its temperature.

De Alwis, Halden & Fryer (1989) stated that electrical conductivity values of a food product determine its feasibility with MEF treatment. Piette, Dostie & Ramaswamy (2001) suggested that MEF heating is possible for foods with σ values in a range between 0.01- 10 S/m. Electrical conductivity, moreover, increases with increasing temperature (Sakr & Liu, 2014).

- **Physical properties**

Food composition, and particle size

Food composition and particle size of the treated product can affect MEF heating. Zareifard, Ramaswamy, Trigui, & Marcotte (2003) studied MEF treatment applied to a two- phase food system (liquid phase was 4% w/w starch solution with 0.5% w/w salt while the solid phase consisted of carrot puree and cubes of different sizes). Authors pointed out that the heating time rose with particles dimension and concentration. Moreover, they observed that electrical conductivity, and therefore the heating rate, decreased when particle size and concentration increased. Castro, Teixeira, Salengke, Sastry, & Vicente (2003) analyzed the effect of MEF heating on strawberry products. They, also, stated that electrical conductivity decreases with solids content increase: this because as the solid content increases, the resistance increases and, thus, the electric current decreases, resulting in a decrease of electrical conductivity (Silva, Santos, & Silva, 2017).

As explained in section 2.1, water content, salt content and, in general, content of ionic and electrolytic components in a food product increases the conductivity of the treated product and, as a consequence, the heating rate during ohmic heating. Marcotte, Trigui, & Ramaswamy (2000) carried out experimental studies on hydrocolloid solutions, prepared in water with salt content varying between 0.25% and 1%, with a voltage gradient of 7 V cm⁻¹. Authors stated that electrical conductivity values, and thus heating rate, increased with salt content. To the counter, instead, fat acts like an electrical insulator: Kim & Kang (2015) evaluated the effect of milk fat on ohmic heating. Sterile cream was mixed with buffered peptone water and milk fat content at 0%, 3%, 7% and 10%. Authors pointed out that heating was faster at lower fat contents.

- **Thermal properties**

Thermal properties of food (especially specific heat and thermal conductivity) also affect MEF heating, as the supplied electrical energy is converted into thermal energy and provide heat to the treated sample. As

described in eq. (2-3), the heat transfer occurring during MEF heating is described by the heat transfer equation by conduction plus a generation term (Marra, Zell, Lyng, Morgan, Cronin, 2009):

$$\rho c_p \frac{\partial T}{\partial t} = \nabla \cdot \lambda \nabla T + Q_{GEN} \quad (2-3)$$

where ρ [kg/m³] is the density, c_p [J/kg K] is the heat capacity, T [K] is the temperature within the sample, t [s] is the process time, λ [W/m K] is the thermal conductivity and Q_{gen} [W/m³] is the specific power source term (described in detail in the next section). Consequently, it is easy to understand that thermal properties (ρ , c_p , λ) have a strong influence on the process and, therefore, on the heating rate of the process.

2.3.2 Process parameters

Electric field strength

In MEF heating, the heat generated inside the food product is proportional to the electrical conductivity and to the electric field strength (given by the ratio between the applied voltage and the distance between the electrodes), as shown in eq. (2-4):

$$Q_{GEN} = \sigma |\nabla V|^2 \quad (2-4)$$

where σ [S/m] is the electrical conductivity and ∇V [V/m] is the gradient of the electrical potential. Therefore, a variation of electric field strength strongly influences the heating of the process and, in particular, its increase leads to an increase in the heating rate (eq. (2-3)).

Frequency and waveform

In MEF heating the common waveform used is sinusoidal. The frequency and waveform impact on the efficiency and quality of the treated food product (Lima, Heskitt, & Sastry, 1999). Lee, Ryu, & Kang (2013), studied the effect of different frequencies (60 Hz to 20 kHz) and waveforms (sine, square and sawtooth) on the heating rate of salsa. They pointed out that the frequency affected the heating rate up to 500 Hz while there was no significant effect on the heating rate when the frequency rose above 1 kHz. Regarding waveform, at 60 Hz, the square wave gave rise to a lower heating rate than sine and sawtooth waves. Imai, Uemura, Ishida, Yoshizaki & Noguchi (1995) observed that from 50 to 10 kHz the time for heat the sample (Japanese white radish) up to 80°C increased about sevenfold.

2.3.3 *MEF heating control parameters*

The process control in MEF heating is a crucial step to optimize the treatment, trying to achieve a uniform heating with high heating rate.

Voltage, current and power applied

The power needed is dependent on the resistance of the food to the voltage gradient and the electric current. Applied voltage can be controlled with a variable autotransformer. To obtain the power needed, at low voltages, current can reach very high values. For this reason, in these conditions, a transformer is used (Roberts, Balaban, Zimmerman, & Luzuriaga, 1998). Another crucial parameter is the current density, that is the ratio between the current and the electrode surface area. The arch discharge can take place when is achieved the value of the critical current density.

In MEF heating, time is function of the applied voltage gradient. Increasing the voltage gradient, the heat generation increases and, thus, the processing time is reduced (Icier, 2009; Icier & Tavman, 2006; M. Zell, Lyng, Morgan, & Cronin, 2009).

Temperature

Temperature plays a fundamental role in MEF heating. As seen in the previous sections, MEF treatment strongly depends on density, thermal conductivity, heat capacity and electrical conductivity, all properties dependent on temperature. For this reason, principally, a good control of temperature is important in MEF processing.

In continuous systems, the power can be arranged using feedback or feed-forward control, measuring the changes in temperature and specific heat capacity. In batch system, instead, the use of thermocouples, placed in one or more points of the sample, is very useful for the control of this parameter.

2.4 *Food processing applications of MEF heating*

MEF technology provides safe, stable and high added value food products, characteristics difficult to achieve through the application of conventional heating methods or others electro- heating methods, such as MW and RF (see section 1.1).

During food processing, a large number of biomolecules, such as proteins, polysaccharides, lipids and functional substances, such as polyphenols and vitamins are lost. These compounds, can be recovered and reused for other type of purposes, such as pharmaceutical products and energy production (Galanakis, 2012; Lin et al., 2013). Pereira et al. (2016)

compared MEF and conventional pre-treatments for recovery of value-added compounds from potatoes. Authors concluded that moderate electric field heating required shorter processing time and lower energy consumption than conventional heating treatment (

Figure 2.4).

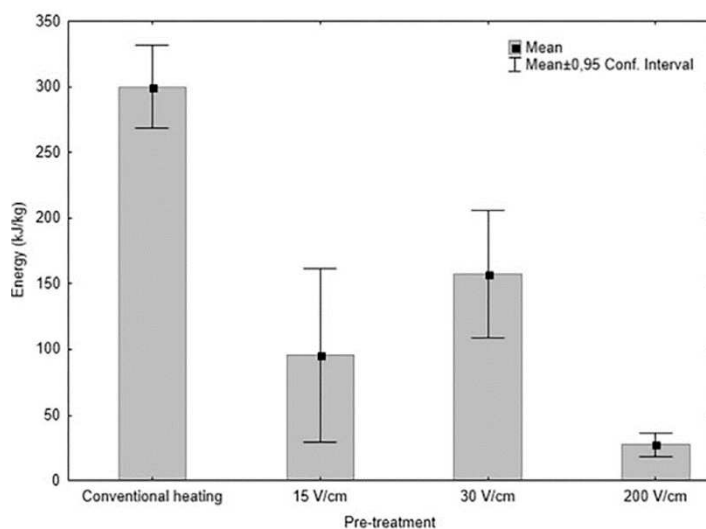


Figure 2.4 Energy consumption comparison between MEF and conventional heating pre-treatments (Pereira et al., 2016).

In food industry, MEF heating include a wide range of applications such as extraction (Loypimai, Moongnarm, Chottanom, & Moontree, 2015), blanching (Allali, Marchal & Vorobiev, 2010), thawing (Liu et al., 2017), cooking (Kanjanapongkul, 2017), peeling (Wongsa-Ngasri & Sastry, 2015), sterilisation and pasteurisation (Achir et al., 2016; Marra, Zell, Lyng, Morgan, Cronin, 2009).

Leizeron & Shimoni (2005) confronted the effect of MEF conventional pasteurisation on properties of orange juice. Authors pointed out that the sample treated with MEF preserved more flavours. Moreover, although both methods avoided for more than 100 days the microbial growth, they stated that the sensory properties of juice treated with MEF were preserved for about 100 days longer respect to product treated with conventional pasteurisation.

In **Table 2.2** is shown a direct comparison between the microorganisms inactivation of MEF and conventional heating methods for different types of microorganisms (Jaeger et al., 2016).

Table 2.2 *Inactivation of microorganisms comparing conventional heating treatment and MEF heating (Jaeger et al., 2016).*

Species	Matrix	Effects	References
<i>Zygosaccharomyces bailii</i>	Phosphate buffer solution	No difference	Palaniappan, Sastry, & Richter, 1992
<i>Escherichia coli</i>	Phosphate buffer Solution	Higher killing rate	Palaniappan, Sastry, & Richter, 1992
<i>Bacillus subtilis</i> spores	0.1% NaCl solution, nutrient solution	Survival rate lowered, D values raised.	Cho, Yousef, & Sastry, 1999
<i>Alicyclobacillus acidoterrestris</i> spores	Orange juice	Faster inactivation	Baysal & Icier, 2010
<i>Escherichia coli</i>	Goat milk	D and Z values lower	Pereira, Martins, Mateus, Teixeira, & Vicente, 2007
<i>Bacillus licheniformis</i> spores	Cloudberry jam	D values lower	Pereira, Martins, Mateus, Teixeira, & Vicente, 2007
<i>Escherichia coli</i> , <i>Salmonella typhimurium</i> , <i>Listeria monocytogenes</i>	Peptone water, apple juice	Stronger inactivation compared to conventional heating	I. K. Park & Kang, 2013
<i>Escherichia coli</i> , <i>Salmonella typhimurium</i> , <i>Listeria monocytogenes</i>	Orange juice, tomato juice	Stronger inactivation in tomato juice than in orange juice	Lee, Sagong, Ryu, & Kang, 2012; Sagong, Park, Choi, Ryu, & Kang, 2011
<i>Escherichia coli</i> , <i>Salmonella enterica</i>	Salsa (chunky tomato-based)	At 25 V/cm inactivation by 5 log units for <i>E. coli</i>	Lee et al., 2013
<i>Bacillus amyloliquefaciens</i> and <i>Geobacillus stearothermophilus</i> spores	0.1% NaCl solution, green pea puree, carrot	In tomato juice inactivation by 3.1 to 4.8 log units, in 0.1% NaCl	Park, Balasubramaniam, Sastry, & Lee, 2013

Moderate Electric Field heating

	puree, tomato juice	solution by 4.6 to 5.6 log units	
<i>Saccharomyces cerevisiae</i>	Phosphate buffer solution	Faster release of cytoplasmic proteins than with conventional heating	Yoon, Lee, Kim, & Lee, 2002

Nair et al. (2014) applied to two types of rice bran, Red Triveni and Basmati, MEF heating as pre-treatment before the extraction, applying an electric field strength of 54 V/cm. They concluded that, using MEF, the processing time was reduced of about 70% - 75% for both types of bran and, moreover, from samples treated with MEF an higher amount of final product was obtained respect to rice treated with only conventional extraction method. De Oliveira, Giordani, Gurak, Cladera-Olivera, & Marczak (2015) extracted pectin from passion fruit comparing conventional extraction method (direct boiling) with MEF extraction. Traditional extraction method required about 2 hours for the treatment, resulting in a significant energy consumption. Moreover, the long time required often led to pectin degradation. MEF, instead, resulted a successful treatment for pectin extraction, especially for that one having a high degree of esterification. Lakkakula, Lima, & Walker (2004) reported that MEF heating was an optimal treatment for the extraction of oil bran. Samples treated with MEF showed a higher yield extraction of about 39% than control samples. Moreover, authors observed that with MEF treatment the lower the frequency applied, the higher the amount of extracted product, phenomenon probably due to electroporation.

Yang et al. (1997) evaluated microbiological safety and sensorial properties of six different stew types, treated with MEF heating, after three years of storage at about room temperature. Authors stated that an optimal storage in terms of quality and microbial security was found.

Zhong & Lima (2003) analyzed if MEF heating applied to sweet potato tissue could improve its vacuum drying rate. Results confirmed that drying rates of the treated samples were faster than untreated ones, with the highest decrease in drying time of 24%.

Engchuan et al. (2014) compared MEF and traditional cooking of pork meat balls. Authors stated that samples treated with Moderate Electric Field resulted more solid and brighter than meat balls treated with traditional method.

Table 2.3 compares the difference in loss nutrients, in terms of “cooking loss”, between meat products treated with MEF and conventional cooking methods.

Table 2.3 “Cooking loss” comparison between MEF heating and conventional heating for meat products (Pathare & Roskilly, 2016; Yildiz-Turp, Sengun, Kendirci, & Icier, 2013).

Product	Method	Cooking loss [%]	References
Pork	MEF heating	9.71- 30.22	Dai et al., 2014
Whole turkey meat	Water bath	22.53-38.51	Zell, Lyng, Cronin, & Morgan, 2010b
	MEF heating- LTLT	25.2	
	MEF heating- HTST	31.3	
Beef muscle (biceps femoris)	Conventional heating	27.0	Zell, Lyng, Cronin, & Morgan, 2009b
	MEF heating	27.7	
	Conventional heating	37.9	
Beef muscle (semitendinosus)	MEF heating- LTLT	29.27	Zell, Lyng, Cronin, & Morgan, 2010a
	MEF heating- HTST	36.29	
	Conventional heating	37.77	

Lascorz, Torella, Lyng, & Arroyo (2016) compared MEF and traditional cooking of shrimps evaluating several aspects such as heating rate, cooking loss, texture and colour. Authors pointed out that samples treated with MEF were cooked faster (40 s independently of size) than shrimps cooked with steam (38 s for small shrimps and 59 s for the large ones). Moreover, shellfish subjected to MEF showed a more uniform cooking than those

cooked traditionally. No differences in texture and cooking loss were observed between samples treated with the two different method. Moreover, shrimps cooked with MEF showed fewer colour changes than samples treated with conventional cooking method.

2.5 *Bubbling phenomena during MEF heating*

As reported in several papers, during MEF heating, with increasing temperature, the bubbling phenomena may occur. Darvishi, Khostaghaza, & Najafi (2013), evaluated the effect of MEF heating on electrical conductivity, heating rate, system performance and pH of pomegranate juice. Voltage gradient applied ranged between 30- 55 V/cm. During this experimental study, authors observed that, when temperature reached about 81 °C, bubbling phenomena started to occur, causing a decrease in electric current and, thus, in electrical conductivity. Authors stated that formation of bubbles could be linked to the release of gas and, consequently, to a concentration of solids due to reactions of electro- chemical nature, which led to an increased resistance to the movement of ions within the treated liquid. Palaniappan & Sastry (1991a), realized an apparatus to measure electrical conductivity of food products applying MEF heating or conventional heating methods. Heating was performed up to 80 – 85 °C, applying a voltage of 140 V and a frequency of 60 Hz. Treated samples were tomato and orange juices. Authors observed that above the temperature of 80 – 85 °C the electric current, and thus electrical conductivity, started to decrease. By observing the sample, authors realized that the decrease in current could be linked to the formation of gas bubbles near the electrodes. Several studies were performed to better understand bubbles phenomena and its cause. Authors pointed out that being both juices of acid nature, this could lead to the potential electrolytic hydrogen bubbles generation. Icier & Ilicali (2005a) heated with MEF up to 70 °C apricot and peach purees applying voltage gradients ranging between 20- 70 V/cm and a frequency of 50 Hz. During the heating it was noted that above 50 °C, especially at high voltage gradients, bubbling phenomena started to occur, and heating was stopped. Moreover, it was observed that when bubbling started electrical conductivity decreased with temperature rise when formation of bubbles started. Due to the occurrence of this phenomena, and the problems linked to them, authors stressed the importance of preventing them by using, for example, inert coated electrodes. Zhao, Kolbe, & Flugstad (1999) devised a method to identify visual electrode corrosion during MEF heating. In this experimental work, they also discussed about bubbling phenomena. Authors stated that gas bubbles were the result of water boiling caused by high current densities or the generation of by- products from oxidation/ reduction reactions.

Therefore, as noted in the experimental works mentioned above, bubbling phenomena occurring during MEF heating cannot be underestimated or

overlooked. Releasing of bubbles requires serious considerations in designing of MEF heater and in the correct choice of the applied voltage gradients.

2.6 Other industrial applications of MEF heating

An important industrial application of MEF is related to the waste treatments, such as sterilization of animal wastes, sewage sludge and compost leachate. Murphy, Powell, & Morrow (1991) evaluated MEF heating suitability for sewage sludge. Sludge had electrical conductivity ranging between 0.2 - 0.6 S/m, at room temperature, and 0.8 - 2.3 S/m at 90 °C: values suitable to treat samples with MEF heating. The heating, in fact, was rapid, uniform and with an energy efficiency of about 98%, resulting very convenient for sterilisation and pasteurisation of sewage sludge. Yin, Hoffmann & Jiang (2018) analyzed *E. Coli* microbial inactivation applying MEF to wastewater sludge. They concluded that, respect to conventional treatments, such as anaerobic digestion, MEF heating was more efficient.

Of recent, another application for MEF is related to its use as electric thermal storage device. Sakr & Liu (2014) suggested that being salts able to store heat, they can be melted and preserved in suitable containers. When energy is needed, these salts can be used in a heat exchange system to release them retained heat.

MEF results suitable also for seawater distillation. Conventional treatment, which exploit the use of steam boilers, bring to the generation of scale that impact on the efficiency of the process. MEF can be used as an alternative heating method, overcoming problems related to boilers (A. M. Assiry, Gaily, Alsamee, & Sarifudin, 2010).

2.7 Summary

The chapter reviewed the basic and working principle of MEF heating. A fundamental characteristic for a performing treatment is that the products to be treated are good conductors of electricity. MEF has become one of the most preferable methods due to its capability to reduce processing time, providing a heating uniformity and, thus, safe and stable food products. The main success of MEF heating is related to the rate of heat generation in the system, for this reason main food properties parameters and process control are discussed. As shown from main food processing and industrial applications, MEF heating is suitable for a wide range of applications. Anyway, numerous studies and research are still needed to better analyse some aspects, some of which: completely understand all the effects produced by of MEF heating, in particular, on heterogeneous food systems. Further

clarifications are also required about MEF heating influence on size, shape and orientation of food products in solid- liquid systems. Moreover, there are still a lot of challenges to control the heating rate during the process, due to variation of electrical conductivity during the treatment.

3 Electrical properties: electrical conductivity

As highlighted in previous section, electrical conductivity is a key property in MEF heating. This section deals, in detail, the effect of different parameters on EC in both liquid and solid foods. Moreover methods of measurement of electrical conductivity are reported too.

3.1 *Liquid foods*

In this section the effects of temperature, electric field strength and ingredients on electrical conductivity of liquid foods are discussed.

3.1.1 *Effect of temperature*

Generally, electrical conductivity increases linearly with temperature. Some exceptions are linked to some components (i.e. starches) that might be subjected to phase transitions or substantial structural changes during the heating (section 3.1.3).

3.1.2 *Effect of electric field strength*

Palaniappan & Sastry (1991a) pointed out that variations of electric field strength in a range between 0 V/cm and 100 V/cm had irrelevant influence on the relationship between electrical conductivity and temperature of orange juice (**Figure 3.1**). This was due to the presence of inert solids that were not affected by the electric field.

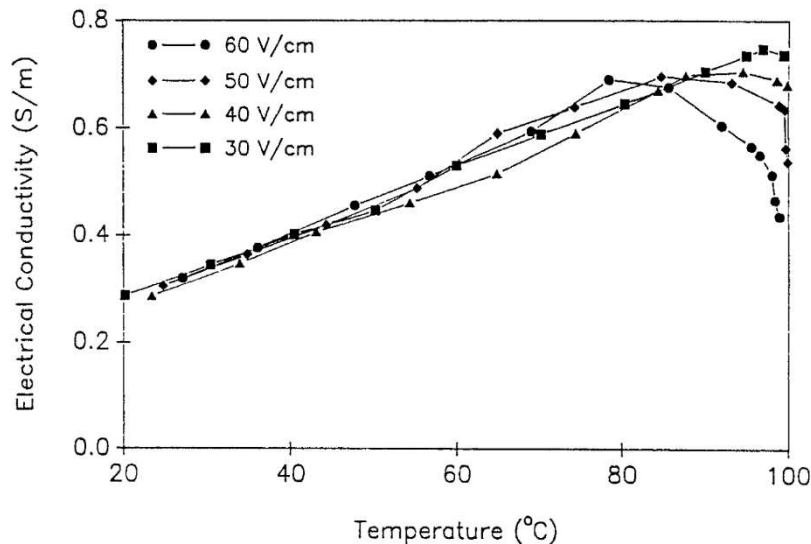


Figure 3.1 Electrical conductivity of orange juice subjected to different electric field strengths. Electrical conductivity decreases at around 100 °C could be due to boiling phenomena (Palaniappan & Sastry, 1991a).

Castro et al. (2003) carried out experimental MEF heating tests using strawberry- based products, to determine the effect of electric field strength on electrical conductivity. Authors observed that, for strawberry pulp at 14.5 ° Brix, the effect of the electrical field strength was negligible.

3.1.3 Effect of ingredients

- **Electrolytic solutes**

The effect of electrolytes, in particular salt, was already discussed in section 2.1. Other electrolytes present in foods are, for example, acids. Moreover, some gums and thickeners could have some charged groups that could contribute on the electrical conductivity.

- **Inert suspended solids**

Generally, suspended solids, such as pulp and cellular solids, are insulators and bring to a reduction of electrical conductivity of the liquid product in which they are dispersed. The particle size of suspended solids can affect the electrical conductivity of the liquid food. An analysis of this influence can be carried out considering, for simplicity, suspended solids as spheres all of the same size. The total volume of the considered solids will be:

$$V_S = n \frac{4}{3} \pi r^3 \quad (3-1)$$

The cross—section area subjected to the electric field will be determined by:

$$A_S = n \pi r^2 \quad (3-2)$$

Substituting eq. (3-1) into eq. (3-2) A_S will be given by:

$$A_S = \frac{3V_s}{4r} \quad (3-3)$$

Thus, the total cross- section of the solids that act like insulators increases as particle size decreases. Consequently, smaller particles will exhibit lower electrical conductivity than coarse ones (Rao, Rizvi, & Datta, 2014). However, as shown in **Figure 3.2**, the opposite situation was observed in case of carrot solids within sodium phosphate solution (Palaniappan & Sastry, 1991b).

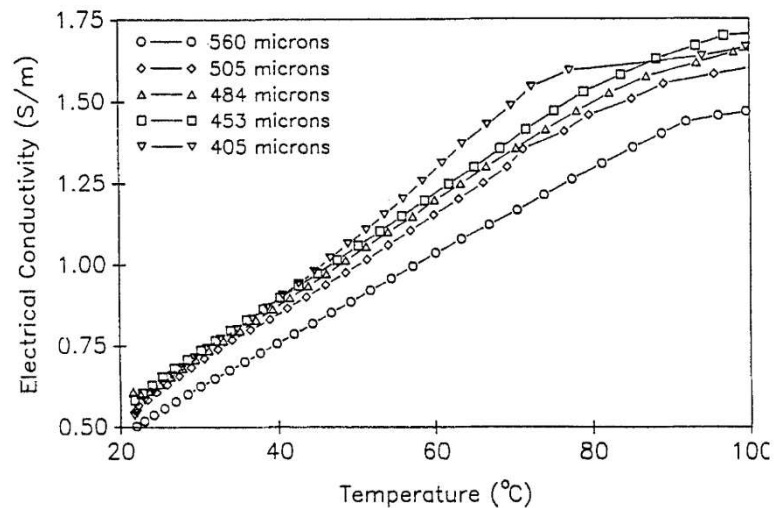


Figure 3.2 Electrical conductivity of carrot solids, with different particles sizes, dispersed in sodium phosphate solution (elaborated from Palaniappan & Sastry, 1991b)

This shows that particle shape and leaching of intracellular constituents can influence and make more complex all the frame of the considered situation.

- **Hydrocolloids**

Several authors analyzed the influence of hydrocolloids on electrical conductivity.

Marcotte, Piette, & Ramaswamy (1998) studied the effect of different hydrocolloids concentration, such as starch, carrageenan, pectin, gelatin and xanthan, on electrical conductivity. Authors pointed out that starch, being a neutral polysaccharide, exhibited the lowest electrical conductivity. Carrageenan and xanthan, instead, being the more charged hydrocolloids among those analyzed, showed the highest electrical conductivity. Pectin, being less charged than carrageenan and xanthan but more charged than starch, exhibited medium electrical conductivity values. Authors obtained the following correlation:

$$\sigma = \sigma_{C,25} + K_T(T - 25) + K_{TC}(T - 25)C \quad (3-4)$$

where:

$$\sigma_{C,25} = K_{C,25}C \quad (3-5)$$

Table 3.1 shows data of parameters $K_{C,25}$, K_T and K_{TC} for the different analyzed hydrocolloids.

Table 3.1 Parameters for electrical conductivity relationships (eqs. (3-4) and (3-5)). $K_{C,25}$ is the concentration parameter at 25 °C; K_T is the temperature parameter; K_{TC} is the interaction parameter between (T-25) and C.

Hydrocolloid	$K_{C,25}$ (S/m %)	K_T (S/m °C)	K_{TC} (S/m% °C)	R^2
Carrageenan	0.1700	8.65×10^{-4}	3.90×10^{-3}	0.9953
Xanthan	0.1330	1.78×10^{-3}	2.46×10^{-3}	0.9990
Gelatin	0.0299	5.29×10^{-5}	7.67×10^{-4}	0.9980
Pectin	0.0305	5.76×10^{-4}	4.81×10^{-4}	0.9955
Starch	0.0130	1.95×10^{-4}	2.71×10^{-4}	0.9985

Marcotte, Trigui, Ramaswamy (2000) analyzed the influence of the addition of salt and citric acid to four hydrocolloid solutions (starch,

4.3%; carrageenan, 1.7%; xanthan, 2%; pectin, 2.5%). Carrageenan and xanthan exhibited, at low salt concentration, the highest electrical conductivity, followed by pectin. Starch, instead, showed the lowest electrical conductivity. Authors obtained a linear regression, eq. (3-6), for each hydrocolloid.

$$\sigma = \sigma_{25} + K_{\sigma T}(T - 25) \quad (3-6)$$

Values of σ_{25} and $K_{\sigma T}$ related to eq.(3-6) are reported in **Table 3.2**.

Table 3.2 Relationship parameters of eq. 3-6 at different salt contents for the various analyzed hydrocolloids (Marcotte, Trigui, Ramaswamy, 2000).

Hydrocolloid	Salt concentration (%)	σ_{25}	$K_{\sigma T}$
Carrageenan (1.7%)	0.25	0.848	0.0199
	0.50	1.371	0.0313
	0.75	1.914	0.0413
	1.0	2.173	0.0481
Xanthan (2%)	0.25	0.889	0.0181
	0.50	1.474	0.0305
	0.75	1.969	0.0396
	1.0	2.162	0.0419
Pectin (2.5%)	0.25	0.691	0.0153
	0.50	1.201	0.0261
	0.75	1.690	0.0349
	1.0	2.195	0.0455
Starch (4.3%)	0.25	0.582	0.0123
	0.50	1.066	0.0204
	0.75	1.544	0.0312
	1.0	2.109	0.0427

Phase transitions of suspended solids

Halden, De Alwis, & Fryer (1990) carried out experiments to establish changes that can take place during MEF heating of foods. In particular, authors observed a variation of the heating slope of a potato slice. Authors attributed this change to starch gelatinization.

Wang & Sastry (1997) analyzed the influence of starch gelatinization on electrical conductivity. Authors noted a negative peak in the electrical conductivity- temperature curve and they represented to the phase transition temperature in the Differential

Scanning Calorimeter (DSC) thermogram. Thus, from this study it was possible to establish that starch gelatinization could be identified measuring electrical conductivity.

Chaiwanichsiri, Ohnishi, Suzuki, Takai, & Miyawaki, (2001) carried out electrical conductivity measurements on potato starch suspension (with salt addition) conventionally heated at 200 kHz. Authors observed an increase of electrical conductivity upon gelatinization. Authors pointed out that this increase was due to the discharge of ions during the gelatinization. Authors explained also the difference of obtained results of Wang & Sastry, (1997) considering that, in this last work, no salt was added.

Through previous cited experimental study, consequently, is possible to confirm that the through the observation of starch gelatinization electrical conductivity has a significant potential.

- **Effect of Non-electrolytic Solutes**

Some substances, such as sucrose, do not give rise to electrically conductive ions in solution. Thus, the presence of this type of substances bring to a less high electrical conductivity of the solution. Castro et al., (2003) analyzed electrical conductivity of strawberry pulps with soluble solids from 14 to 59.5 °Brix, obtained by addition of sucrose. Authors pointed out that, as shown in **Figure 3.3**, as sugar content increased, electrical conductivity value decreased.

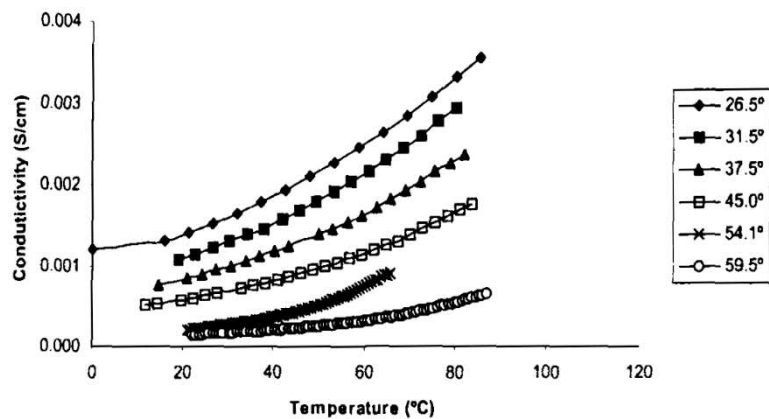


Figure 3.3 Influence of sugar content in strawberry pulp on electrical conductivity (Castro et al., 2003).

3.2 Solid foods

In this section are presented the effects that microstructure of the material, temperature, electric field strength, frequency and ingredients have on the electrical conductivity.

3.2.1 Effect of temperature and electric field strength

- **Gels and Noncellular solids**

As observed by Yongsawatdigul, Park, & Kolbe (1995) with Pacific whiting surimi paste, in noncellular solids, generally, electrical conductivity increases linearly with temperature. As shown in **Figure 3.4**, Castro et al., (2003), instead, observed a slight non-linear increase of electrical conductivity with temperature for strawberry jelly.

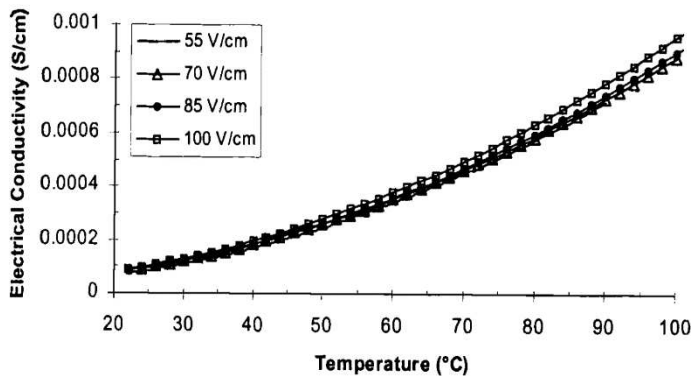


Figure 3.4 Electrical conductivity of strawberry jelly at different electric field strengths (Castro et al., 2003).

Various reasons can be advanced for this type of effect, such as the breakdown of the gel that can bring to a lower drag of ions and, thus, to a higher electrical conductivity at higher temperatures.

Electric field strength, generally, has not strong effects on electrical conductivity behavior. Castro et al., (2003) in addition to the effect of temperature on the electrical conductivity of strawberry jelly, analyzed also the possible effects of the electric field strength. Authors pointed out that electric field strength had a slight effect on the electrical conductivity. Moreover, Yongsawatdigul et al., (1995), pointed out that electric field strength had a slight effect on the electrical conductivity of surimi paste and this could be attributed to electrochemical reactions that occurred at the electrode surfaces.

- **Solids with undisrupted cellular structure**

In solids having a cellular structure, such as, fruits and vegetables electrical conductivity is affected by both temperature and electric field strength. Palaniappan & Sastry, (1991b) compared the effects on the electrical conductivity of three different vegetables heated conventionally and with MEF. Until about 70 °C, the electrical conductivity of products heated with conventional method showed moderate changes with temperatures. After 70 °C, the cellular structure broke down and, consequently, electrical conductivity showed a significant increase, as shown in **Figure 3.5**.

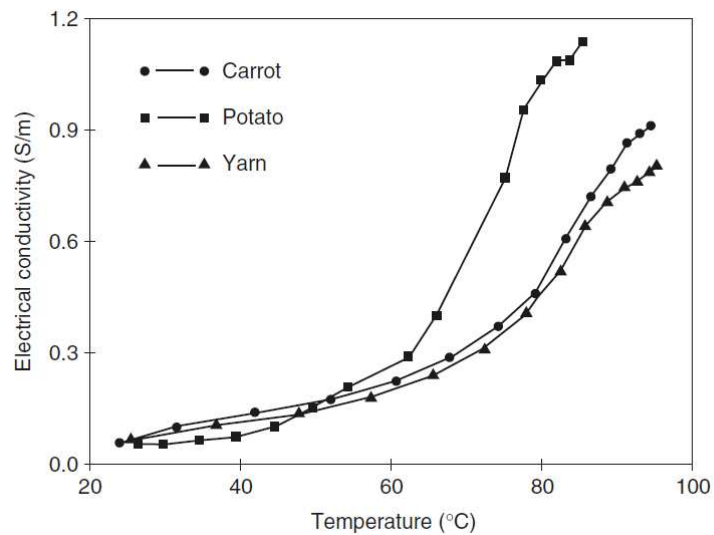


Figure 3.5 *Electrical conductivity of vegetable tissue (carrot, potato and yam) conventionally heated* (elaborated from Palaniappan & Sastry, 1991b).

For carrots, for example, increasing the electric field strength, as shown in **Figure 3.6**, the change in electrical conductivity became less sharp and, at sufficiently high electric field strengths, the electrical conductivity-temperature trend assumed a linear evolution. Therefore, this means that a sample subjected to MEF undergone to cellular structure breakdown at lower temperatures than when is conventionally heated.

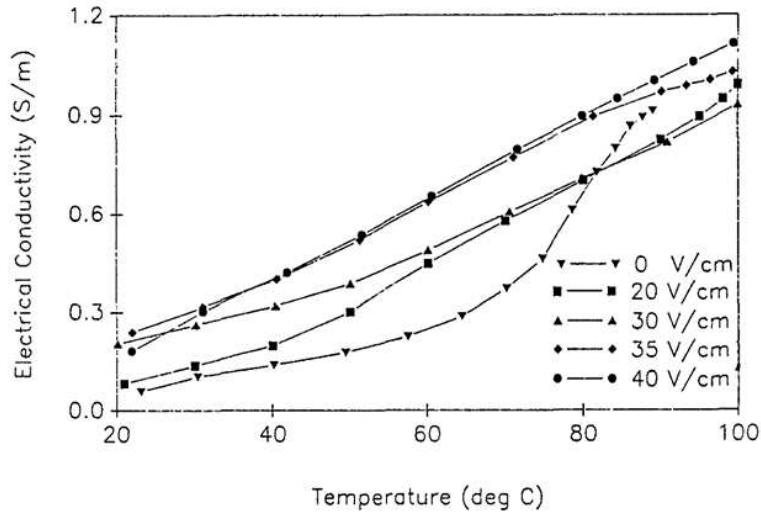


Figure 3.6 Electrical conductivity of carrot tissue subjected to various electric field strength (elaborated from Palaniappan & Sastry, 1991b).

- **Effect of ingredients**

The effect that various ingredients have on electrical conductivity of solid foods is similar to that one they have on liquid foods (section 3.1.3).

For solid foods particles, to increase the electrical conductivity the most commonly used method is the addition of salt by infusion method. Wang & Sastry (1993a,b) applied the salt infusion method to potato. Authors pointed out that the utilized method was successful only for external layers of the treated vegetable. The effect of salt addition on electrical conductivity obtained by authors is shown in **Figure 3.7**.

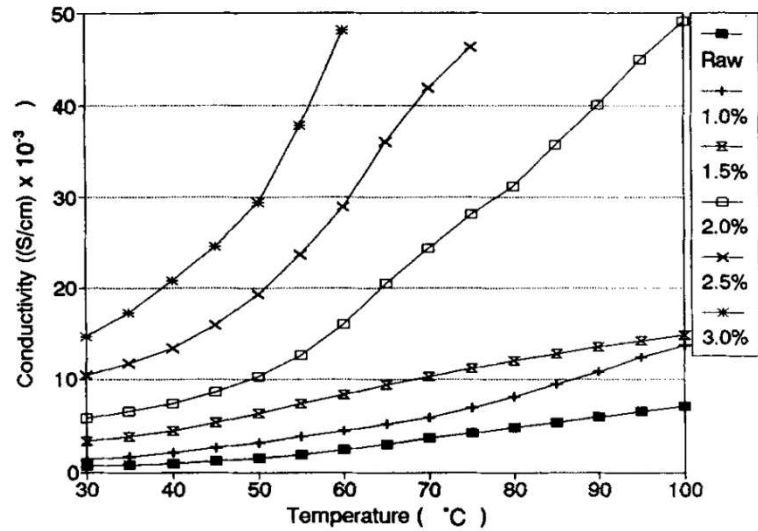


Figure 3.7 Effect of salt infusion at different concentrations on the electrical conductivity (Wang & Sastry, 1993b).

3.3 Measurement methods of electrical conductivity

A sample scheme of a system used to measure electrical conductivity is shown in **Figure 3.8**. As shown in figure, the system consists of a treatment cell, in this case of cylindrical shape, with two electrodes inserted at its ends. In the geometric centre is inserted a thermocouple to allow the measurement of the temperature.

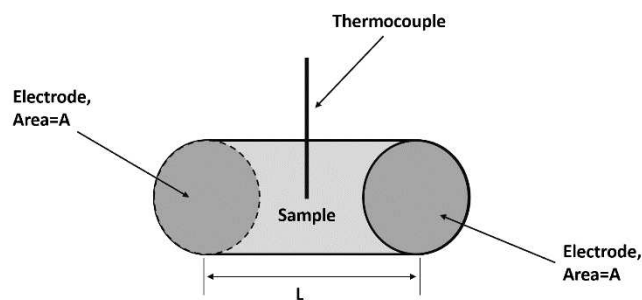


Figure 3.8 Classic system used to measure electrical conductivity.

This type of system for electrical conductivity measurements offers different advantages:

- Treated samples have a definite shape. Thus, the calculation of cell constant K is simplified.
- A thermocouple allows the measurement of temperature. It is possible to use more than one thermocouple to monitor the temperature in different points of the system. Temperature measurements is a critical step, being electrical conductivity strongly dependent on it.
- Both solids and liquid samples may be treated. Liquids takes the form of the treatment cell containing them. Solid foods, instead, can be cut to make them take the shape of the vessel that contains them.
- Thermocouples and electrodes can be locked up using O-rings or packing glands, allowing, in this way, the system to work at pressures higher than the atmospheric one.
- Heating the sample with MEF, electrical conductivity can be measured continuously as function of temperature and frequency.

Difficulties encountered during MEF heating process and the precautions to be taken are:

- It is important to ensure a good contact between the electrodes and the sample to be treated. In other words, it is important to guarantee the best contact between electrode and sample, applying the due pressure without breaking the food sample structure.
- Measurement of the temperature is crucial, and it is of fundamental importance avoiding electrical interferences. The use of optical fibres can be the optimal choice, though is quite difficult to keep the in place if it-to-out pressure gradient is established. In this regard, thermocouples must be isolated by coating them, for example using coated Teflon thermocouples. This solution, however, avoids electrical interferences but leads to slow response times. This solution, therefore, could be a problem in case of rapid MEF heating processes.

An alternative way to accelerate the response time is, for example, the use of fibre- optic sensors.

The measurement of electrical conductivity can be carried out, then, by connecting the system to a power source, applying an electric field and measuring continuously current and temperature. Electrical conductivity can be then measured.

In case the sample to be treated is particularly delicate and cannot be subjected to particular physical stresses, an indirect method of measurement may be used. The sample to be treated can be placed in the treatment cell

and the space between the ends of the sample and the electrodes can be filled with a fluid of known electrical conductivity (**Figure 3.9**).



Figure 3.9 *Electrical conductivity measurement method for particularly delicate sample*

The system shown in the figure above can be considered as a set of resistances in series and the electrical conductivity of the sample can be evaluated. This method, however, has a disadvantage: if the electrical conductivity of the fluid is different from the sample's one, the measurement of the electrical conductivity could be compromised.

In case of liquid foods for electrical conductivity measurement can also be used the following devices:

- **Conductive sensors** can be at 2- electrodes or 4- electrodes. With the first ones, the device consists of a meter and a probe with two metal electrodes placed at a certain distance from each other. For electrical conductivity measurements, the probe is put in contact with the sample and an AC voltage is applied between the electrodes. Current passing through the sample is the measurement signal. Being applied current and voltage known, the sample resistance is known and, thus, also the conductance value.

Conductivity sensors at 4- electrodes consist of a meter and a probe with two pairs of electrodes. In this type of device, the two pairs of outer electrodes measure the current, while the two pairs of inner electrodes measure applied voltage.

- **Inductive sensors** consist of a probe in which electrodes are replaced by two toroidal coils. Both coils are covered with a corrosion- resistant plastic body and must be completely immersed in the liquid. One coil is the drive, the other one is the receive coil. For the conductivity measurement, an alternating voltage is applied to the drive coil, which causes a voltage in the liquid neighbouring the coil. This voltage gives rise to a ionic current flow which, in turn, causes an electronic current in the receive coil. The induced current is proportional to the conductance of the solution and is measured by the analyzer. Knowing the conductance of the solution

and cell constant, the device returns the electrical conductivity value

The conductivity sensors at 2- electrodes are well used for low conductivity applications. Sensor at 4- electrodes, instead, are suitable for moderate to high conductivity applications. Inductive sensors are well used for corrosive solutions and, bearing the fouling, for solutions with high content of suspended solids.

3.4 Summary

This chapter discussed the effects of temperature, electric field strength and ingredients on the electrical conductivity of both liquid and solid foods. Moreover, different methods for electrical conductivity measurement were discussed.

4 Preliminary trials on MEF heating

In Chapter 4 are described the preliminary trials and relative materials and methods used, related to the experimental work at the University of Salerno and during the international mobility at UCD (University College Dublin, Belfield, Dublin 6, Ireland).

4.1 Raw materials for MEF heating test

In this section are described raw materials used to carry out the experimental work at University College Dublin (UCD, Ireland) where a first MEF equipment existed. This methodology as then be applied in the subsequent MEF heating trials run at University of Salerno (UNISA, Italy), also discussed herein.

4.1.1 Meatballs

There are always issues related to wasting food for laboratory experiments. In the past, chemicals such as carbo methyl cellulose were used as food analog for ohmic heating test (Icier & Illicali 2005b). In this experimental work, as raw materials it was decided to use food with the purpose of analyzing an actual possible meal characterized by its heterogeneity, thus chicken meatballs and reconstituted potato flakes. Pre-cooked and frozen chicken meatballs were purchased in Ikea stores (Huvudroll, Ikea Italia, Baronissi, Italy, for the tests run at University of Salerno; Alemansrätten, Ikea, Dublin, Ireland, for the test run at UCD).

Alemansrätten meatballs were made with minced chicken meat (61%), chicken skin, onion, potato starch, salt (1.6%) and spices. Meatball diameter was about 3 cm. **Table 4.1** show nutritional values for 100 g of product.

Table 4.1 *Nutritional values for 100 g of Alemansrätten chicken meatballs.*

Nutritional values	
Energy [kJ]	794
Fat* [g]	13
* of which saturates [g]	4.2
Carbohydrate [g]	5.2
** of which sugars [g]	0.8
Proteins [g]	13
Salt [g]	1.6

Huvudroll meatballs were made with minced chicken meat (69%), chicken skin, onions, corn starch, salt (1.5%) and spices. **Table 4.2** shows nutritional values for 100g of product.

Table 4.2 *Nutritional values for 100 g of Huvudroll chicken meatballs.*

Nutritional values	
Energy [kJ]	778
Fat* [g]	13
* of which saturates [g]	3.2
Carbohydrate [g]	4.9
** of which sugars [g]	0.6
Proteins [g]	13
Salt [g]	1.5

4.1.2 Reconstituted flakes potatoes

Reconstituted potato flakes were obtained mixing potato flakes (Erin Foods Ltd., Thurles, Co. Tipperary, Ireland, for the tests performed at UCD; Crastan, Pisa, Italy, for tests performed at University of Salerno), pure dried vacuum salt (INEOS Enterprises, Weston Point, Runcorn, Chesire WA7 4HB, UK for the tests run at UCD; Conad Soc. Coop., Italy, for tests run at University of Salerno), unsalted butter (Tesco, Dublin, Ireland, for the tests carried out at UCD; Conad Soc. Coop., Italy, for tests carried out at University of Salerno) and distilled water.

4.2 Samples preparation

To perform experimental tests, different formulations of reconstituted potato flakes (RPF) were prepared both at UCD and at the University of Salerno, as shown in **Table 4.3**.

Table 4.3 Samples composition used at UCD and UNISA.

	Unsalted butter	Salt	Potato flakes	Distilled water	USED @
Composition 1 w/w [%]	5.00	5.70	23.70	65.60	UCD
Composition 2 w/w [%]	4.90	10.90	19.80	64.40	UCD
Composition 3 w/w [%]	-	2.75	12.68	84.57	UNISA
Composition 4 w/w [%]	-	1.39	12.86	85.74	UNISA
Composition 5 w/w [%]	-	0.74	12.95	86.31	UNISA
Composition 6 w/w [%]	-	0.37	13.00	86.63	UNISA
Composition 7 w/w [%]	5.80	2.90	18.80	72.50	UNISA
Composition 8 w/w [%]	5.80	5.70	16.00	72.50	UNISA
Composition 9 w/w [%]	5.80	0.00	21.70	72.50	UNISA

For convenience, reconstituted potato flakes obtained from composition 1 and composition 2 will be indicated using the acronym RPF; reconstituted potato flakes obtained from composition 3, 4, 5, 6 will be identified with acronym RPFNB; reconstituted potato flakes obtained with compositions 7, 8 and 9 will be referred to acronym RPFB.

To perform experimental tests at UCD, the predefined amount of salt and unsalted butter (**Table 4.3**) were added to boiled distilled water and mixed with a scoop, until the butter was melted and salt was dissolved. The obtained mixture was put in a pan mixer (Kenwood chef classic, model KM331, Kenwood Ltd., Havant, UK) with a dough hook. Subsequently, potato flakes were slowly added in the mixer, set at the lowest speed, to prevent the formation of air bubbles. Once potato flakes were completely incorporated, the mixing continued for about 1 minute, to ensure a correct and complete mixing. Obtained reconstituted potato flakes were packaged with a wrap plastic film, to prevent moisture evaporation



Figure 4.1 *Reconstituted potato flakes storage in wrap plastic film.*

Subsequently, reconstituted potato flakes samples were retained in an incubator (10 A, 230 V, 50 Hz; Model KB 53, Binder, Tuttlingen, Germany) at 2°C until needed for use.

Chicken meatballs were stored in a freezer at -20°C and, subsequently, retained in the incubator at 2°C overnight (10 A, 230 V, 50 Hz; Model KB 53, Binder, Tuttlingen, DE) before the experiments.

For experimental work at UNISA, the fixed quantity of salt and butter for RPF, or the only fixed quantity of salt for RPFNB, were added and mixed to boiling water. Once butter was melted and salt dissolved, the mixture was put in a pan and potato flakes were slowly added. Mixing was carried out using a hand whisk and was continued until potato flakes were completely mixed. Reconstituted potato flakes were put in wrap plastic film, to avoid the evaporation of water and transferred in a refrigerator overnight at 5 °C.

Chicken meatballs were stored in a freezer overnight at -20 °C.

Before the experiments, reconstituted potato flakes and meatballs were left at room temperature, to allow both to reach the same uniform temperature.

4.3 *Meatballs configuration*

For the experimental work, chicken meatballs and reconstituted potato flakes were positioned in a MEF heating treatment cell, considering different system configurations, to evaluate the effects of load and position of meatballs on MEF heating. Configurations used for RPF, RPFNB and RPF are shown respectively in **Figure 4.2**, **Figure 4.3**, **Figure 4.4**.

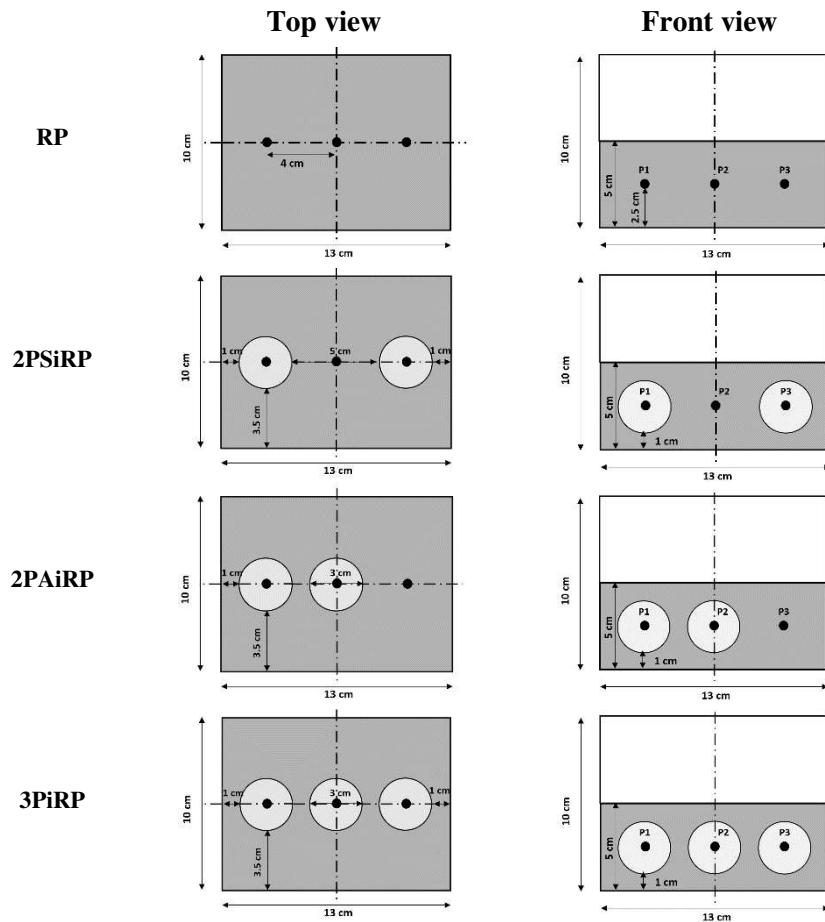


Figure 4.2 Top and front view of the different configurations analyzed. White big circles represent chicken meatballs. Black points represent temperature measurement points. Grey sections represent the portions of space occupied by reconstituted potato flakes (RPF).

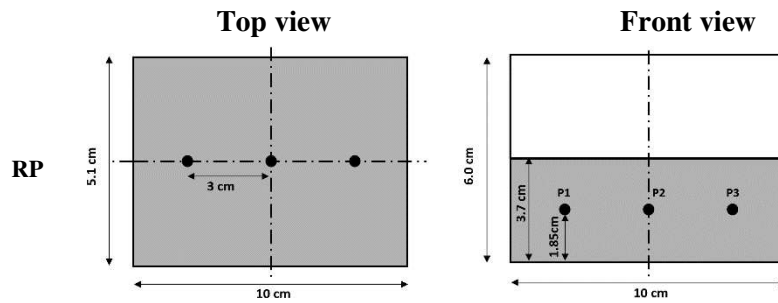


Figure 4.3 Top and front view of the different configurations analyzed. Black points represent temperature measurement points. Grey sections represent the portions of space occupied by reconstituted potato flakes (RPFNB).

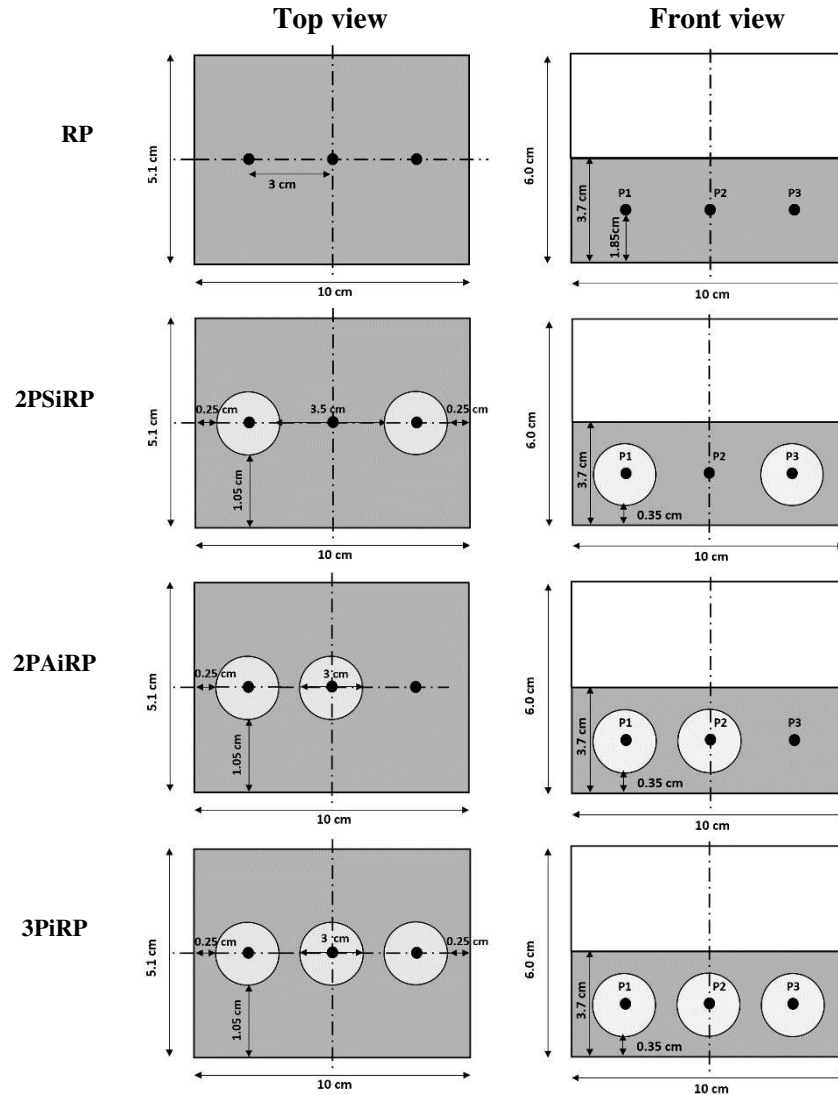


Figure 4.4 Top and front view of the different configurations analyzed. White big circles represent chicken meatballs. Black points represent temperature measurement points. Grey sections represent the portions of space occupied by reconstituted potato flakes (RPF).

As shown in **Figure 4.2**, **Figure 4.3** and **Figure 4.4**, one homogeneous system, composed by RPF, RPFNB or RPFB and three different heterogeneous systems, composed by reconstituted potato flakes (RPF or

RPF) and meatballs, were analyzed. Heterogeneous configurations were composed by two chicken meatballs located in reconstituted potato flakes at positions P1 and P3 (2PSiRP); two chicken meatballs located in reconstituted potato flakes at positions P1 and P2 (2PAiRP); and three chicken meatballs located in RPF at the three positions P1, P2 and P3 (3PiRP).

4.4 MEF heating equipment

In this section the equipment used to carry out the experimental MEF heating work at University College Dublin and the equipment designed and used for MEF heating experimental tests at University of Salerno are described.

4.4.1 MEF heating equipment at University College Dublin

MEF heating system utilized for experimental work at UCD (**Figure 4.5**) was a batch system constituted by an AC variable power supply unit (15 A, 0-250 V, 50 Hz; C- Tech Ltd, Chester, UK); a rectangular treatment cell (height 10 cm, length 15 cm and width 10 cm) with two platinized titanium electrodes of 9.5 cm x 9 cm, with a gap of 13 cm between them (

Figure 4.6); three T- type electrically insulated thermocouples to check the temperature of the sample at the established measurement points P1, P2, P3 (**Figure 4.7**).

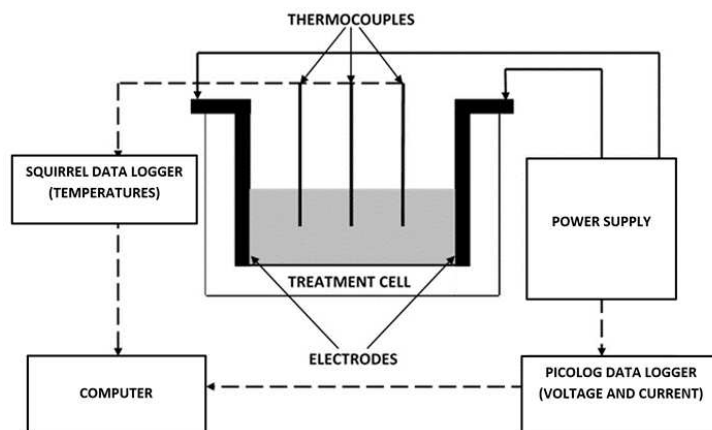


Figure 4.5 MEF heating equipment.

MEF treatment cell was open on top, allowing to the three thermocouples to be placed at the established positions P1, P2 and P3 (**Figure 4.7**).

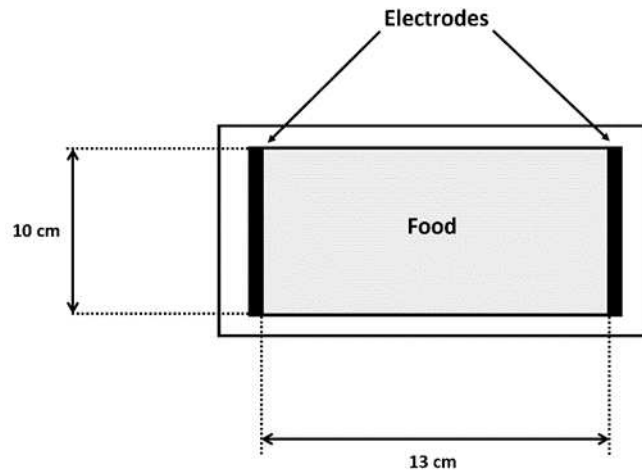


Figure 4.6 *Top view of MEF heating treatment cell.*

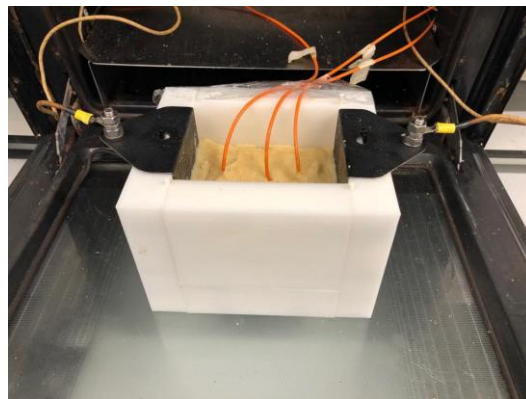


Figure 4.7 *MEF heating cell with three thermocouples inserted in positions P1, P2 and P3.*

PicoLog V6 data logger (Model No. R5.06.3, Pico Technology Ltd, St. Neots, UK) was utilized to record current and voltage values.

A data logger (Squirrel SQ2040 Series Data Loggers, Grant Instrument Ltd., Cambridge, UK) was used to register the temperature values every second.

MEF heating was carried out in an in an interlocked safety cabinet in which all the electrical connections were housed, to guarantee experiments could be performed safely from a health and safety perspective.

4.4.2 MEF heating equipment at University of Salerno

The experimental apparatus realized at University of Salerno consisted, principally, of a power supply system, a data acquisition systems and a MEF heating treatment cell, which are described in the following sections.

A simplified schematic diagram of the system built is shown in **Figure 4.8**.

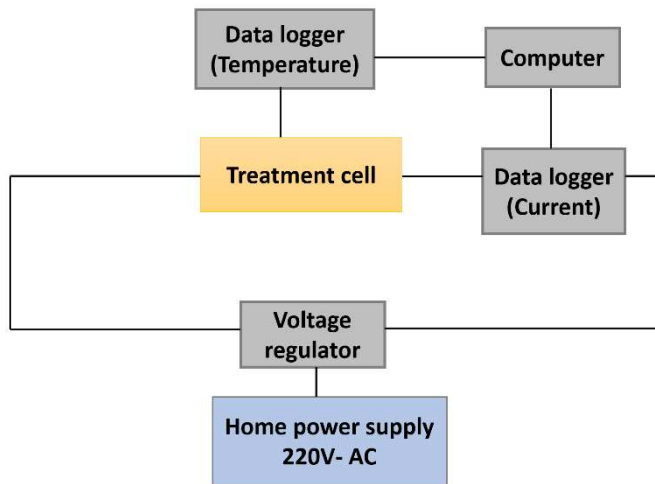


Figure 4.8 Schematic diagram of MEF heating setup.

- **Treatment cell**

Initially, for the design of MEF heating apparatus the attention was focused on the realization of a rectangular treatment cell. Subsequently, in anticipation of future tests to be carried out, a cylindrical cell was realized too.

Rectangular treatment cell

As mentioned in section 2.2 the main criteria to consider for the realization of a MEF heating treatment cell are:

- It should be of insulating material
- It should be able to withstand process temperature

- Should not impart off- flavour to the product

Based on the above criteria and considering that beyond to being adapted for alimentary uses, it is transparent and therefore it allows a direct visual of the treated product conditions, for the construction of ohmic heating chamber glass (**Figure 4.9**) was selected.

Technical specifications of treatment cell are given in **Table 4.4**.



Figure 4.9 Rectangular treatment cell.

Table 4.4 Technical specifications of MEF heating rectangular treatment cell.

Length [cm]	Width [cm]	Height [cm]	Distance between electrodes [cm]
10	5.1	6.0	9.6

The edges of glass treatment cell were joined together using a cementing material (silicon paste) as reinforcement to form a leak proof chamber. The choice fell on silicon paste because it is able to withstand temperatures of above 600 °C. The cementing material has been applied on the outside edges of the chamber.

Cylindrical treatment cell

Standing on the above cited criteria for the realization of MEF heating treatment cell, another treatment cell, for further future experiments, was realized of cylindrical shape (**Figure 4.10**). Considering its resistance to abrasion, impermeability and ease of use and maintenance, this time, the choice of the material for the treatment cell fell on PVC (Polyvinyl chloride).

Technical specifications of PVC treatment cell are reported in **Table 4.5**.



Figure 4.10 *Cylindrical treatment cell*

Table 4.5 *Technical specification of MEF heating cylindrical cell.*

Length [cm]	Internal diameter [cm]	External diameter [cm]	Distance between electrodes [cm]
5.4	3.0	3.5	4.0

The cell was closed using a threading system at both ends ensuring, thus, watertight.

- **Electrodes**

In MEF heating, the desired electric current from the source to the sample is transmitted by metal electrodes. In this case, they were designed for the specific purpose considering technical specifications of treatment cells.

As reported in section 2.2, the material used for electrodes in MEF heating chamber should have, principally, the following features:

- It should be of food grade and non-corrosive
- It should be workable and provide smooth finish

To meet the minimum requirements above discussed, food grade stainless steel 316 was selected as electrodes material. Electrodes realized for both rectangular and cylindrical cell are shown in **Figure 4.11(a)** and **Figure 4.11(b)**.

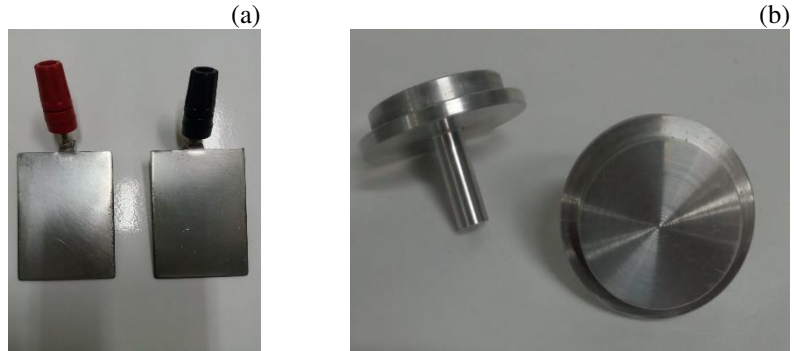


Figure 4.11 (a) rectangular cell electrodes. (b) cylindrical cell electrodes

- **Voltage regulator**

Considering the specifications of the first cell treatment realized (rectangular cell), for the choice of the best voltage regulator rough calculations have been carried out to better understand the necessary technical specifications. Since the prototype MEF heating unit had as its primary purpose the treatment of food products, reference was made to meat-based sauces, the composition of which has been rearranged considering a classic home-made meat soup.

In **Table 4.6** is shown the main composition of meat-based sauce analyzed.

Table 4.6 Meat-based sauce composition.

Sauce compounds	Composition [%]
Beef	45
Olive oil	15
Tomato	30
Water	10

Considering an initial treatment temperature of 25 °C and a final treatment temperature of 100 °C, the following electrical conductivities were computed for beef and tomato using correlation models shown in **Table 4.7**.

Table 4.7 Electrical conductivities for beef and tomato (Palaniappan & Sastry, 1991a,b).

Sauce compounds	Correlation	σ_{25} [S/m]	K [$^{\circ}\text{C}^{-1}$]	M_S [%]
Beef	$\sigma = \sigma_{25} [1 + K(T - 25)]$	0.440	0.016	-
Tomato	$\sigma = \sigma_{25} [1 + K(T - 25)] - 0.101M_S$	0.863	0.174	0.15

M_S is the solid concentration [%], σ_{25} [S/m] is the electrical conductivity at 25°C, K [$^{\circ}\text{C}^{-1}$] is the temperature compensation constant and T [$^{\circ}\text{C}$] is the temperature.

For the different compounds, electrical conductivities at 100 °C are shown in **Table 4.8**:

Table 4.8 Electrical conductivities of meat-based sauce compounds.

Sauce compounds	σ_{100} [S/m]	Reference
Beef	0.968	Palaniappan & Sastry, 1991b
Oil	0.00	Ushie, Osang, Ojar, Ohakwere-eze, Alozie, 2014
Tomato	12.11	Palaniappan & Sastry, 1991a
Water	0.792	Shrestha et al., 2017

Knowing the electrical conductivity of the different sauce compounds, the electrical conductivity of meat-based sauce was calculated, obtaining 4.15 S/m.

The resistance of the sample was evaluated as follows:

$$R = \frac{1}{\sigma} \cdot \frac{L}{A} \quad (4-1)$$

where L [m] is the distance between the electrodes, σ [S/m] is the electrical conductivity of the sauce and A [m²] is the cross-section of the material in the treatment cell.

In the particular case, the width (W) was 0.051 m (**Table 4.4**) and, considering a filling height of 0.05 m, A was 0.0025 m². Making calculations, R got 9.08 Ω .

Assuming an applied power of 1500 W, current and voltage were evaluated from eq. (2-1) and eq. (2-2), obtaining a current value of 12.86 A and a voltage value of 116.7 V.

In summary, considering a nominal power value of 1500 W, the following values were taken into account:

Table 4.9 *Values obtained for the equipment.*

H_{filling} [m]	W [m]	A [m ²]	σ [S/m]	R [Ω]	I [A]	V [V]
0.05	0.051	0.0025	4.15	9.08	12.86	116.7

Taking into account the obtained values in **Table 4.9**, in particular current and voltage values, a voltage regulator VAM20F-1N (K-Factor srl, Castellarano, Italy), shown in **Figure 4.12**, was chosen and purchased, to ensure the required process parameters previously computed.



Figure 4.12 *Voltage regulator, VAM20F-1N (K-Factor srl)*

Technical specifications of the selected voltage regulator are shown in **Errore. L'origine riferimento non è stata trovata.**

Table 4.10 *Voltage regulator, technical specifications.*

Model	Current [A]	Max Power [kVA]	Voltage input [V]	Voltage output [V]
VAM20F-1N	20	5.0	230	0-250

- **Temperature measurements and data acquisition systems**

During the experimental tests carried out, which will be then treated in the next sections, temperature measurements were carried out using

insulated thermocouple (**Figure 4.13**). In particular, to avoid interferences with the electrical field, FEP (fluorinated ethylene propylene) coated T-type thermocouples (TC misure e controlli s.r.l., Torino, Italy) were used, with an operating temperature up to 250 °C.



Figure 4.13 FEP coated thermocouples (TC- direct, Torino, Italy)

4.5 MEF heating procedure

For experimental tests carried out at UCD, at each trial treatment cell was loaded (with only potatoes or potatoes and meatballs), as described in section 4.3, up to a height of 5 cm. In course of the loading of RPF, attention has been paid to avoid the formation of air bubbles and to guarantee an optimal contact between the sample and the electrodes. Once the cell was completely loaded, thermocouples were positioned in RPF and on the meatball surface and core, depending on the experiments that have been carried out, at the established points (P1, P2, P3, see section 4.3). Thermocouples were fixed with scotch tape to one edge of the cell, to avoid possible movements. Temperature's readings were registered using Squirrel View Plus Edition. RPF and RPF with meatballs were heated from a dimensionless temperature of 0.00 to 0.70. Firstly, experiments were carried using an applied voltage of 30 V for all configurations, as described in section 4.3, and compositions (5.7% and 10.9 % salt content, see section 4.2). Subsequently, further tests were carried out applying different voltages (20 V, 30 V and 40 V) using 2PSiRP configuration with RPF at 5.7% salt content. P2 was used as a control point. Every test was carried out in triplicate.

For experimental MEF heating tests carried out at University of Salerno, for each trial treatment cell was loaded up (with only potatoes or with potatoes and meatballs) up to a height of 3.7 cm. Also in this case, care was taken during the filling of the cell to prevent the formation of air bubbles. Thermocouples were fixed, using a home-made stand to avoid possible movements, at the three measurement key points (P1, P2, P3, - section 4.3).

Before performing experimental tests, treatment cell was insulated inside a commercial oven (Whirlpool Europe, Biandronno, Italy) equipped with an interlock dispositive. Tests were run considering a target time of 4 minutes

for the homogeneous system RPFNB, 2.33 minutes for the homogeneous system RPFB and 4.33 minutes for the heterogeneous system RPFB and meatballs. Tests were performed at 30 V, 40 V and 50 V using for each system configurations discussed in section 3.3. Every test was carried out in triplicate.

4.6 Electrical conductivity measurements

According to Joule's 1st law, in MEF the heat generated into the material, in the specific case into the food, is proportional to the square of the electric field strength and to the electrical conductivity of the product. Electrical conductivity is the capability of a material to conduct electric current. It is function of temperature, concentration of the electrolytes, heating time and type of pre-treatment (Varghese et al., 2012). Electrical conductivity is given by (Zhu, Zareifard, Chen, Marcotte, & Grabowski, 2010):

$$\sigma = \frac{L}{A} \frac{1}{R} = \frac{L}{A} \frac{I}{V} = K G \quad (4-2)$$

where σ is the electrical conductivity [S/m], L [m] is the distance between the electrodes, A [m²] is the cross-section area of the sample, R [Ω] is the resistance, I [A] is the current, V [V] is the applied voltage, G [S] is the conductance (which is the reciprocal of the electrical resistance) and K [1/m] is the cell constant (given by the ratio of L/A).

Both at UCD and University of Salerno, electrical conductivity measurements were performed using an experimental setup whose schematic diagram is shown in **Figure 4.14**.

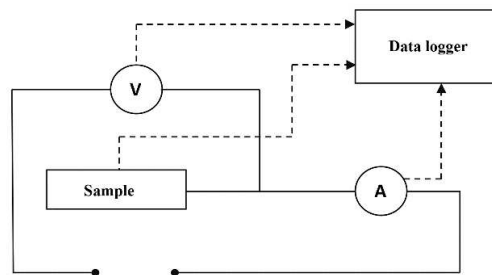


Figure 4.14 Experimental setup used to carry out electrical conductivity measurements.

At UCD, electrical conductivity measurements for RPF and chicken meatballs were carried out using a MEF heating system composed by a

treatment cell (**Figure 4.15**), positioned within an interlocked safety cabinet, and a portable power supply (10 A, 0- 270 V, 50 Hz; Model No. CMCTV10, Carroll & Meinell Transformers Ltd, Stockton- on- Tees, UK). A hole along the cylindrical cell permitted the insertion of an insulated K-type thermocouple in the geometric center of the sample (**Figure 4.16**). Two multimeters were used to record current and voltage.

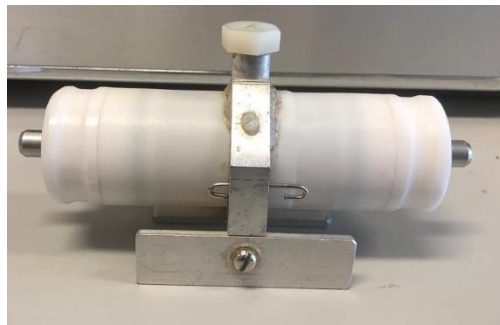


Figure 4.15 Electrical conductivity treatment cell.

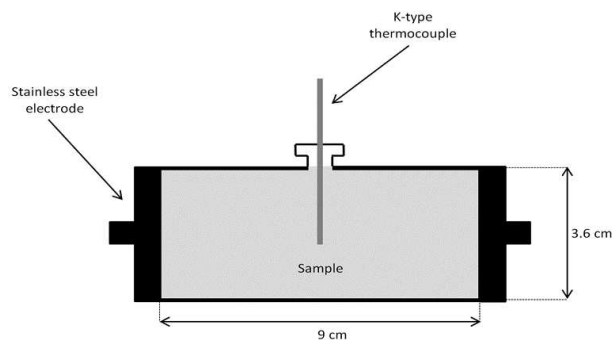


Figure 4.16 Front view of the treatment cell for electrical conductivity measurements.

The treatment cell used was cylindrical with a length of 11 cm and an internal diameter of 3.6 cm. The end caps were in the form of stainless-steel electrodes and they were held in the right position using a spring system to maintain contact and avoid sample leakages. Distance between the electrodes was 9 cm.

Before carrying out electrical conductivity tests, the cylindrical cell was calibrated (see section 4.7).

For electrical conductivity measurements, samples (RPF or meatballs) were taken from an incubator (10 A, 230 V, 50 Hz; Model KB 53, Binder GmbH, Tuttlingen, Germany) at 2 °C and located in the treatment cell. To avoid the formation of air bubbles during the filling, that could limit the passage of the current, the foodstuffs were carefully loaded and compressed within the cell. Care was also taken to be sure that samples were in good contact with the electrodes. Tests were performed using an applied voltage of 20 V at 50 Hz. Samples were heated from 5 °C to 75 °C. Current and voltage were recorded every 5 °C. Electrical conductivity measurements, for both reconstituted potato flakes (at 5.7% and 10.9 % salt content) and chicken meatballs, were performed in triplicate.

At University of Salerno, electrical conductivity measurements were performed using MEF heating system and rectangular treatment cell described in section 4.4.2. The filling of the treatment cell was faithful to the description carried out in section 4.5. Measurements were carried out considering a target time of 4 minutes for the homogeneous system RPFNB and 2.33 minutes for the homogeneous system RPFB. Experimental electrical conductivity measurements were performed in triplicate at 30 V and 50 Hz.

4.7 *Electrical conductivity treatment cells calibration*

This section deals calibrations of cylindrical cell used to perform electrical conductivity measurements at University College Dublin and rectangular and cylindrical cell calibrations designed and used at University of Salerno.

4.7.1 *Cylindrical cell calibration (UCD)*

Before performing experimental tests, the cylindrical treatment cell used at UCD, was calibrated. Five aqueous KCl solutions at 0.05 M, 0.15 M, 0.25 M, 0.35 M, 0.50 M were heated with MEF. Voltage and current experimental values were recorded at 25 °C. For each KCl aqueous solution, three replicates were performed. Knowing, from experimental, voltage and current values, and knowing the electrical conductivity values from literature (Vanýsek, 1998), the conductivity cell constant K , given by the ratio L/A (see section 4.6), was calculated for each KCl composition. In **Table 4.11** are reported obtained cell constant values. For each KCl solution an average value of K , obtained from the three replicates, is reported.

Table 4.11 *Electrical conductivity and K values of KCl aqueous solutions.*

KCl [M]	$\sigma_{literature}$ [S/cm] (Vanýsek, 1998)	$K_{average}$ [1/cm]
0.05	0.0067	0.50 ± 0.002
0.15	0.0174	0.58 ± 0.001
0.25	0.0283	0.58 ± 0.005
0.35	0.0393	0.63 ± 0.008
0.50	0.0592	0.65 ± 0.01

Subsequently, cell calibration was validated using NaCl solutions at 0.02, 0.05 and 0.17 M. Voltage and current experimental values were recorded at 25 °C. Electrical conductivity of NaCl solutions was calculated from eq. (4-2) (section 4.6) using the average value (0.59 1/cm) of the cell constant values evaluated above (**Table 4.11**). Obtained electrical conductivity values were compared with those in Vanýsek (1998). In **Table 4.12** are reported obtained electrical conductivity values for each NaCl composition. In particular, for each NaCl formulation, an average value of σ , obtained from the three replicates, is reported.

Table 4.12 *Comparison between experimental and literature electrical conductivity values of NaCl aqueous solution.*

NaCl [M]	$\sigma_{average}$ [S/cm]	$\sigma_{literature}$ [S/cm] (Vanýsek, 1998)
0.02	0.0026 ± 0.00002	0.0023
0.05	0.0057 ± 0.00003	0.0055
0.17	0.0180 ± 0.00002	0.0180

4.7.2 Rectangular cell calibration (UNISA)

At University of Salerno, to carry out calibration of rectangular treatment cell, five aqueous NaCl solutions at 0.4% [w/v], 0.8% [w/v], 1.2% [w/v], 1.6% [w/v] and 2.0% [w/v] were heated with MEF. Obtained voltage and current experimental values were recorded at 25 °C. For each NaCl solution

were performed three replicates. Obtained electrical conductivity experimental values were compared with literature ones (**Table 4.13**).

Table 4.13 Comparison between experimental and literature electrical conductivity values for rectangular treatment cell calibration.

NaCl [%]	$\sigma_{experimental}$ [mS/cm]	$\sigma_{literature}$ [mS/cm] (Poisson, 1980)
0.4	7.2 ± 0.0	7.5
0.8	14.1 ± 0.0	14.3
1.2	21.3 ± 0.1	20.8
1.6	27.1 ± 0.1	27.1
2.0	32.0 ± 0.2	33.0

4.7.3 Cylindrical cell calibration (UNISA)

For cylindrical treatment cell designed at Unisa, calibration was performed using three aqueous solutions at 1% [w/v], 1.5% [w/v] and 2% [w/v] heated with MEF. Obtained experimental values of current and voltage were recorded at 25 °C. For each NaCl solution, tests were performed in three replicates. For the calibration, experimental and literature electrical conductivity values were compared (**Table 4.14**).

Table 4.14 Comparison between experimental and literature electrical conductivity values for cylindrical treatment cell calibration.

NaCl [%]	$\sigma_{experimental}$ [mS/cm]	$\sigma_{literature}$ [mS/cm] (Poisson, 1980)
1	17.1 ± 0.0	17.6
1.5	24.8 ± 0.1	25.6
2	32.5 ± 0.2	33.0

4.8 Statistical Analysis

Statistical analysis was carried out utilizing one- way analysis of variance (ANOVA) in Excel (Microsoft Office 2010 Professional Plus, Microsoft Corporation, New Mexico, USA). When ANOVA revealed significant differences ($P < 0.05$) Tukey pairwise comparison test was performed.

Obtained results show a standard deviation less or equal to 5%.

4.9 Summary

The chapter deals the raw materials, equipment and methods used to perform MEF heating experiments on homogeneous and heterogeneous food systems, composed by only reconstituted potato flakes and reconstituted potato flakes and meatballs respectively, with different compositions and system configurations, at University College Dublin. Moreover, the design, materials and methods related to MEF equipment realized and utilized to carry out MEF heating experimental tests on homogeneous and heterogeneous food systems, composed by only reconstituted potato flakes and reconstituted potato flakes and meatballs at different compositions and system configurations, at University of Salerno are discussed.

5 MEF heating: results and discussions

Chapter 5 deals results obtained from the experimental work carried out at University College Dublin. The main purpose of the work was to evaluate MEF heating feasibility of a heterogeneous food system composed by reconstituted potato flakes (at different compositions) and meatballs. Four different configurations of chicken meatball in reconstituted potato flakes were analyzed. The MEF heating behavior of a homogeneous food system, constituted by reconstituted potato flakes (at different compositions), was examined too. Moreover, electrical conductivity measurements of reconstituted potato flakes and meatballs are reported too.

5.1 Electrical conductivity of chicken meatballs and RPF

Electrical conductivity of chicken meatballs, from 31 °C to 75 °C, and RPF (5.7% and 10.9% salt content) from 5 °C to 75 °C is shown in **Figure 5.1**.

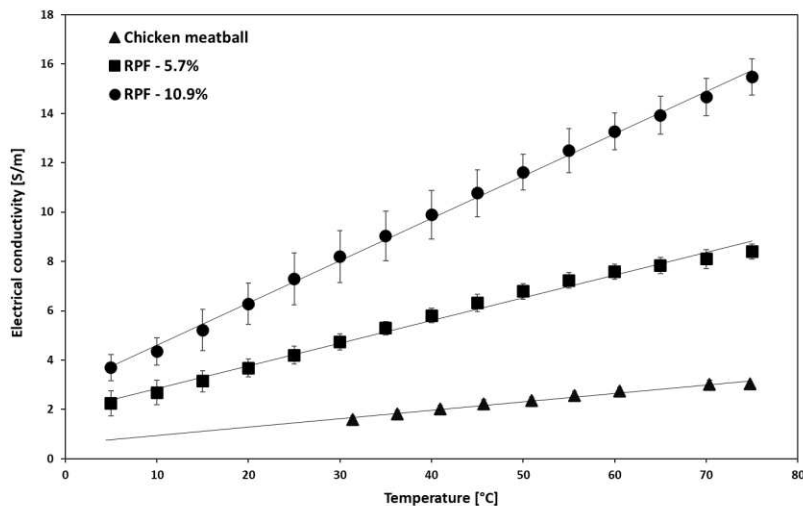


Figure 5.1 Electrical conductivity of chicken meatballs and RPF at 5.7% and 10.9% salt content (20 V, 50 Hz).

As shown in **Figure 5.1**, electrical conductivity of reconstituted potato flakes, at 5.7% and 10.9% salt content, and chicken meatball exhibit a linear increase with respect to temperature. The electrical conductivities of chicken meatball ranging between 1.59 ± 0.15 S/m, at 31 °C, and 3.03 ± 0.16 S/m at 75 °C, values in good agreement with Zell, Lyng, Cronin, & Morgan (2009b). Cited authors performed electrical conductivity measurements for different types of meats (beef, pork, lamb, chicken and turkey) and reported a linear increase of σ versus temperature. In the cited paper, electrical conductivity values of chicken meat, with 0.21% salt content, were about 0.6 S/m, at 5 °C, and 1.50 S/m at 75 °C. In the present experimental work, salt content of chicken meatball was 1.6% and, therefore, the electrical conductivity values are mostly in agreement, being slightly higher than σ values found in literature.

For reconstituted potato flakes at 5.7% salt content, electrical conductivity values were found ranging between 2.25 ± 0.52 , at 5 °C, and 8.39 ± 0.31 , at 75 °C; at 10.9% salt content, instead, electrical conductivity was between 3.7 ± 0.53 , at 5 °C, and 15.49 ± 0.73 , at 75 °C. This means that electrical conductivity values for RPF increased with temperature and salt content. These obtained results are in agreement with previous literature works: Marcotte, Trigui, & Ramaswamy (2000) carried out experimental estimations on four hydrocolloid solutions, prepared in water varying the amount of salt from 0.25% to 1%, applying a voltage gradient of about 7 V cm^{-1} . Authors stated that electrical conductivity values increased with temperature and salt content.

In **Errore. L'origine riferimento non è stata trovata.** are reported the linear regressions of electrical conductivity versus temperature for RPF at 5.7% and 10.9% salt content and chicken meatballs.

Table 5.1 Linear regression of electrical conductivity (S/m) in function of temperature (°C).

Product	σ [S/m]	R^2
RPF – 5.7% salt	$0.0920 T + 1.9226$	0.9897
RPF – 10.9% salt	$0.1715 T + 2.8874$	0.9979
Chicken meatballs	$0.0340 T + 0.6087$	0.9829

5.2 Temperature-time profile of MEF heating

in homogeneous system

Temperature-time evolutions are discussed using a centred definition for a reduced temperature, defined as follows:

$$T_{red} = \frac{T - T_0}{T_{sat} - T_0} \quad (5-1)$$

where T is the punctual temperature, T_0 the initial temperature and T_{sat} is fictitious saturated temperature (100 °C).

System configuration and reconstituted potato flakes formulations used for this study are reported in section 4.3.

The temperature- time evolution at key points P1, P2 and P3 for homogeneous RPF systems at 5.7% and 10.9% salt content, heated using RP configuration (section 4.3), are reported in **Figure 5.2**.

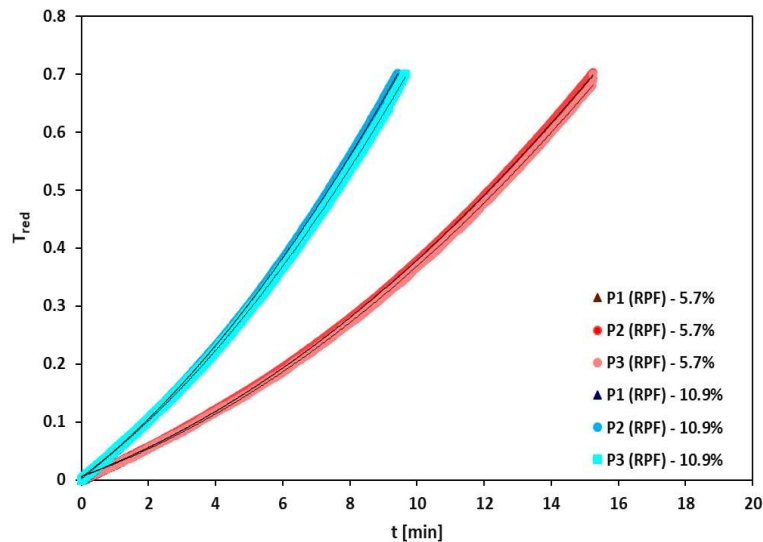


Figure 5.2 Temperature- time evolution in key points (P1, P2 and P3) of the homogeneous system RPF at 5.7% and 10.9% salt content (30 V, 50 Hz).

For each salt content, the three investigated points follow similar temperature evolutions (results related to 10.9% salt content fall under the blue coloured lines, the ones related to 5.7% salt content remain comprised in the red tone lines) and, therefore, RPF samples undergo uniform heating. This uniformity can be clarified considering that reconstituted potato flakes, to both considered compositions, are homogeneous, in terms of electrical and thermo-physical properties and spatial potential distribution. RPF at 10.9% salt content, having higher electrical conductivity, heat faster than reconstituted potato flakes with lower salt content (5.7%), reaching the target temperature of 72 °C in 9 min and 51 s; the second ones (5.7% salt content), instead, need 15 min and 24 s. It is easy to conclude that salt content affects the MEF heating and thus the processing time of the system: the higher the

quantity of salt in the foodstuff, the higher the amount of ions that move from an electrode towards the other one and, thus, higher is the electrical conductivity that, together with the local potential variation, affects the power generated inside the system.

Obtained curves are in good agreement with other literature works: Marra, Zell, Lyng, Morgan, Cronin (2009) evaluated the heat transfer during MEF heating of RPF. Authors developed a mathematical model and compared experimental results with obtained virtual ones. Applying a voltage gradient of about 9 V cm^{-1} , they considered two different conditions. In the first case, they considered that analyzed sample was thermally insulated ($U=0 \text{ W m}^{-2} \text{ K}^{-1}$); in the second case, instead, they considered heat transfer coefficients between 5 and $100 \text{ W m}^{-2} \text{ K}^{-1}$. With a heat transfer coefficient of $5 \text{ W m}^{-2} \text{ K}^{-1}$, temperature- time evolutions were consistent with those one obtained in this experimental work. This heating behaviour, considering a constant local potential variation due to the sample's uniformity, is caused by the increase of electrical conductivity with respect to temperature.

5.3 Temperature evolution for heterogeneous system with different configurations

Figure 5.3 and **Figure 5.4** show the temperature- time evolutions in key points P1, P2 and P3 of the heterogeneous system 2PSiRP (section 4.3) with RPF at 5.7% and 10.9% salt content.

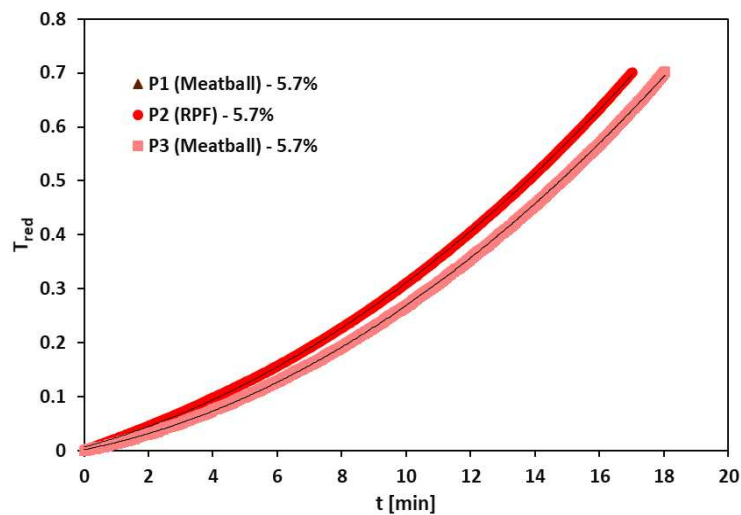


Figure 5.3 Temperature- time evolutions in key points

(P1, P2 and P3) of the system 2PSiRP at 5.7% salt content (30 V, 50 Hz).

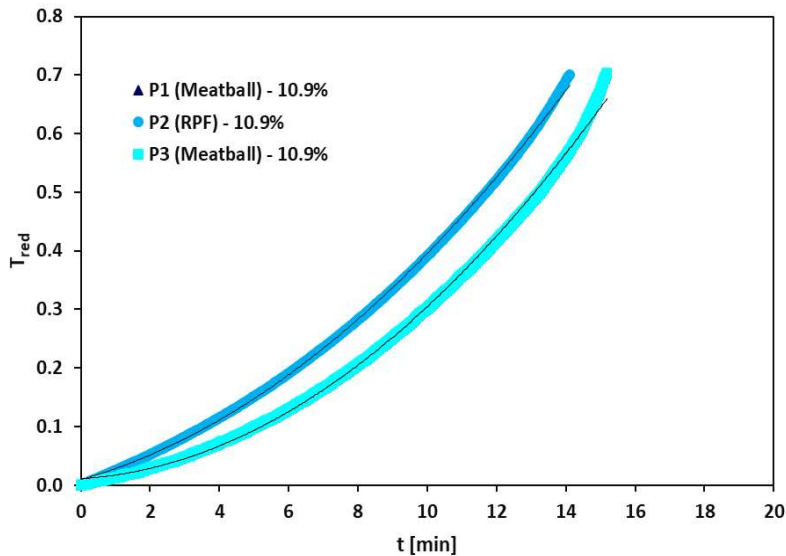


Figure 5.4 Temperature- time evolutions in key points (P1, P2 and P3) of the system 2PSiRP at 10.9 % salt content (30 V, 50 Hz).

When a heterogeneous food system is subjected to MEF heating, the temperature- time evolution of each treated product depends on its electrical conductivity. In this case, respect to the previous situation analyzed, the food products associated to the three key points change, and, consequently, the time to reach the target temperature varies too.

During these experiments the temperature at the meatballs core follow exactly the same temperature evolution (the triangular markers representing the temperature at point P1 are covered by the light blue squared markers representing P3). As shown in **Figure 5.3** and **Figure 5.4**, the temperature-time evolution of the two meatballs (P1 and P3 which temperature evolutions overlap one with each other), followed closely that one of the surrounding RPF, therefore reconstituted potatoes flakes and their composition influence meatballs heating. In both salt compositions (5.7 % and 10.9%), however, the point P2, related to RPF, was heated slightly faster than meatballs. In 5.7% salt content, RPF (P2) reached 72°C in 17 min and 2 s, while meatballs (P1 and P3) needed 18 min and 3 s. At 10.9% salt content, instead, RPF (P2) arrived at 72°C in 14 min and 12 s, while meatballs (P1 and P3) needed 15 min and 18 s. It's easy to see, comparing **Figure 5.3** and

Figure 5.4, that a more significant temperature difference between RPF and meatballs was reached during heating in 10.9% salt content.

In a heterogeneous system, the higher the electrical conductivity of the product, the higher the specific thermal power generated by the MEF system, thus, the quicker the heating. If only the electrical conductivity is taken into account, being that one of RPF higher than that one of meatballs, a quicker heating has to be expected for reconstituted potato flakes with respect to meatballs. Obtained results, instead, exhibit a small temperature difference between the two considered food product: this because, in addition to electrical conductivity, other variables also play a fundamental role and have to be considered. The electrical energy dissipated as heat in the food system is given by the product between the food electrical conductivity and the square value of electrical potential local variation (eq. (2-4)). This means that the specific power source depends on the local variation of the electrical potential more than on the electrical conductivity.

To investigate if meatballs position in RPF can influence them heating, a different configuration was analyzed. Chicken meatballs, in this case, were placed in position P1 and P2 (as in **Figure 4.2**).

Figure 5.5 and **Figure 5.6** show temperature- time evolution of a heterogeneous system composed by two meatballs placed at positions P1 and P2 and RPF, with 5.7% and 10.9% salt content, at position P3, applying 2PAiRP configuration.

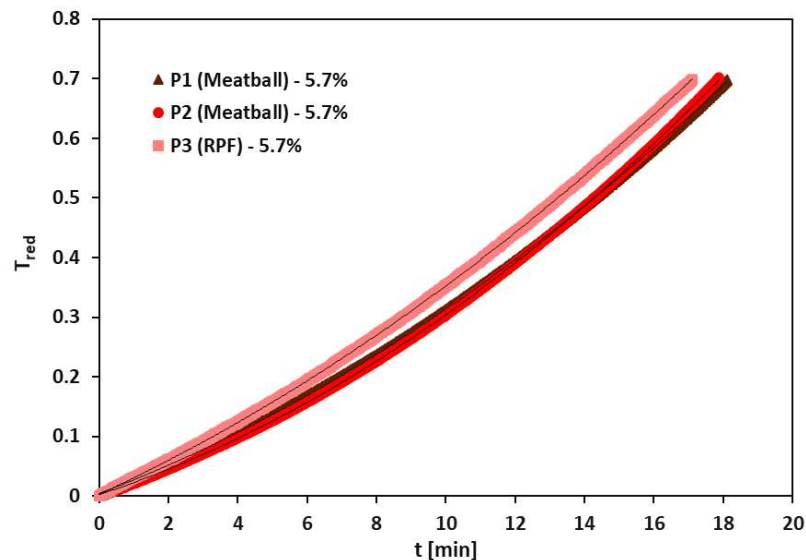


Figure 5.5 Temperature- time evolutions in key points (P1, P2 and P3) of the system 2PAiRP at 5.7 % salt content (30 V, 50 Hz).

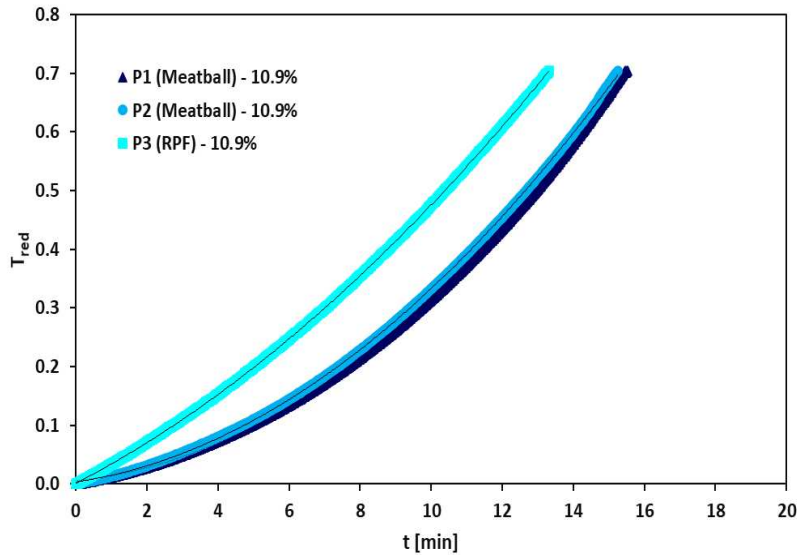


Figure 5.6 Temperature- time evolutions in key points (P1, P2 and P3) of the system 2PAiRP at 10.9 % salt content (30 V, 50 Hz).

By varying the position of the meatballs, consequently, the heating in P1, P2 and P3 changes as a result of the different foodstuffs related to the three key points (meatball instead of RPF in P2 and RPF instead of meatball in P3). Also in this case meatballs heating is affected by RPF composition: the time to reach 72 °C, in case of 5.7% salt content is 18 min for meatballs (P1 and P2), and 17 min and 12 s for RPF (P3), some seconds less than meatballs. In 10.9% salt content, instead, there is a higher difference between meatballs and RPF heating: meatballs reach 72 °C in 15 min and 39 s, instead the RPF in 13 min and 32 s. In any case, the time to reach the target temperature in the meatballs core is about the same in both heterogeneous configurations analyzed until now (2PSiRP and 2PAiRP). Obtained results, therefore, establish that meatball heating is not affected by meatballs position but, probably, it could be influenced by foodstuff geometry: the spherical geometry of meatballs give to them a different and higher local potential variation than the RPF in which they are dispersed. The higher local potential variation in meatballs compensates their lower electrical conductivity values than RPF, generating quite similar power values in the different key points and obtaining, thus, a good heating uniformity in the heterogeneous system.

After confirming the independence of the heating from meatballs position, a new system configuration was analyzed adding a third meatball to the previous configuration (2PAiRP): this new configuration, 3PiRP, had three meatballs positioned in P1, P2 and P3.

As shown in **Figure 5.7** and **Figure 5.8**, also in this case, the temperature- time evolution of the three meatballs follow the same trend and the heating times, for each of the analyzed compositions at 5.7% and 10.9% salt content, were quite similar.

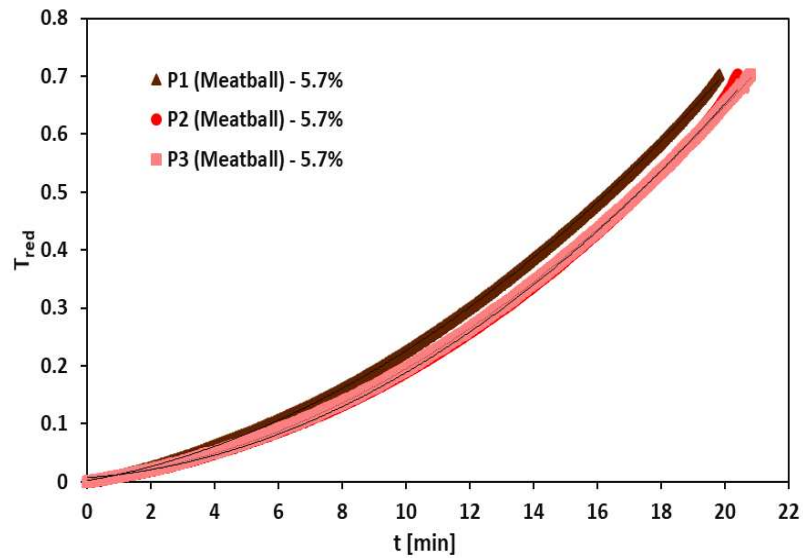


Figure 5.7 Temperature- time evolutions in key points (P1, P2 and P3) of the system 3PiRP at 5.7 % salt content (30 V, 50 Hz).

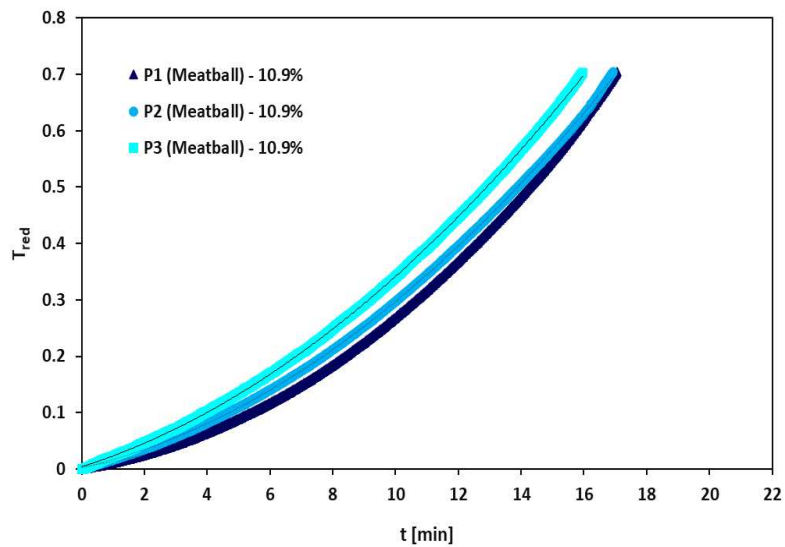


Figure 5.8 Temperature- time evolutions in key points (P1, P2 and P3) of the system 3PiRP at 10.9 % salt content (30 V, 50 Hz).

The time to reach the target temperature in the meatballs core (P1, P2 and P3) is 20 min and 35 s in 5.7% salt content and 16 min and 65 s in 10.7% salt content.

Although meatballs in 5.7% and 10.9% RPF salt content had the same composition (and, thus, the same physical properties) they were heated differently. This behaviour confirms that meatballs are influenced from the surrounding environment, and thus from the different salt content in RPF. Moreover, meatballs heating depends also on the number of meatballs in the system. It is also important to note that the non linear nature of the heating curves is indicative of the increase in electrical conductivity with temperature.

To better understand the dependence of meatballs heating on RPF compositions and type of configuration, a comparison between the processing times is shown in **Table 5.2**.

Table 5.2 Processing time to reach 72°C in meatballs core for the different configurations surrounded by RPF at 5.7% or 10.9% salt content.

Configuration	5.7% salt content	10.9% salt content
	t_{meatball} [min]	t_{meatball} [min]
2PSiRP	18.03± 0.00	15.18± 0.02
2PAiRP	18.00± 0.01	15.39± 0.03
3PiRP	20.35± 0.01	16.65± 0.03

Considering the configurations with the same number of meatballs (2PSiRP and 2PAiRP), both in 5.7% and 10.9% salt content, the time to reach 72 °C in the meatballs core is quite the same (about 18 min at 5.7% salt content and about 15 min at 10.9% salt content), confirming that the meatballs heating is affected by the salt content of the surrounding RPF.

In configuration with three meatballs (3PiRP) the time to reach the target temperature was 20 min and 35 s for 5.7% salt content and 16 min and 65 s for 10.9% salt content. Processing times for 3PiRP are higher than the ones of the previous two analyzed configurations (2PSiRP and 2PAiRP) for both salt compositions: this confirms that the processing time is not influenced by the system configuration, i.e. the position of meatballs, but by the number of meatballs in the system. Moreover from **Table 5.2** is possible to observe that the time to reach the target temperature in meatballs core is always higher if they are dispersed in RPF at 5.7% salt content.

Table 5.3 shows the processing time for both RPF and meatballs at the two different salt contents and configurations analyzed.

Table 5.3 Processing time to reach target temperature in P1, P2, P3 for the different configurations at 5.7% and 10.9% salt content.

Configuration	5.7% salt content			10.9% salt content		
	t_{meatball} [min]	t_{RPF} [min]	Δt [min]	t_{meatball} [min]	t_{RPF} [min]	Δt [min]
RP	-	15.24 \pm 0.00	-	-	9.51 \pm 0.00	-
2PSiRP	18.03 \pm 0.00	17.02 \pm 0.01	1.01	15.18 \pm 0.02	14.12 \pm 0.01	1.06
2PAiRP	18.00 \pm 0.01	17.12 \pm 0.00	0.88	15.39 \pm 0.03	13.32 \pm 0.01	2.07
3PiRP	20.35 \pm 0.01	-	-	16.65 \pm 0.03	-	-

Considering the difference between the processing time for RPF and meatballs (in different configurations), there is a good compromise in salt content for RPF: in 5.7%, the difference of heating time between RPF and meatballs remains below 1 min and 01s; in 10.9% salt content the heating time is reduced by about 20% for RPF and by about 16% for meatballs, but the difference between their time processing increases up to 2 min and 7 s.

5.4 Effect of different applied voltages on temperature- time evolution in heterogeneous system

The impact of different applied voltages (20 V, 30 V and 40 V) on temperature- time evolution of the heterogeneous system 2PSiRP at 5.7% salt content was investigated. **Figure 5.9** and **Figure 5.10** show temperature-time evolutions in P3 (meatball) and P2 (RPF), varying the applied voltage.

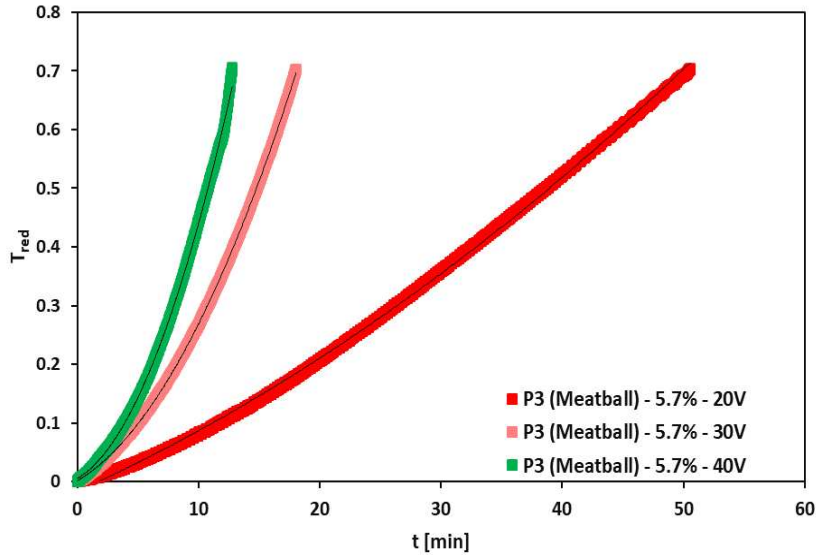


Figure 5.9 Temperature-time evolution in meatball core (P3) of the system 2PSiRP at 20 V, 30 V, 40 V and 5.7% salt content.

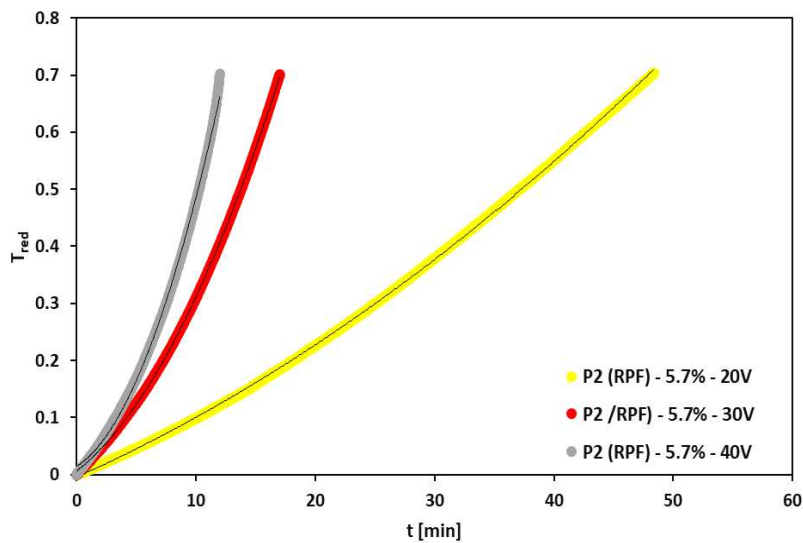


Figure 5.10 Temperature-time evolution in RPF (P2) of the system 2PSiRP at 20 V, 30 V, 40 V and 5.7% salt content.

The temperature- time evolutions in the examined points P3 and P2 show different slopes (dT/dt) in line to applied voltage: the higher the applied voltage, the greater the slope of the curves. As a consequence, therefore, the

time processing to reach the target temperature can be reduced increasing the applied voltage. In particular, the time required to reach 72 °C in the meatball core was 50 min and 55 s, 18 min and 03 s and 12 min and 77 s, whereas RPF needed 48 min and 40 s, 17 min and 02 s and 12 min, respectively at 20 V, 30 V and 40 V.

Obtained results are consistent with several literature works. Darvishi, Khostaghaza & Najafi (2013) evaluated the effect of MEF heating on pomegranate juice applying voltage gradients of 30, 35, 45 and 55 V/cm. Authors stated that as the voltage gradient increased, the processing time reduced. De Halleux, Piette, Buteau, & Dostie (2005) evaluated MEF cooking of Bologna ham applying a voltage of 64, 76, and 103 V. They observed a considerable reduction in treatment time as the applied voltage increased.

Table 5.4 *Errore. L'origine riferimento non è stata trovata.* shows the specific power source (W m^{-3}) generated by the applied voltage in meatballs core and RPF of the system 2PSiRP in 5.7% salt content.

Table 5.4 *Specific power source in RPF and meatballs core of the system 2PSiRP at 20 V, 30 V, 40 V and 5.7% salt content.*

Applied voltage [V]	$Q_{\text{GEN}} \cdot 10^{-6} [\text{W/m}^3]$	
	Meatball	RPF
20	0.97	0.86
30	2.94	2.53
40	4.68	4.21

Results show that an increase of the applied voltage from 20 V to 30 V triples the specific power source in both meatballs and RPF. A further increase of the applied voltage from 30 V to 40 V conduces to an increase of specific power source of about 65% for meatballs and 67% for RPF.

Being the tested system heterogeneous, it was interesting to analyse the thermal behaviour at the interface between meatball and RPF. For this reason, the temperature on meatball surface was recorded for the configuration 2PSiRP in 5.7% and 10.9% salt content, in position P1.

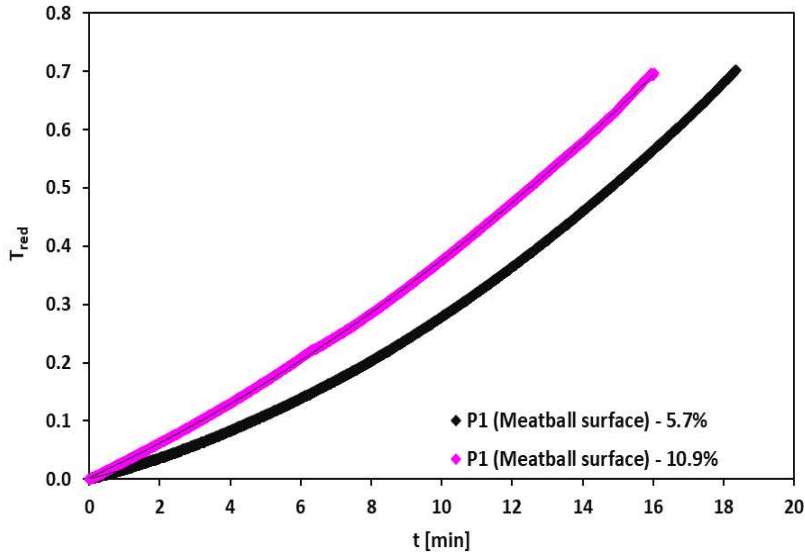


Figure 5.11 Temperature-time evolution on the surface of meatball in key point P1 of the system 2PSiRP in RPF containing 5.7% and 10.9% salt content (30 V, 50 Hz).

As shown in **Figure 5.11** the temperature- time evolution on the surface of the meatball is affected by the salt content of the surrounding RPF. At 5.7% the time to reach 72°C on the meatball surface is 18 min and 35 s, instead at 10.9% salt content is 16 min and 2 s. Obtained results are in good agreement with the previous obtained data: the higher the RPF salt content in which meatballs are dispersed, the higher the electrical conductivity and, thus, the shorter the heating time to reach 72°C.

Comparing temperature- time evolutions of the system 2PSiRP in 5.7% salt content (**Figure 5.3**) with the ones in **Figure 5.11**, the time to reach the target temperature in meatballs core is similar to that of the meatball surface (respectively, 18 min and 3 s and 18 min and 35 s), confirming a good uniform heating. RPF, instead, heats faster (17 min and 2 s) than meatball core and surface. Considering 10.9% salt content, the time to reach 72°C in meatball core, **Figure 5.4**, and meatball surface **Figure 5.11**, is quite the same also in this case (respectively, 15 min and 18 s and 16 min). In the same way, RPF heats faster (14 min and 12 s) than meatball core and surface.

This experimental study confirms that the heating uniformity of a heterogeneous food system subjected to MEF heating can be obtained with the appropriate differentiation of the electrical conductivity of the system constituents. In this particular case, the best heating uniformity can be

achieved with a heterogeneous food system composed by RPF and meatballs in 5.7% salt content.

5.5 Power density generated in MEF heating

In MEF heating the time necessary to reach a specific temperature, and thus the heating rate of the system, depends on the power generated in the food product, which depends, in turn, on the on the electrical conductivity of the product and on the square value of the local variation of the electrical potential, as shown in eq. (2-4).

The evaluation of power generated inside the meatballs, for the different compositions and configurations, is shown in **Table 5.5**.

Table 5.5 Specific power source generated inside meatballs for the different configurations in 5.7% and 10.9% salt content.

Configuration	RPF 5.7%	RPF 10.9%
	$Q_{GEN} \cdot 10^{-6}$ [W/m ³]	$Q_{GEN} \cdot 10^{-6}$ [W/m ³]
2PSiRP	2.94	4.19
2PAiRP	2.66	3.79
3PiRP	2.82	3.31

The specific power source generated inside meatballs in RPF at 5.7% salt content is always smaller than the ones at 10.9% salt content. Having the meatballs the same electrical conductivity, this means that the higher the amount of salt in RPF in which meatballs are dispersed, and the higher the local variation of the electrical potential inside the meatballs.

As shown in **Table 5.6**, the specific power source generated in meatballs and RPF at 5.7% salt content in 2PSiRP and 2PAiRP configurations is quite similar, confirming that the heating uniformity between meatballs and reconstituted potato flakes is due to the higher local variation of the electrical potential inside the meatballs which compensates their lower electrical conductivity than potatoes.

Table 5.6 Specific power source in meatballs core and RPF, at 5.7% salt content, of the systems 2PSiRP and 2PAiRP.

Configuration	Meatballs core	RPF
	$Q_{GEN} \cdot 10^{-6}$ [W/m ³]	$Q_{GEN} \cdot 10^{-6}$ [W/m ³]
2PSiRP	2.94	2.53
2PAiRP	2.66	2.26

5.6 *Summary*

In this chapter, the MEF heating suitability of a heterogeneous food system composed by chicken meatballs, in four different configurations, dispersed in reconstituted potato flakes at two different salt contents (5.7% and 10.9%) has been discussed.

Obtained results, showed that MEF can heat uniformly food products with quite different electrical conductivity values. In particular, in the analyzed system, meatballs dispersed in RPF at 5.7% salt content, heated similarly to RPF. In case of RPF at 10.9% salt content, lower the time required to reach the target temperature but the larger the extent of the heating difference between meatballs and RPF, which is indicative of a less uniform heating. Results showed also that meatballs heating time did not depend on their relative position, though it was affected by the number of meatballs in the system. The best heterogeneous system heated resulted that one at 5.7% salt content and it was demonstrated that, considering a range of applied voltages (in this study, 20 V, 30 V and 40 V), an optimal value of applied voltage exists (30 V, in this case). In particular, at 20 V the difference in time-to-target between RPF and meatballs increased, while at 40 V there was not a good compromise between the energy to be supplied (considering the higher voltage of 40 V) and the difference in heating time to reach the target temperature between the two foodstuffs.

6 MEF heating: comparison of homogeneous and heterogeneous food systems

Chapter 6 deals experimental results obtained from the experimental work carried out at University of Salerno. A direct comparison with experimental results obtained from food systems analyzed at University College Dublin (discussed in chapter 5) is examined too.

6.1 MEF heating of homogeneous food system

In this section experimental results obtained by MEF heating of RPFNB and RPFB homogeneous system are discussed. Electrical conductivity measurements for both analyzed systems are discussed too.

Also in this case, temperature-time evolutions are discussed using a centred definition for a reduced temperature (see section 5.2).

System configuration and reconstituted potato flakes formulations used for this study are reported in section 4.3.

6.1.1 MEF heating of homogeneous system RPFNB

In this section results obtained applying MEF heating to the homogeneous food system RPFNB at different salt content and 30 V, 40 V and 50 V are discussed. Electrical conductivity measurements of the system are shown too.

- **Electrical conductivity**

Electrical conductivity of RPFNB (0.37%, 0.74%, 1.39%, 2.75% salt content) at temperature range from 26 °C to 44 °C, is shown in **Figure 6.1**.

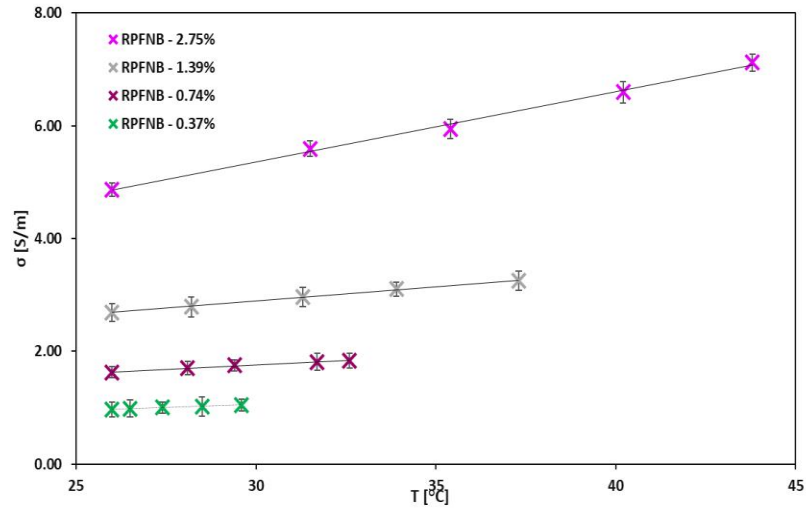


Figure 6.1 Electrical conductivity of RPFNB at 0.37%, 0.74%, 1.39%, 2.75% salt content (30 V, 50 Hz).

As shown in table above, experimental electrical conductivity values increase with temperature and with the amount of salt added during the sample preparation. Also in this case, as in the previous section, obtained results are in good agreement with Marcotte, Trigui & Ramaswamy (2000).

Electrical conductivity data, at 0.37% salt content, ranging between 0.97 ± 0.13 S/m, at 26 °C, and 1.05 ± 0.11 S/m, at 30 °C; at 0.74% salt content electrical conductivity values were between 1.63 ± 0.10 , at 26 °C, and 1.84 ± 0.13 , at 33 °C; at 1.39% salt content electrical conductivity varies between 2.69 ± 0.16 S/m and 3.25 ± 0.17 , in a temperature range from 26 °C to 37 °C; at 2.75% salt content electrical conductivity values ranging between 4.87 ± 0.12 S/m, at 26 °C, and 7.12 ± 0.15 S/m, at 44 °C

In **Table 6.1** are reported the linear regressions of electrical conductivity versus temperature for RPFNB at different salt contents.

Table 6.1 Linear regression of electrical conductivity [S/m] as function of temperature [°C] for the homogeneous system RPFNB.

Product	σ [S/m]	R^2
RPFNB – 0.37% salt	$0.0208T + 0.432$	0.9961
RPFNB – 0.74% salt	$0.0317T + 0.8095$	0.9977
RPFNB – 1.39% salt	$0.0508T + 1.3689$	0.9933
RPFNB – 2.75% salt	$0.1244T + 1.6252$	0.9966

- **Temperature- time evolution of MEF heating applied to homogeneous food system**

In **Figure 6.2**, for a target processing time of 4 minutes, the temperature-time evolution, at measurement point P2 of the homogeneous system RPFNB (0.37%, 0.74%, 1.39%, 2.75% salt content), using RP configuration (section 4.3), is reported.

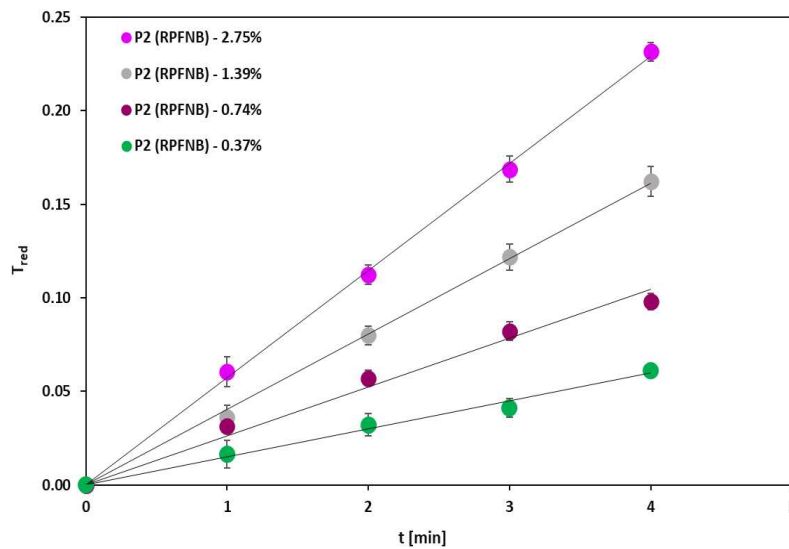


Figure 6.2 Temperature- time evolution in key point P2 of the homogeneous system RPFNB at 0.37%, 0.74%, 1.39%, 2.75% salt content (30 V, 50 Hz).

As shown in figure, at the same processing time, reconstituted potato flakes at higher salt content, having higher electrical conductivity, reach higher T_{red} than reconstituted potatoes with lower salt content. Obtained results, therefore, are in good agreement with what is reported in section 5: MEF heating is affected by the salt content in the system.

A direct comparison between dimensionless temperatures reached at the target time, for RPFNB at different salt contents is shown in **Table 6.2**.

Table 6.2 Comparison of T_{red} reached at target time of 4 minutes for RPFNB at 0.37%, 0.74%, 1.39% and 2.75% salt content.

Sample	Time [min]	T_{red}
RPFNB – 0.37% salt	4	0.06 ± 0.0012
RPFNB – 0.74% salt	4	0.10 ± 0.0044
RPFNB – 1.39% salt	4	0.16 ± 0.008
RPFNB – 2.75% salt	4	0.23 ± 0.005

Linear functions fitting temperature-time evolutions of the analyzed reconstituted potato flakes at different salt contents, are reported in **Table 6.3**.

Table 6.3 Linear regressions of T_{red} as function of time [min] for the homogeneous system RPFNB.

Salt content [%]	T_{red}	R^2
0.37%	$0.015t$	0.9965
0.74%	$0.0262t$	0.9947
1.39%	$0.0404t$	0.9996
2.75%	$0.0573t$	0.9997

Effect of applied voltage on temperature- time distribution

The effect of the applied voltage (30 V, 40 V, 50 V) to the system during MEF heating was investigated in measurement point P2, using RP configuration, for RPFNB at different salt contents (0.37%, 0.74%, 1.39%, 2.75%).

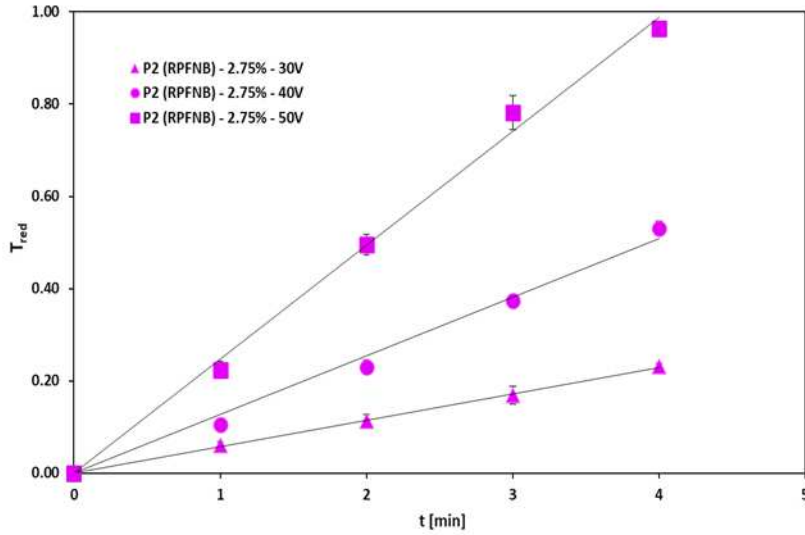


Figure 6.3 Temperature time evolution in key point P2 of the system RPFNB at 30 V, 40 V, 50 V and 2,75% salt content.

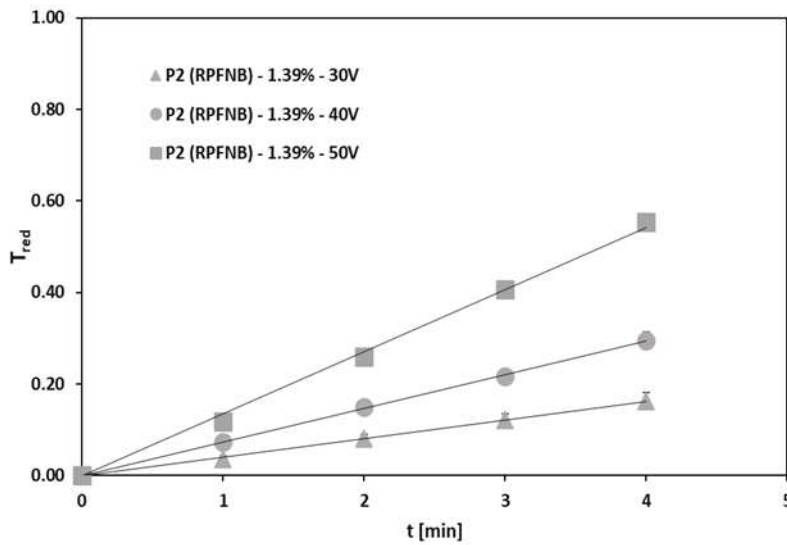


Figure 6.4 Temperature time evolution in key point P2 of the system RPFNB at 30 V, 40 V, 50 V and 1.39% salt content.

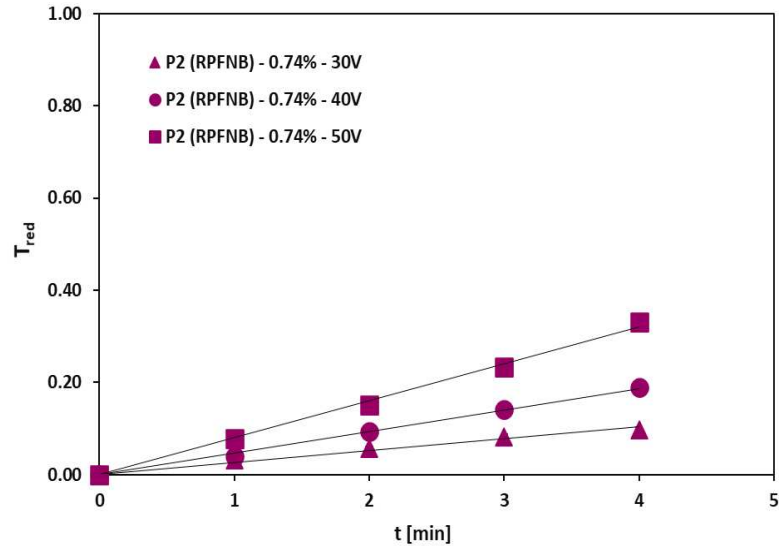


Figure 6.5 Temperature time evolution in key point P2 of the system RPFNB at 30 V, 40 V, 50 V and 0.74% salt content.

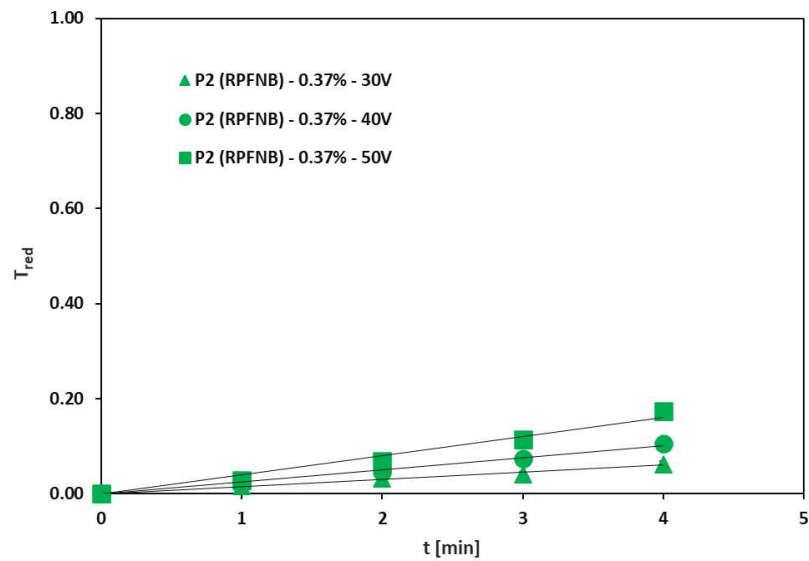


Figure 6.6 Temperature time evolution in key point P2 of the system RPFNB at 30 V, 40 V, 50 V and 0.37% salt content.

As shown in **Figure 6.3**, **Figure 6.4**, **Figure 6.5** and **Figure 6.6**, at each salt composition, as the applied voltage increase, the slope of the curve (dT/dt) increases. Consequently, at a fixed time, increasing the applied

voltage, T_{red} increases in turn. Obviously, as shown in **Table 6.4** higher is the salt content in the system, higher is the applied voltage and, thus, higher is the reached dimensionless temperature.

Table 6.4 *Dimensionless temperature reached at target time of 4 minutes for RPFNB homogeneous system at 0.37%, 0.74%, 1.39%; 2.75 % salt content and 30 V, 40 V, 50 V.*

Salt content	Voltage [V]	T_{red}
0.37%	30	0.06 ± 0.01
	40	0.10 ± 0.01
	50	0.17 ± 0.01
0.74%	30	0.10 ± 0.00
	40	0.19 ± 0.01
	50	0.33 ± 0.00
1.39%	30	0.16 ± 0.02
	40	0.30 ± 0.02
	50	0.55 ± 0.02
2.75%	30	0.23 ± 0.01
	40	0.53 ± 0.02
	50	0.96 ± 0.01

6.1.2 Reconstituted potato flakes with butter (RPFNB)

- **Electrical conductivity**

Electrical conductivity of the homogeneous system RPFNB 0%, 2.9%, 5.7% salt content at temperature ranging from 24 °C to 50 °C is shown in **Figure 6.7**.

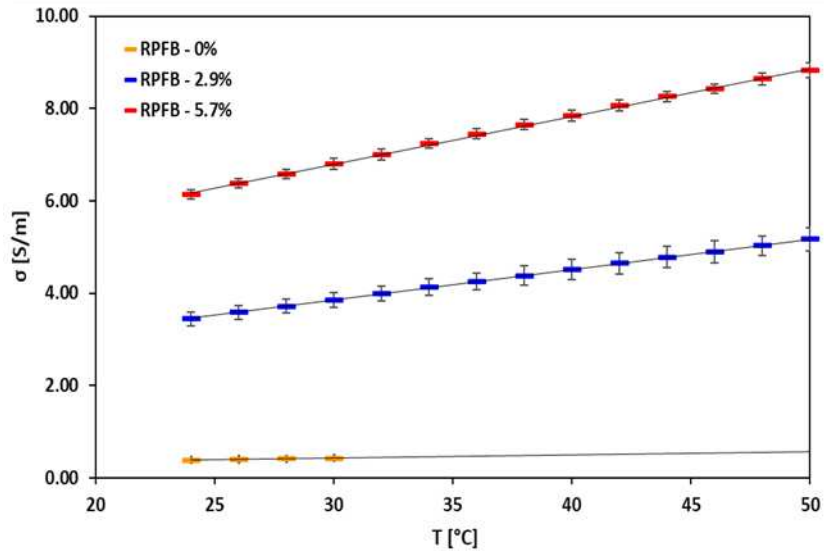


Figure 6.7 Electrical conductivity of RPFB at 0%, 2.9%, 5.7% salt content (30 V, 50 Hz).

At 0 % salt content electrical conductivity varies between 0.39 ± 0.01 , at 24 °C, and 0.43 , at 30 °C; at 2.9% salt content electrical conductivity is 3.44 ± 0.15 , at 24 °C, and 5.17 ± 0.25 , at 50 °C; at 5.7% salt content electrical conductivity ranging between 6.14 ± 0.09 and 8.83 ± 0.16 , at a temperature range from 24 °C to 50 °C

Also, in this case, electrical conductivity values increase with temperature and salt content.

In **Table 6.5** are reported trend curves fitting experimental conductivity values versus temperature for the analyzed homogeneous system.

Table 6.5 Linear regression of electrical conductivity [S/m] as function of temperature [°C] for the homogeneous system RPFB.

Product	σ [S/m]	R^2
RPFB – 0% salt content	$0.0067T + 0.2275$	0.9996
RPFB – 2.9% salt content	$0.066T + 1.8707$	0.9997
RPFB – 5.7% salt content	$0.1033T + 3.7$	0.9992

- **Temperature- time evolution of the homogeneous food system**

In **Figure 6.8** is reported temperature- time evolution, at key points P1, P2, P3 using RP configuration, of the homogeneous system RPFB (0%, 2.9%, 5.7% salt content).

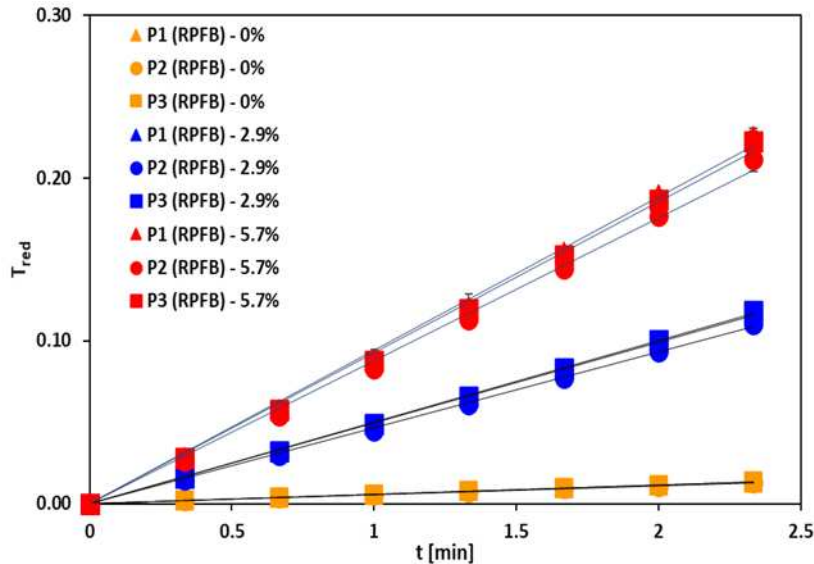


Figure 6.8 Temperature time evolution in key points (P1, P2, P3) of the system RPFNB at 0%, 2.9%, 5.7% salt content (30 V, 50 Hz).

For each investigated salt content, the three key points follow very similar temperature-time evolutions, thus the system RPFNB is subjected to uniform heating. As discussed in section 5, the heating uniformity can be explained considering the uniformity of the sample in terms of electrical, thermo-physical properties and spatial potential distribution.

As shown in figure above, at the same time, T_{red} value increases with increasing salt content. As discussed previously, an higher salt content in the homogeneous system, means higher electrical conductivity values and, thus, higher temperature values are reached. For better clarity, **Table 6.6** shows the dimensionless temperature (T_{red}) values reached at the target time of 2.33 min for the different analyzed salt content.

Table 6.6 Dimensionless temperature reached at target time for the homogeneous system RPFNB at 0%, 2.9% and 5.7% salt content (30 V, 50 Hz).

Salt content	Target time [min]	T_{red}
0%	2.33	0.01 ± 0.00
2.9%	2.33	0.12 ± 0.00
5.7%	2.33	0.22 ± 0.01

In **Table 6.7** are reported trends fitting for temperature-time evolution of the analyzed RPF homogeneous system at different salt contents.

Table 6.7 Linear trend of Θ as function of time [min] for the homogeneous system RPF.

Salt content	T_{red}	R^2
0%	$0.0057t$	1
2.9%	$0.0487t$	0.9998
5.7%	$0.0915t$	0.9991

- **Effect of applied voltage on temperature- time distribution for the homogeneous system RPF**

Figure 6.9, Figure 6.10, Figure 6.11 show the effect of applied voltages (30 V, 40 V, 50 V) to the system RPF at key points P1, P2, P3 and RP configuration, at 0%, 2.9% and 5.7% salt content.

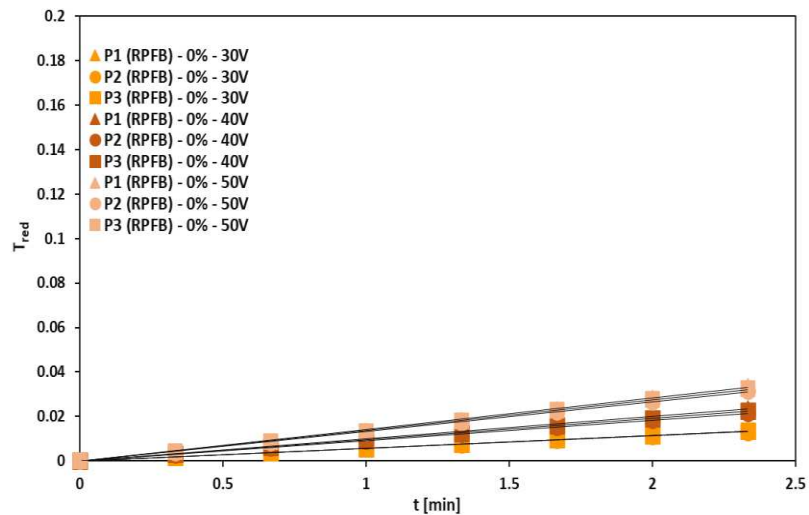


Figure 6.9 Temperature- time evolution in key points P1, P2, P3 of the system RPF at 30 V, 40 V, 50 V and 0% salt content.

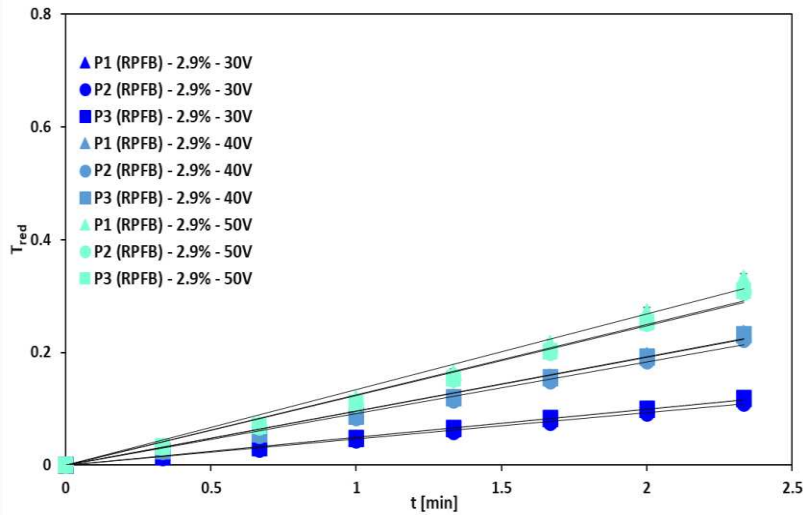


Figure 6.10 Temperature- time evolution in key points *P1*, *P2*, *P3* of the system RPFb at 30 V, 40 V, 50 V and 2.9% salt content.

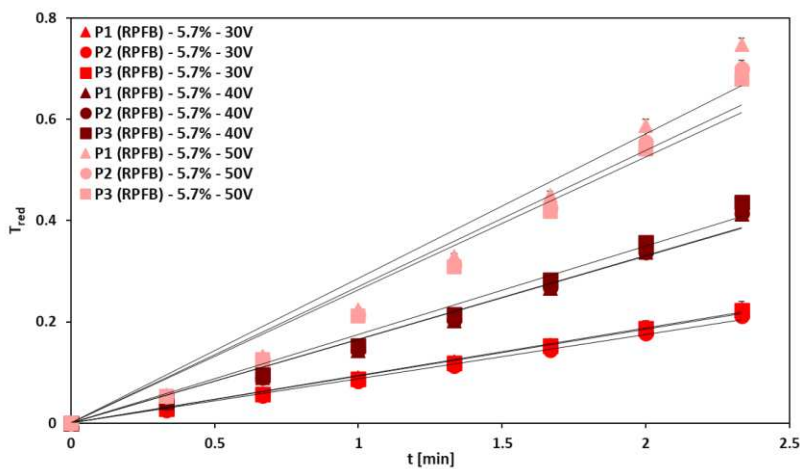


Figure 6.11 Temperature- time evolution in key points *P1*, *P2*, *P3* of the system RPFb at 30 V, 40 V, 50 V and 5.7% salt content.

As shown in figures above, also in this case, at each analyzed composition, increasing the applied voltage, increases the slope of the curve and, thus, the dimensionless temperature reached at a fixed time. A direct comparison between T_{red} reached at target time of 2.33min in function of different voltages is shown in **Table 6.8**.

Table 6.8 Dimensionless temperature reached at target time for RPFB homogeneous system at 30 V, 40 V, 50 V and 0%, 2.9%, 5.7% salt content.

Salt content	Voltage [V]	T_{red}
0%	30	0.01 ± 0.00
	40	0.02 ± 0.00
	50	0.03 ± 0.00
2.9%	30	0.12 ± 0.00
	40	0.23 ± 0.00
	50	0.32 ± 0.01
5.7%	30	0.22 ± 0.01
	40	0.42 ± 0.01
	50	0.71 ± 0.01

6.1.3 Temperature- time evolution comparison

between homogeneous food systems

In **Figure 6.12** a direct comparison of temperature- time evolution for homogeneous systems RPFB and RPF at 5.7% salt content is shown.

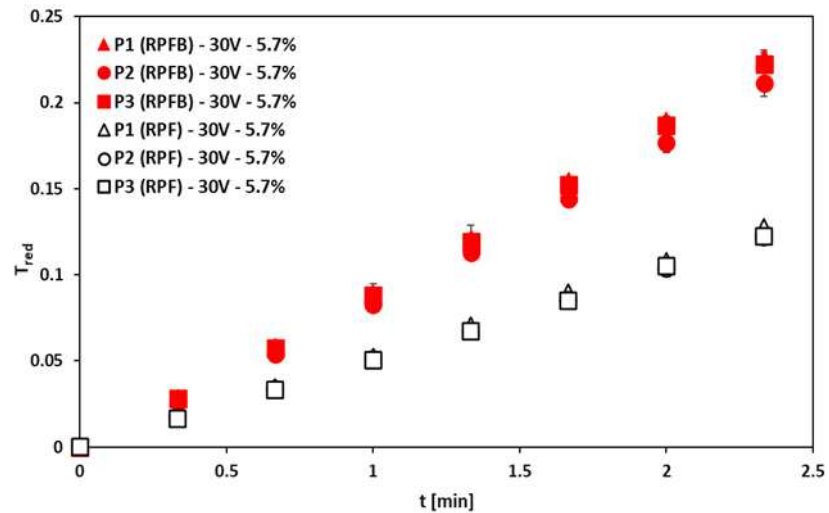


Figure 6.12 Temperature- time evolution comparison between homogeneous systems RPFB and RPF at 5.7% salt content (30 V, 50 Hz).

The two analyzed homogeneous systems (RPFB and RPF) are characterized by the same salt content (5.7%) and, thus, similar electrical conductivity values; consequently, at a fixed processing time, the same temperature had to be expected for both systems. Instead, as shown in figure above, RPFB reach higher T_{red} than homogeneous system RPF. Indeed, RPFB at 2.33 min reach a dimensionless temperature of 0.22 ± 0.01 , instead RPF reach, at the same time, a T_{red} of 0.12 ± 0.01 .

In MEF heating, as mentioned also in section 5, the higher is the electrical conductivity of the system, the higher the specific thermal power generated by MEF and, thus, the greater the heating. Referring to eq. (2-4), considering, as said before, that homogeneous systems have similar electrical conductivities, this means that, as in section 5, the local variation of the electrical potential play a key role.

RPFB and RPF were heated in two different treatment cells having different distances between the electrodes (L); consequently, the two homogeneous systems were subjected to different electric field strengths (**Table 6.9**).

Table 6.9 Distance between the electrodes and electric field strengths applied for the two homogeneous system RPFB and RPF at 5.7% salt content (30 V, 50 Hz).

Sample	L [cm]	Applied voltage [V]	Electric field strength [V/cm]
RPFB	13	30	0.43
RPF	10	30	0.30

As shown in **Table 6.9** RPFB system was subjected to an electric field strength higher (0.43 V/cm) than RPF (0.30 V/cm) and, thus, its greater heating is clarified.

Confirming the above, considering that the heating rate (dT/dt) is represented by the slope of the curve, in **Table 6.10** are shown linear regressions for both homogeneous food system RPFB and RPF.

Table 6.10 Linear functions of T_{red} in function of time [min] for homogeneous systems RPFB and RPF at 5.7% salt content (30 V, 50 Hz).

Sample	T_{red}	R^2
RPFB – 5.7%	$0.0915t$	0.9991
RPF – 5.7%	$0.0524t$	0.9998

As shown in table above, RPFB have a heating rate higher (0.0915 1/s) than RPF (0.0524 1/s), confirming that RPFB is subjected to a quicker heating than RPF.

6.2 MEF heating applied to heterogeneous food system

In this section experimental results obtained heating with MEF heterogeneous system composed by RPFB and meatballs are discussed. In section 4.3 systems configurations, reconstituted potato flakes and meatballs formulations utilized for this experimental study are reported.

Also, in this case, a reduced temperature (eq. (5-1)) has been used.

6.2.1 Temperature- time evolution of MEF heating applied to heterogeneous food system

In **Figure 6.13** and **Figure 6.14** temperature-time evolutions in key points P1, P2, P3 of the heterogeneous system RPFB at 2.9% and 5.7% salt content, using 2PSiRP, configuration are shown.

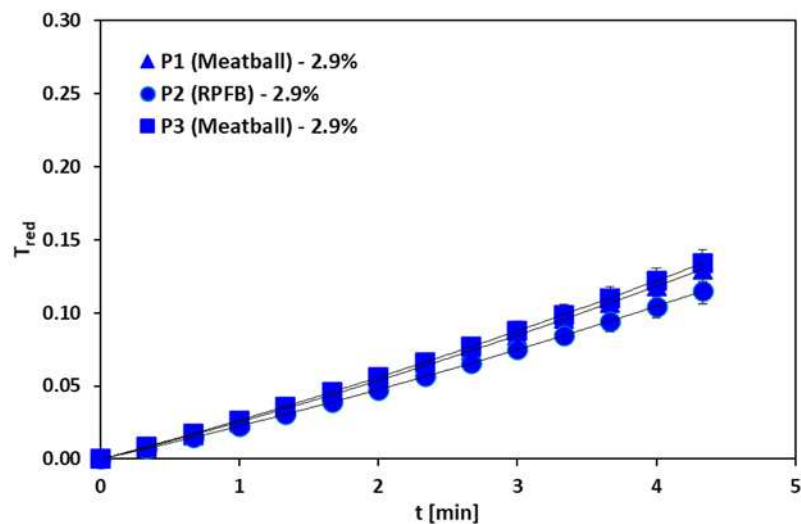


Figure 6.13 Temperature- time evolution in key points P1, P2, P3 of the heterogeneous system RPFB using 2PSiRP at 2.9% salt content (30 V, 50 Hz).

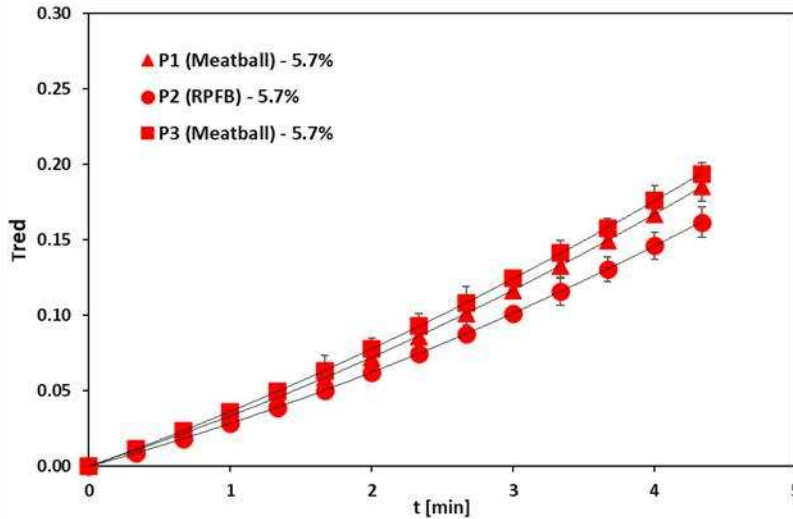


Figure 6.14 Temperature- time evolution in key points P1, P2, P3 of the heterogeneous system RPFB using 2PSiRP at 5.7% salt content (30 V, 50 Hz).

As shown in **Figure 6.13**, RPFB system at 2.9% salt content is subjected to a good uniform heating between mashed potatoes and meatballs. As in section 5, a more consistent difference in temperature between mashed potatoes and meatballs is found at the higher salt content (5.7%) of the heterogeneous system.

At 2.9% salt content, both meatballs, in position P1 and P3, at target time of 4.33, reached a dimensionless temperature of 0.13 ± 0.01 . Reconstituted potato flakes instead reached a T_{red} of 0.11 ± 0.01 . In 5.7% salt content, instead, meatballs, in position P1 and P3, reach 0.19 ± 0.01 , while RPFB arrive to 0.16 ± 0.01 dimensionless temperature.

However, having potatoes higher electrical conductivity than meatballs, makes strange to note that RPFB are subjected to lower heating than meatballs. As also explained previously the electrical energy dissipated in form of heat is affected by the electrical conductivity but, also, by the local variation of electrical potential. Thus, the higher heating of meatballs than potatoes may be related to their higher local potential variation, due probably to their spherical shape and to meatballs proximity to the electrodes. In other words, meatballs could be more affected, than RPFB, by the local variation of the electrical potential. Thus, local variation of potential has a greater impact, compared to electrical conductivity, on the specific power source.

6.2.2 Effect of applied voltage on temperature- time distribution for heterogeneous system with configuration 2PSiRP

In Figure 6.15, Figure 6.16, Figure 6.17,

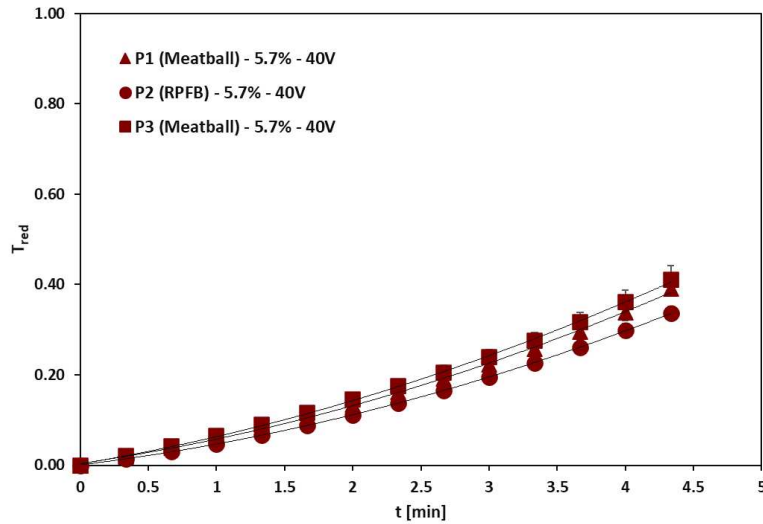


Figure 6.18 the influence of applied voltage (50 V, 40 V) on MEF heating of heterogeneous system RPFb with meatballs, using 2PSiRP, at 2.9% and 5.7% salt content is illustrated.

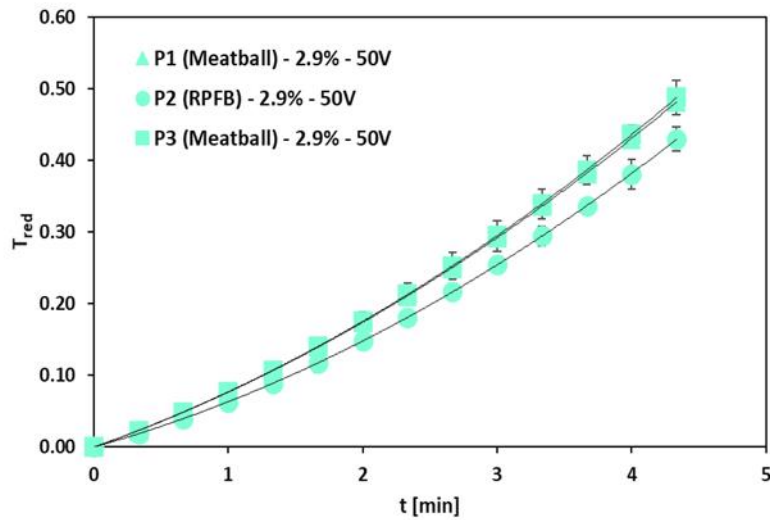


Figure 6.15 Temperature- time evolution in key points P1, P2, P3 of the heterogeneous system RPFb and meatballs (2PSiRP) at 50 V and 2.9% salt content.

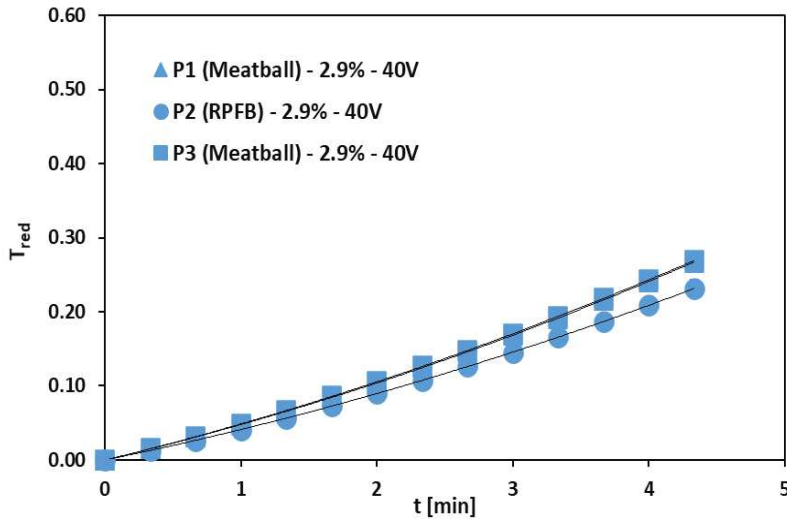


Figure 6.16 Temperature- time evolution in key points P1, P2, P3 of the heterogeneous system RPFb and meatballs (2PSiRP) at 40 V and 2.9% salt content.

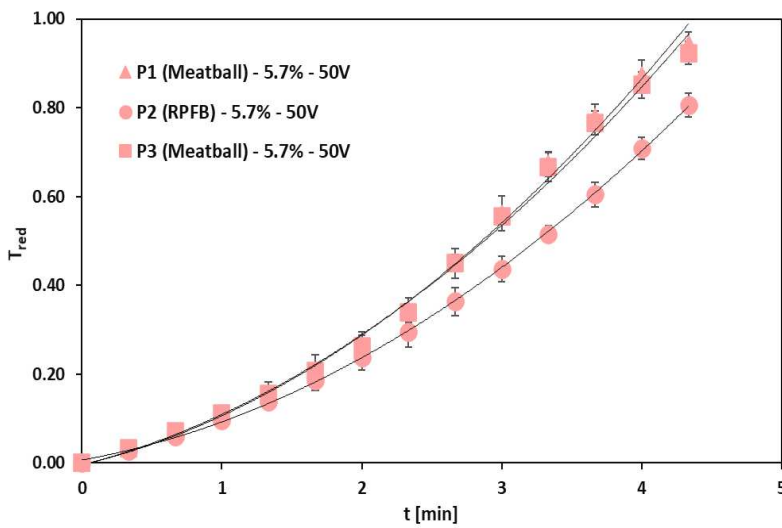


Figure 6.17 Temperature- time evolution in key points P1, P2, P3 of the heterogeneous system RPFb and meatballs (2PSiRP) at 50 V and 5.7% salt content.

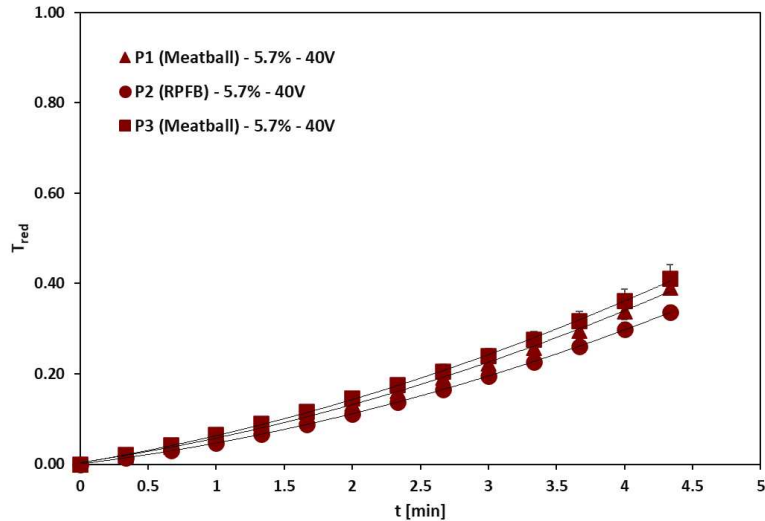


Figure 6.18 Temperature- time evolution in key points *P1*, *P2*, *P3* of the heterogeneous system RPFb and meatballs (2PSiRP) at 40 V and 5.7% salt content.

As shown in figures above, for both analyzed compositions, higher is the applied voltage and higher is T_{red} reached at a fixed time. In other word, at a fixed time, higher the voltage applied and greater the heating. **Table 6.11** show T_{red} reached at target time and different applied voltages for 2.9% and 5.7% salt content.

Table 6.11 T_{red} reached at target time for RPFb heterogeneous system at 30 V, 40 V, 50 V and 2.9%, 5.7% salt content.

Salt content	Voltage [V]	T_{red}		
		Meatball P1	Meatball P3	RPFb
2.9%	30	0.13±0.01	0.13±0.01	0.11±0.01
	40	0.27±0.01	0.27±0.01	0.23±0.01
	50	0.48±0.01	0.49±0.02	0.43±0.02
5.7%	30	0.19±0.01	0.19±0.01	0.16±0.01
	40	0.41±0.02	0.58±0.01	0.42±0.00
	50	0.94±0.03	0.92±0.03	0.81±0.03

As in section 5, meatball position was changed to understand the effect of its position in the heating of the system. For this reason, position 2PAiRP

(see section 4.3) was investigated. In particular, one meatball was changed from position P3 to position P2.

Figure 6.19 and **Figure 6.20** illustrate temperature- time evolutions of the system RPFb with meatballs, in key points P1, P2 and P3, at 2.9% and 5.7% salt content, with 2PAiRP configuration.

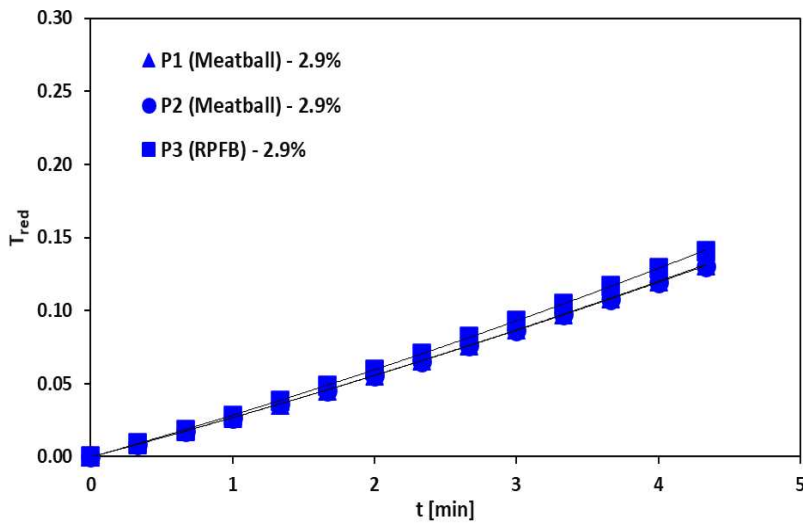


Figure 6.19 Temperature- time evolution in key points P1, P2, P3 of the heterogeneous system RPFb with meatballs, using 2PAiRP configuration, at 2.9% salt content (30 V, 50 Hz).

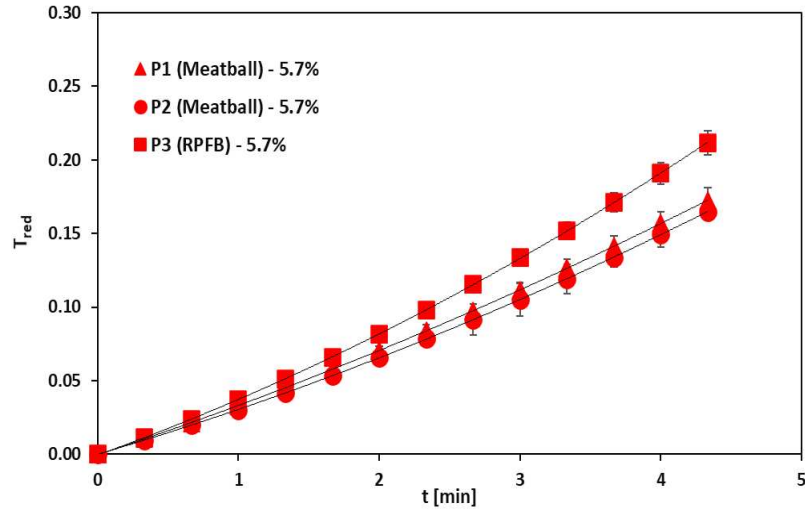


Figure 6.20 Temperature- time evolution in key points P1, P2, P3 of the heterogeneous system RPFB with meatballs, using 2PAiRP configuration, at 5.7% salt content (30 V, 50 Hz).

As shown in figures, at both compositions, meatballs evolutions follow closely the one of mashed potatoes, confirming, also in this case, that meatballs are influenced from the salt content of the surrounding environment. Moreover, as in the previous analyzed configuration, an higher difference in temperature between potatoes and meatballs is shown in 5.7% salt content.

At 2.9% salt content, meatball in position P1 and P2, at target time reach respectively 0.13 ± 0.00 . RPFB, instead, at the same time reach 0.14 ± 0.02 . At 5.7% salt content, instead, meatballs reach 0.17 ± 0.00 , while mashed potatoes 0.21 ± 0.01 . In **Table 6.12** a direct comparison between dimensionless temperatures reached by meatballs at 2.9% and 5.7% salt content, using 2PSiRP and 2PAiRP configuration is shown.

Table 6.12 Dimensionless temperature reached at target time for heterogeneous system using 2PSiRP and 2PAiRP configurations at 2.9% and 5.7% salt content (30 V, 50 Hz).

Configuration	2PSiRP		2PAiRP	
	Meatballs		Meatballs	
	P1	P3	P1	P2
2.9% salt content	0.13 ± 0.01	0.13 ± 0.01	0.13 ± 0.00	0.13 ± 0.00
5.7% salt content	0.19 ± 0.01	0.19 ± 0.01	0.17 ± 0.00	0.17 ± 0.00

Comparing data in table above is possible to observe that, at 2.9% salt content, both analyzed configurations reach the same dimensionless temperature. At 5,7% salt content, the two configurations have 0.02 of difference in dimensionless temperature. Thus, in any case, the temperature reached in meatball core is the same in both analyzed heterogeneous configurations. Obtained results, thus, determine that meatball heating is not affected by their position in the system. Also in this case, is consistent to confirm that meatball heating is influenced by their geometry that give to them a greater variation of local potential variation than potatoes.

Having confirmed that local potential variation is due to meatball geometry and proximity to the electrodes, it would expect that meatball P2 would heat less than meatball P1. Instead, two meatballs, at each salt content, reach the same temperature.

6.2.3 Effect of applied voltage on temperature- time distribution for heterogeneous system with configuration 2PAiRP

In **Figure 6.21**, **Figure 6.22**, **Figure 6.23** Temperature- time evolution in key points P1, P2, P3 of the heterogeneous system RPFb and meatballs (2PAiRP) at 50 V and 5.7% salt content. and **Figure 6.24** the impact of applied voltage (50 V, 40 V) on MEF heating of heterogeneous food system RPFb with meatballs, applying 2PAiRP configuration, at 2.9% and 5.7% salt content is shown.

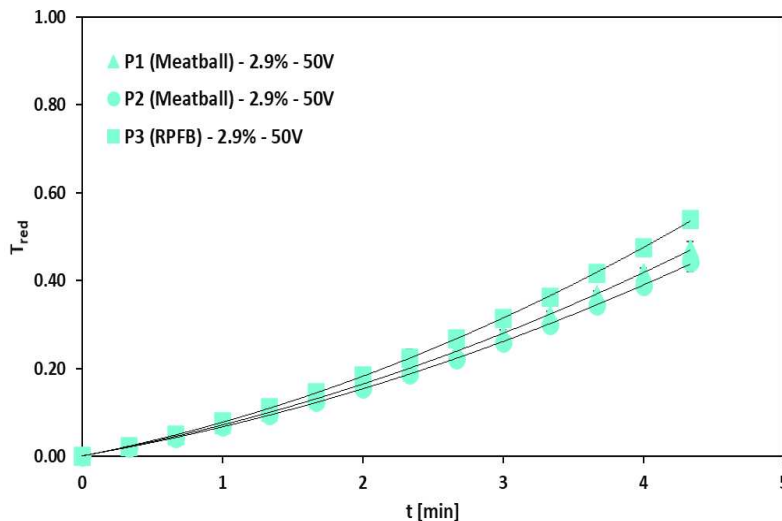


Figure 6.21 Temperature- time evolution in key points P1, P2, P3 of the heterogeneous system RPFb and meatballs (2PAiRP) at 50 V and 2.9% salt content.

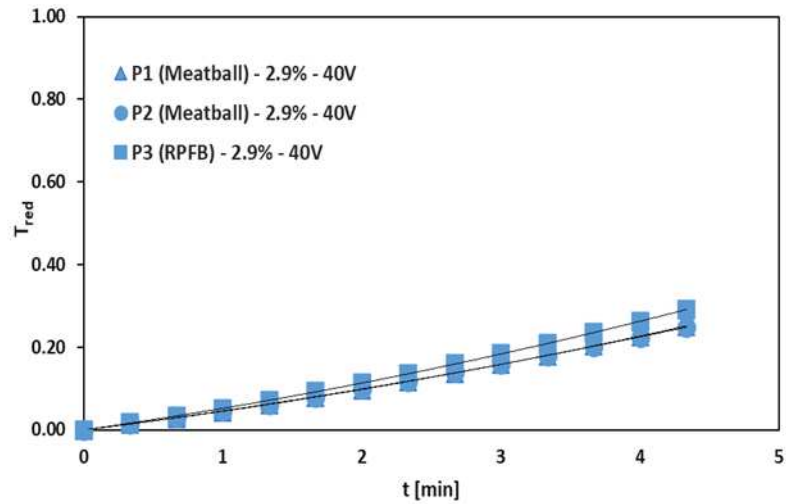


Figure 6.22 Temperature- time evolution in key points P1, P2, P3 of the heterogeneous system RPFB and meatballs (2PAiRP) at 40 V and 2.9% salt content.

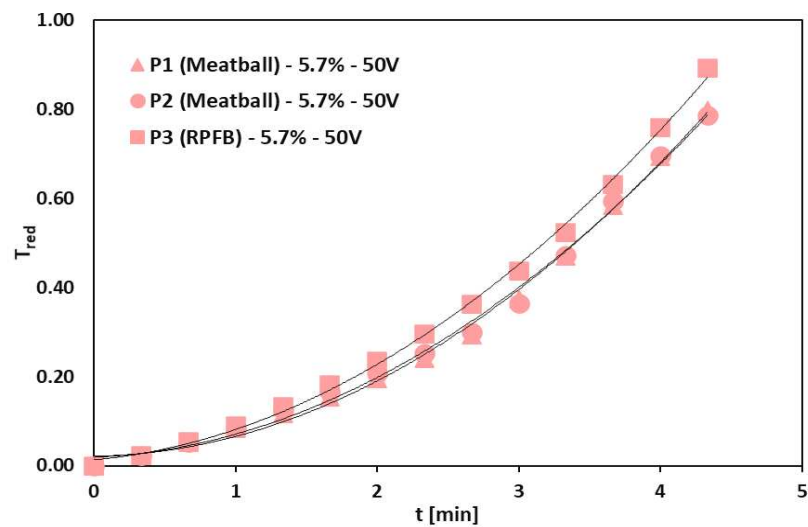


Figure 6.23 Temperature- time evolution in key points P1, P2, P3 of the heterogeneous system RPFB and meatballs (2PAiRP) at 50 V and 5.7% salt content.

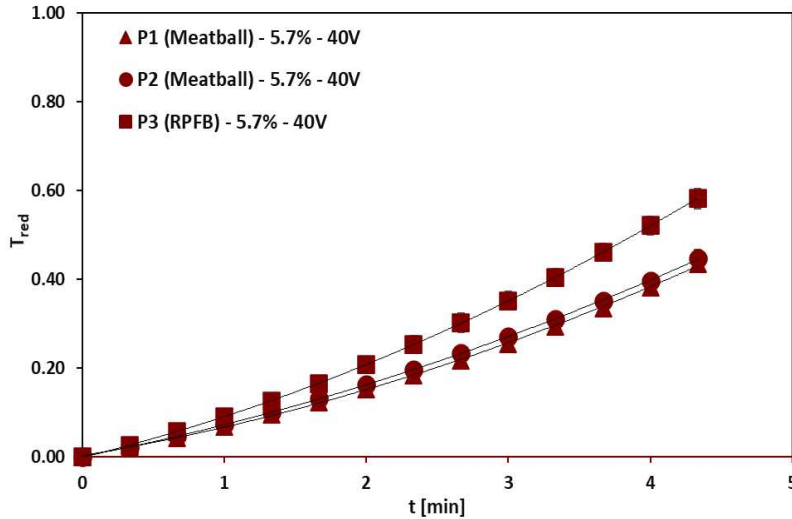


Figure 6.24 Temperature- time evolution in key points *P1*, *P2*, *P3* of the heterogeneous system *RPFB* and meatballs (*2PAiRP*) at 40 V and 5.7% salt content.

Both 2.9% and 5.7% salt contents, increasing the voltage, at a fixed time, exhibit higher dimensionless temperature reached. **Table 6.13** shows different T_{red} reached by heterogeneous food systems analyzed at 2.9% and 5.7% salt content and 30 V, 40 V, 50 V applied voltages.

Table 6.13 T_{red} reached at target time for *RPFB* heterogeneous (*2PAiRP*) system at 30 V, 40 V, 50 V and 2.9%, 5.7% salt content.

Salt content	Voltage [V]	T_{red}		
		Meatball P1	Meatball P3	RPFB
2.9%	30	0.13±0.00	0.13±0.00	0.14±0.02
	40	0.25±0.01	0.25±0.01	0.29±0.01
	50	0.47±0.01	0.44±0.02	0.54±0.06
5.7%	30	0.17±0.00	0.17±0.00	0.21±0.01
	40	0.44±0.01	0.45±0.02	0.58±0.02
	50	0.80±0.00	0.79±0.01	0.89±0.04

A new configuration, having three meatball in position *P1*, *P2* and *P3* was analyzed, to evaluate the effect of the number of meatballs in the system.

Figure 6.25 and **Figure 6.26** show temperature time evolution of the heterogeneous system composed by three meatballs at 2.9% and 5.7% salt content using *3PiRP* configuration.

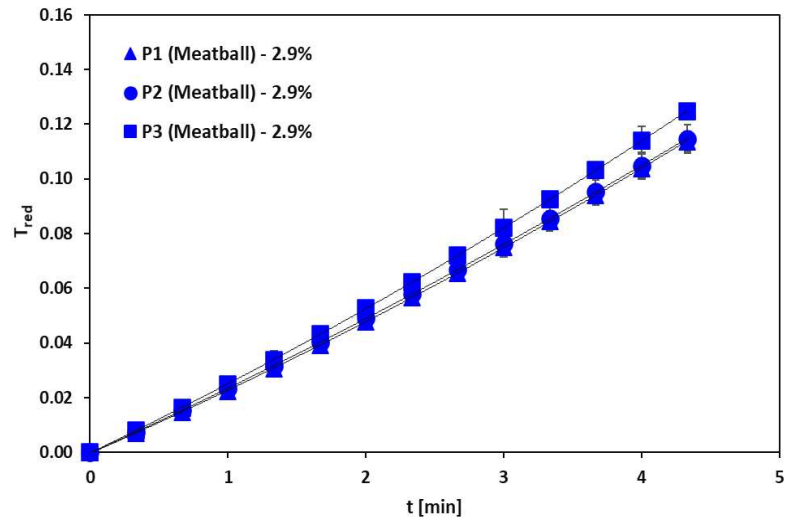


Figure 6.25 Temperature- time evolution in key points P1, P2, P3 of the heterogeneous system RPFb with meatballs, using 3PiRP configuration, at 2.9% salt content (30 V, 50 Hz).

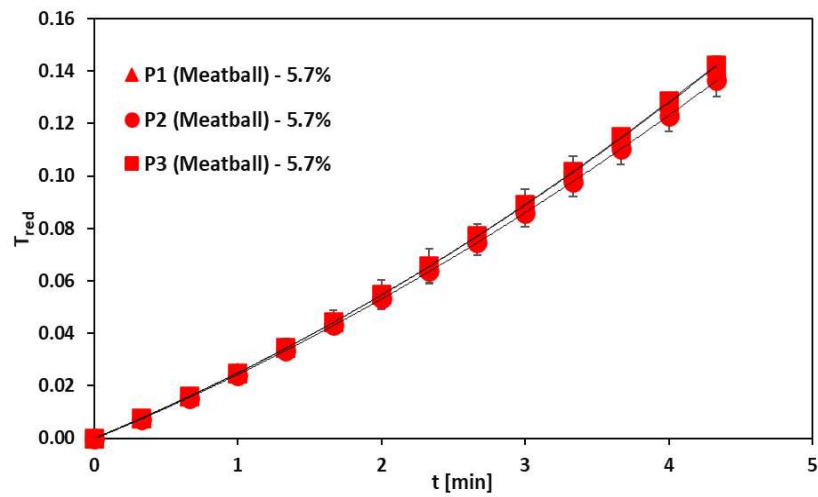


Figure 6.26 Temperature- time evolution in key points P1, P2, P3 of the heterogeneous system RPFb with meatballs, using 3PiRP configuration, at 5.7% salt content (30 V, 50 Hz).

In both analyzed salt compositions, the three meatballs show a good heating uniformity. At 2.9% salt content meatballs, at target time of 4.33 min, respectively in position P1, P2 and P3 reach a dimensionless temperature of 0.11 ± 0.00 , 0.11 ± 0.01 and 0.12 ± 0.00 . At 5.7%, instead, all three meatballs in position P1, P2 and P3 arrive at T_{red} of 0.14 ± 0.00 . Reaching meatballs at 2.9% salt content a lower temperature than meatballs at 5.7% content, also in this case is confirmed the dependence of meatball heating from salt content contained in reconstituted potato flakes in which they are dispersed.

In **Table 6.14** are shown temperature reached at target time of 4.33 min for the different configurations analyzed (2PiRP, 2PAiRP, 3PiRP)

Table 6.14 Comparison between T_{red} at target time for 2PSiRP, 2PAiRP, 3PiRP configurations at 2.9% and 5.7% salt content and 30 V.

	2PSiRP		2PAiRP		3PiRP		
	Meatballs		Meatballs		Meatballs		
Salt content	P1	P3	P1	P2	P1	P2	P3
2.9% salt	0.13 ± 0.01	0.13 ± 0.01	0.13 ± 0.00	0.13 ± 0.00	0.11 ± 0.00	0.11 ± 0.01	0.12 ± 0.00
5.7% salt	0.19 ± 0.01	0.19 ± 0.01	0.17 ± 0.00	0.17 ± 0.00	0.14 ± 0.00	0.14 ± 0.00	0.14 ± 0.00

In case of 3PSiRP configuration, for both analyzed composition, the temperature reached at target time is always lower than other two configurations (2PSiRP, 2PAiRP) confirming that the heating is influenced by the number of meatballs in the system.

Also in this case, considering the proximity of meatballs P1 and P3 to the electrodes an higher heating had to be expected than meatball P2. Meatballs, instead, reach about the same dimensionless temperature.

6.2.4 Effect of applied voltage on temperature- time distribution for heterogeneous system with configuration 3PiRP

The influence of applied voltage (50 V, 40 V) on the heating of the system has been analyzed for the heterogeneous system RPFb with meatballs at 2.9% and 5.7% salt content, applying configuration 3PiRP.

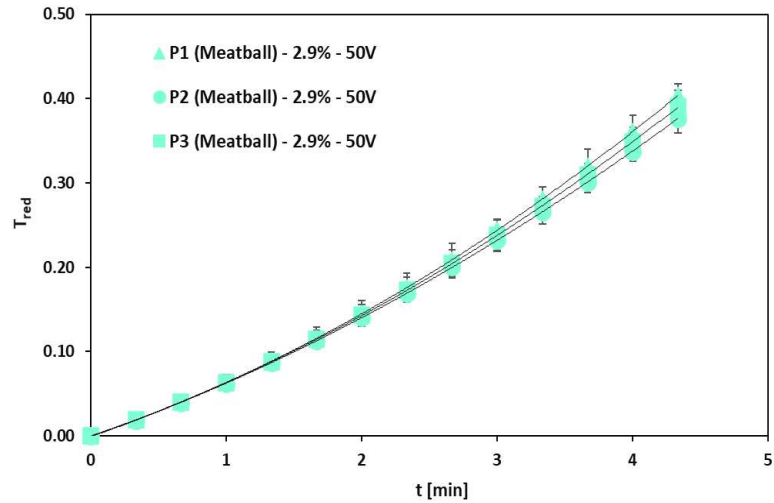


Figure 6.27 Temperature- time evolution in key points P1, P2, P3 of the heterogeneous system RPFB and meatballs (3PiRP) at 50 V and 2.9% salt content.

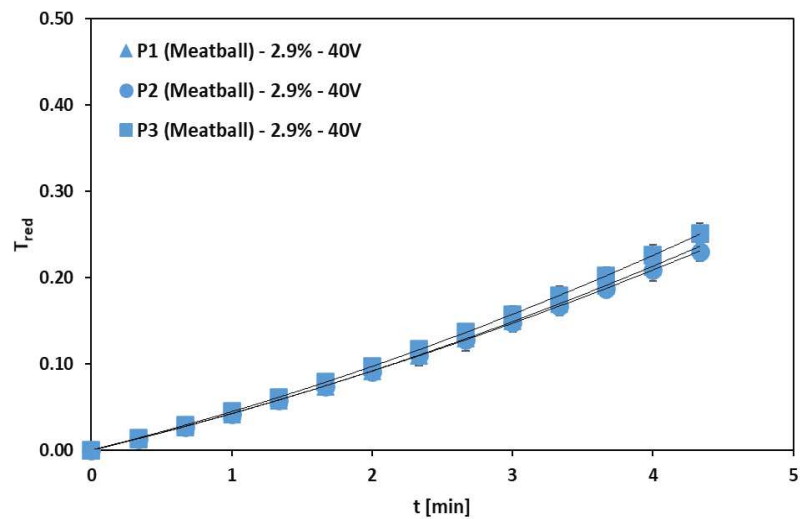


Figure 6.28 Temperature- time evolution in key points P1, P2, P3 of the heterogeneous system RPFB and meatballs (3PiRP) at 40 V and 2.9% salt content.

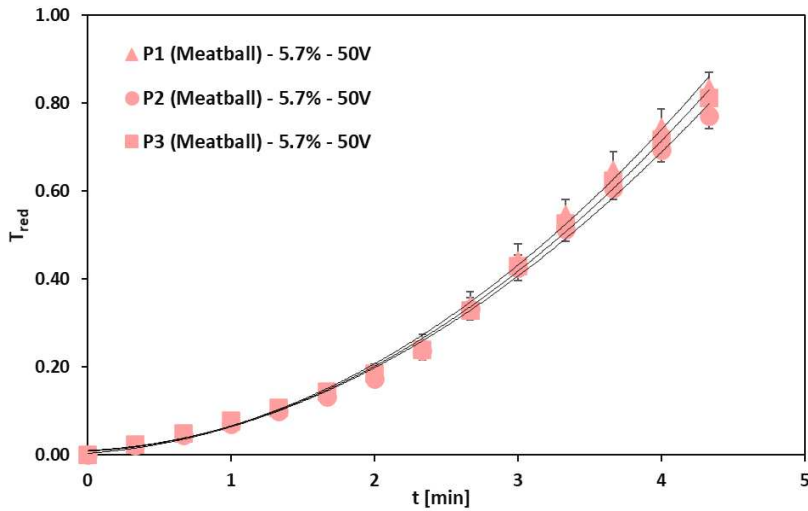


Figure 6.29 Temperature- time evolution in key points *P1*, *P2*, *P3* of the heterogeneous system RPFB and meatballs (3PiRP) at 50 V and 5.7% salt content.

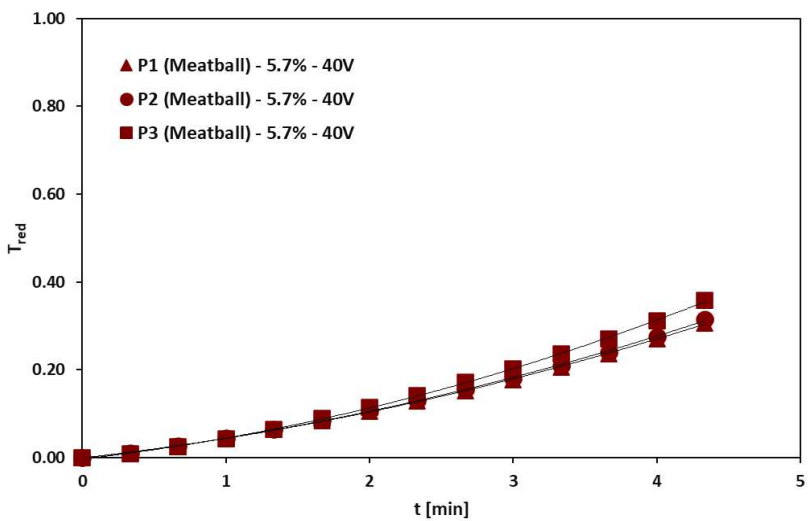


Figure 6.30 Temperature- time evolution in key points *P1*, *P2*, *P3* of the heterogeneous system RPFB and meatballs (3PiRP) at 40 V and 5.7% salt content.

Also in this case, at the same salt content, higher is the applied voltage to the system and higher is the dimensionless temperature reached at the same

time. For simplicity a direct comparison between temperature reached at 30 V, 40 V and 50 V, for both analyzed composition, is reported in **Table 6.15**

Table 6.15 T_{red} reached at target time for RPFB heterogeneous (3PiRP) system at 30 V, 40 V, 50 V and 2.9%, 5.7% salt content.

Salt content	Voltage [V]	T_{red}	T_{red}	T_{red}
		Meatball P1	Meatball P3	RPFB
2.9%	30	0.11±0.00	0.11±0.01	0.12±0.00
	40	0.24±0.01	0.23±0.01	0.25±0.01
	50	0.40±0.01	0.38±0.02	0.39±0.02
5.7%	30	0.14±0.00	0.14±0.00	0.14±0.00
	40	0.31±0.01	0.32±0.01	0.36±0.01
	50	0.84±0.03	0.77±0.03	0.81±0.01

At high voltages, especially at 5.7% salt content, differences between dimensionless temperature reached at P1, P2 and P3 could be linked to the beginning of physical- chemical phenomena.

6.3 Summary

In this chapter, first of all, results obtained applying MEF heating to the homogeneous systems RPFNB (0.37%, 0.74%, 1.39%, 2.75% salt content, key point P2) applying 30 V, 40 V and 50 V, are discussed. Results showed that, considering the same processing time, higher the salt content, higher the temperature reached. Moreover, considering the same salt composition, higher the applied voltage, higher the temperature reached from the system.

Subsequently, another homogeneous system RPFB (0%, 2.9%, 5.7% salt content, key points P1, P2, P3) was analyzed. Results showed that, for each investigated salt content, homogeneous system underwent uniform heating. Also in this case, considering analysing different applied voltages (30 V, 40 V, 50 V), increasing the applied voltage, increased the reached temperature at a fixed time.

A direct comparison between RPFB and RPF homogeneous system (at 5.7% salt content and 30 V) was carried out: RPFB reached an higher temperature than RPF, this because RPFB was subjected to an electric field strength higher than the other homogeneous system.

Subsequently, an heterogeneous system composed by RPFB and meatballs was heated with MEF. Different system configurations (2PSiRP, 2PAiRP, 3PiRP), applied voltages (30 V, 40 V, 50 V) and salt content (2.9% and 5.7%) were analysed.

MEF heating: comparison of homogeneous and heterogeneous food systems

Results showed that meatballs spherical shape and their proximity to the electrodes can influence the heating. Moreover, also in this case, higher the applied voltage and, at a fixed time, greater the heating.

7 Simulation of MEF heating

In this chapter is discussed the analysis of a simulator able to numerically solve a mathematical model of MEF heating of foods. The comparison between experimental results obtained applying MEF heating to a heterogeneous food system composed by reconstituted potato flakes RPFB and meatballs and modelling aspects related to the simulation (on the same heterogeneous food system) of MEF processing is presented too.

7.1 MEF heating modelling

The possibility to build a virtual tool able to simulate the outcome of a process undoubtedly leverages the exploration of so called "what-if" scenarios of a given process. Such a tool can be of great aid when designing/conducting a MEF heating process. In this section, the comparison between the results provided by a numerical simulator and experimental results (section 6) obtained applying MEF heating to the heterogeneous food system composed by reconstituted potato flakes RPFB, at 2.9% and 5.7% salt content, and meatballs (section 4.3) applying a voltage of 30 V and 40 V is presented. For building the numerical simulator, a commercial software COMSOL Multiphysics (Comsol AB, Sweden) have been used. Physical properties description used and modelling implementation are discussed in detail too.

7.1.1 Measurement of physical properties

Physical properties were evaluated in accord to procedures of previously published works (Lyng, Arimi, Scully, & Marra, 2014; Marra, F., Zell, M., Lyng, J.G., Morgan, D.J. Cronin, 2009). Mashed potatoes and meatballs electrical conductivity (σ) was investigated throughout the cell equipment filled with only mashed potatoes and only minced meatballs, respectively. Conductivity was so calculated according to the eq.1 of Marra, Zell, Lyng, Morgan, Cronin (2009). Thermal conductivity (λ) and volumetric heat capacity (H_p) were measured with a portable handheld device for thermal properties (KD2 Pro, Decagon, WA, USA). The measurements were performed on sets of 50 single tests on mashed potatoes and meatballs at different temperatures. Finally, density (ρ) measurements were performed on samples at single temperature (298.15 K).

Table 7.1, Table 7.2, Table 7.3 report evaluated physical properties for RPFNB, at 2.9% and 5.7% salt content, and meatballs.

Table 7.1 Physical properties best fitting as function of temperature of mashed potatoes RPFNB 2.9% salt. The temperature T is in $^{\circ}\text{C}$.

σ [S/m]	λ [W/m K]	\mathbf{Hp} [MJ/m ³ K]	ρ [kg/m ³]
0.0629T+1.929	0.0005T+0.4554	0.0024T+3.1624	946.72

Table 7.2 Physical properties best fitting as function of temperature of mashed potatoes RPFNB 5.7%. The temperature T is in $^{\circ}\text{C}$.

σ [S/m]	λ [W/m K]	\mathbf{Hp} [MJ/m ³ K]	ρ [kg/m ³]
0.1139T+2.4384	0.0026T+0.4262	0.0092T+2.9604	991.80

Table 7.3 Physical properties best fitting as function of temperature of meatball. The temperature T is in $^{\circ}\text{C}$.

σ [S/m]	λ [W/m K]	\mathbf{Hp} [MJ/m ³ K]	ρ [kg/m ³]
0.0357T+0.6573	0.0044T+0.2985	0.0082 T+2.977	1065.00

7.1.2 Modeling implementation

To be able to run a series of virtual simulations, a mathematical model of MEF heating was developed, as described in the following sections.

- **Transport equations and modeling tools**

The heat transfer phenomena that take places during ohmic heating of a solid-like food-domain such as the analyzed heterogenous system, are described by the classical unsteady state heat equation by conduction plus a generation term (Marra, Zell, Lyng, Morgan, Cronin, 2009)

$$\rho C_p \frac{\partial T}{\partial t} = \nabla \cdot \lambda \nabla T + Q_{GEN} \quad (7-1)$$

where T is the temperature within the sample, t is the process time, λ is the thermal conductivity, ρ is the density, C_p is the heat capacity and the last term represent the heat generation source where σ is the electric conductivity and $|\nabla V|$ the modulus of the gradient of electrical potential.

According to quasi-static approach, the electrical potential distribution within the sample can be computed using the following Laplace equation:

$$\nabla \cdot \sigma \nabla V = 0 \quad (7-2)$$

While the electrical conductivity depends on temperature, eqs. (7-1) and (7-2) are dependent one to each other and the problem must be solved in a coupled form.

A complete cell geometry was designed using Solidworks software (Solidworks corp., Dessault Systems, Paris, France) and a final assembled geometry was imported into Comsol software (Comsol AB, Sweden) environment to define the model builder structure. Custom materials were created respectively for mashed potato and meatballs in accord to the physical properties previously defined. Silica glass and AISI 304 stainless steel Comsol library materials were used respectively for treatment cell and electrodes. Heat transfer and electric current modules were implemented to describe the system. Its opportune coupling with multi-physics correlated electromagnetic heating module were computed to simulate the MEF equipment.

A reduced temperature variable was defined as:

$$T_{red} = \frac{T - T_0}{T_{sat} - T_0} \quad (7-3)$$

where T is the punctual temperature, T_0 the starting temperature of the measured position, and T_{sat} fictitious saturated temperature equal to 373.15.

7.1.3 Initial and boundary conditions

It is assumed that the entire sample is at an initial uniform voltage, $V_0=0$ and temperature T_0 (301.15 K, as it was the average value of the sample temperature measured after the cell filling manual operations).

As boundary conditions for the heat transfer equation, continuous domains were considered assuming ideal conductive transport between mashed potatoes, electrodes, and glass interfaces domains. For the external surfaces, different considerations were done. The external lower face of the glass cell was considered adiabatic due to the oven insulation. All others glass and steel surfaces in contact with external surrounding (air) were considered as convective heat walls with external natural convection. The upper mashed potato face is in free air and the moisture loss heat transfer was assimilated to an overall convective heat flux as:

$$q_{eq} = h (T_{air} - T) \quad (7-4)$$

here h was considered ranging from 5 to 100 W/m^2K and different simulations tests were preliminary performed in accordance with the literature (Carson, Willix, & North, 2006)

The electric equation boundary conditions were considered as perfect insulation surfaces for all boundaries except of the hereafter considered ones. A fixed voltage over the connector face of one electrode and a ground condition on the other electrode connector face were imposed. The interfacial surfaces between mashed potatoes and electrodes and between mashed potatoes and meatballs were considered as an electric contact surfaces where current flux J is described by:

$$J = h_c (V_1 - V_2) \quad (7-5)$$

h_c was the electric conductance in S/m^2 and after different parameter optimization runs, its values were estimated and reported in **Table 7.4** for every interface type. Finally, half body symmetry boundary condition was considered also to reduce the simulation computational efforts.

7.1.4 Numerical solution solver implementation

The implemented model was solved by the Comsol software. A multi-sweep study respectively for electric field (3 and 4 V/cm) and materials (MP29 and MP57) was implemented. Frequency domain (50 Hz) and time depending (0 to 4.5 minutes) solvers were used respectively for electric current and heat transfer equations.

Numerical tests were performed with different mesh parameters to evaluate the simulation results and to find the best mesh settings. The set providing the best spatial resolution for the considered domain and for which the solution was found to be independent of the grid size, was composed of 125311 tetrahedrons, 16634 triangles boundary elements, 988 edge elements, 58 vertex elements with 367894 of degree of freedom (**Figure 7.1**).

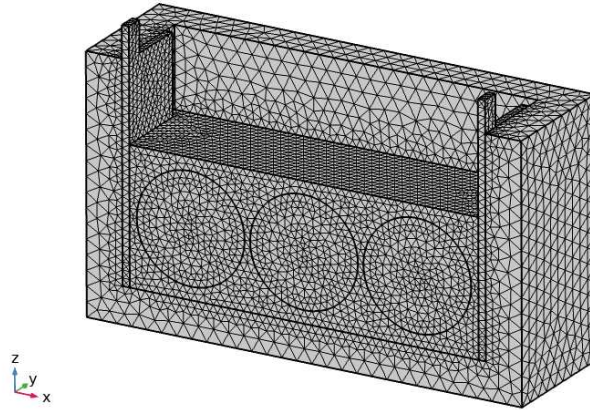


Figure 7.1 Mesh structure of the analyzed system.

7.2 Results and discussion

An analysis of the model 3D plots was firstly done. After that, an appropriate comparison of the MEF experimental profiles and the model prediction was presented.

7.2.1 Model 3D plots analysis

The numerical solutions can be presented in a series of 3D plots where heat losses, electric field, and interfacial electric conductance variational analysis were performed.

Figure 7.2 shows four examples of a temperature slice plot after 4 minutes of MEF heating for mashed potato salt concentration equal to 2.9%, assuming an equivalent heat transfer coefficient h (Eq. (7-4)) values of 5, 25, 50 and 100 $\text{W}/(\text{m}^2 \text{K})$, having also considered an applied voltage of 30 V and the **Table 7.4** values for electric conductance. Going from lower to higher heat transfers, higher difference among top surface and core temperature was observed. However, in accord to different surface temperature measurement during ad-hoc test experiments, no more than 3 °C of difference was registered among surface and core mashed-potato temperatures. On the base of these tests, 5 $\text{W}/(\text{m}^2 \text{K})$ was used for the other model simulations.

No appreciable differences were observed on the lateral surfaces heat loss considering firstly natural convection and secondly perfect wall insulation.

Figure 7.3 shows three examples of electric field slice plot after 4 minutes of MEF heating for MP29 and MP57, considering an equivalent

heat transfer coefficient h (eq. (7-4)) value of $5 \text{ W}/(\text{m}^2 \text{ K})$, having also imposed applied voltages of 30V and 40V and the **Table 7.4** values for electric conductance. The higher applied voltage, the higher is the resulting electric field as expected. Moreover, a considerable reduced electric field homogenization could be observed for a higher salt concentration of mashed potato.

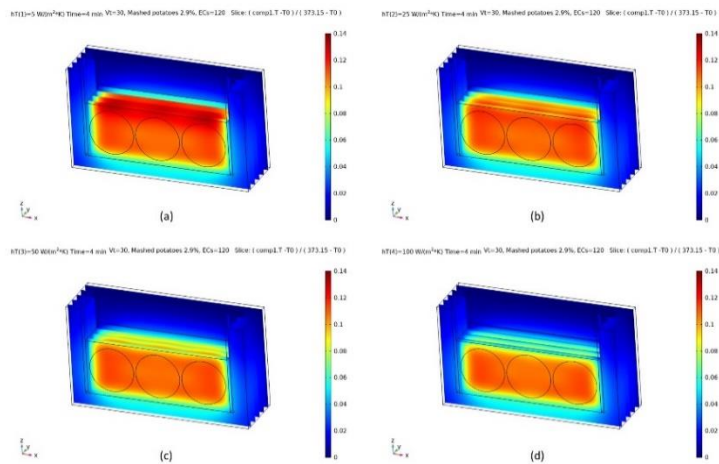


Figure 7.2 Slice plot of temperature within the considered system after 4min with an applied voltage of 30 V and reconstituted potato flakes (RPF) at 2.9% salt content. (a) $h=5 \text{ W}/(\text{m}^2 \text{ K})$, (b) $h=25 \text{ W}/(\text{m}^2 \text{ K})$, (c) $h=50 \text{ W}/(\text{m}^2 \text{ K})$ and (d) $h=100 \text{ W}/(\text{m}^2 \text{ K})$

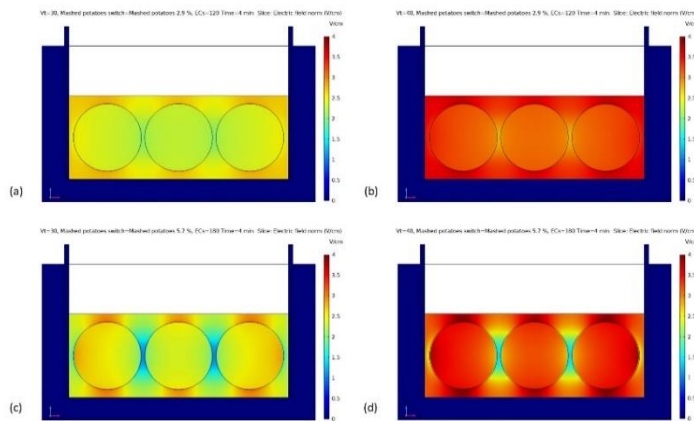


Figure 7.3 Electric field plot after 4min with Applied voltages equal to 30V (a, c) and 40V (b, d), reconstituted potato flakes (RPF) at 2.9% (a, b) and 5.7% (c, d), $h=5 \text{ W}/(\text{m}^2 \text{ K})$.

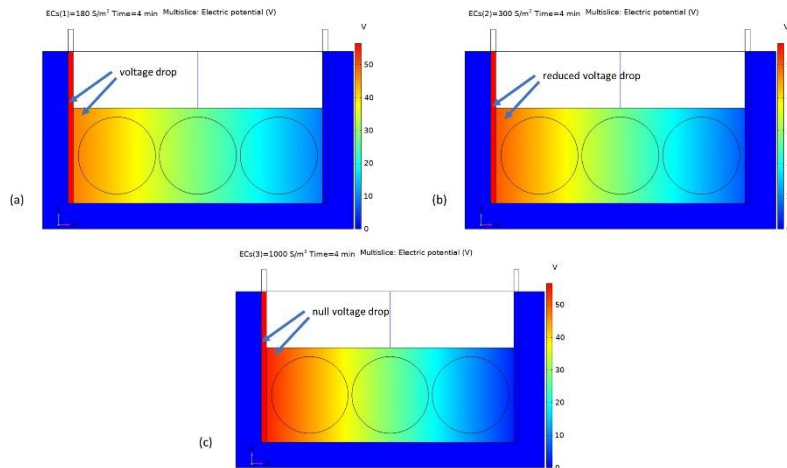


Figure 7.4 Electric potential slice plot after 4 minutes of MEF heating. Reconstituted potato flakes at 2.9% salt content, $h=5$ $W/(m^2 K)$, applied voltage of 40 V, hc (MP29MB)=800 S/m^2 . (a) hc (MP29steel)=180 S/m^2 , (b) hc (MP29steel)=300 S/m^2 , (c) hc (MP29steel)=1000 S/m^2 .

Figure 7.4 shows three examples of electric potential slice plot after 4 minutes of MEF heating for mashed potato salt concentration equal to 2.9%, considering an equivalent heat transfer coefficient h (eq. (7-4)) value of 5 $W/(m^2 K)$, having also imposed applied voltages of 40 V and electric conductance equal to 180, 300 and 1000 S/m^2 for MP57-steel interfaces, 800 S/m^2 for MP57-MB interfaces.

As expected, an increasing of the interface electric conductance will decrease the voltage drop across the in-contact materials. For very high values the electric contact is like ideal contact. After an optimization analysis of the MEF heating experimental/model curves comparison, a set of optimal electric conductance interface values are estimated and reported in **Table 7.4**. Needs to be remarked that the showed potential is the punctual electric potential while the applied potential is the sinusoidal Root Mean Square (RMS) value.

Table 7.4 *Electric conductance for mashed potato 2.9% (MP29) and 5.7% (MP57) - steel and mashed potato (MPXX) – meatball (MB) interfaces.*

Interface	h_c [S/m^2]
MP29-steel	120
MP57-steel	180
MP29-MB	800
MP57-MB	800

7.2.2 MEF profiles experimental comparison

Hereafter an experimental MEF heating of the investigated heterogeneous system (RPFB and meatballs), respectively for 30 and 40 V applied potential, for both 2.9% and 5.7% of reconstituted potato flakes salt concentration were reported and compared with the model predictions.

In **Figure 7.5a**, the comparison of temperature evolution (model predicted and experimentally measured at the chosen points P1, P2 and P3) for an applied voltage of 30 V, is reported. The model prediction shows a good agreement with the experimental results and drives the heating curve within the maximum of experimental standard deviation of 5%. It is worthwhile remarking that the model expectancy shows the external points temperatures higher than the central one as expected for the electrode proximity.

For higher voltage (**Figure 7.5b**), experimental temperature evolution shows a deviation from model prediction for longer times probably due to the rising of other phenomena not considered by the model.

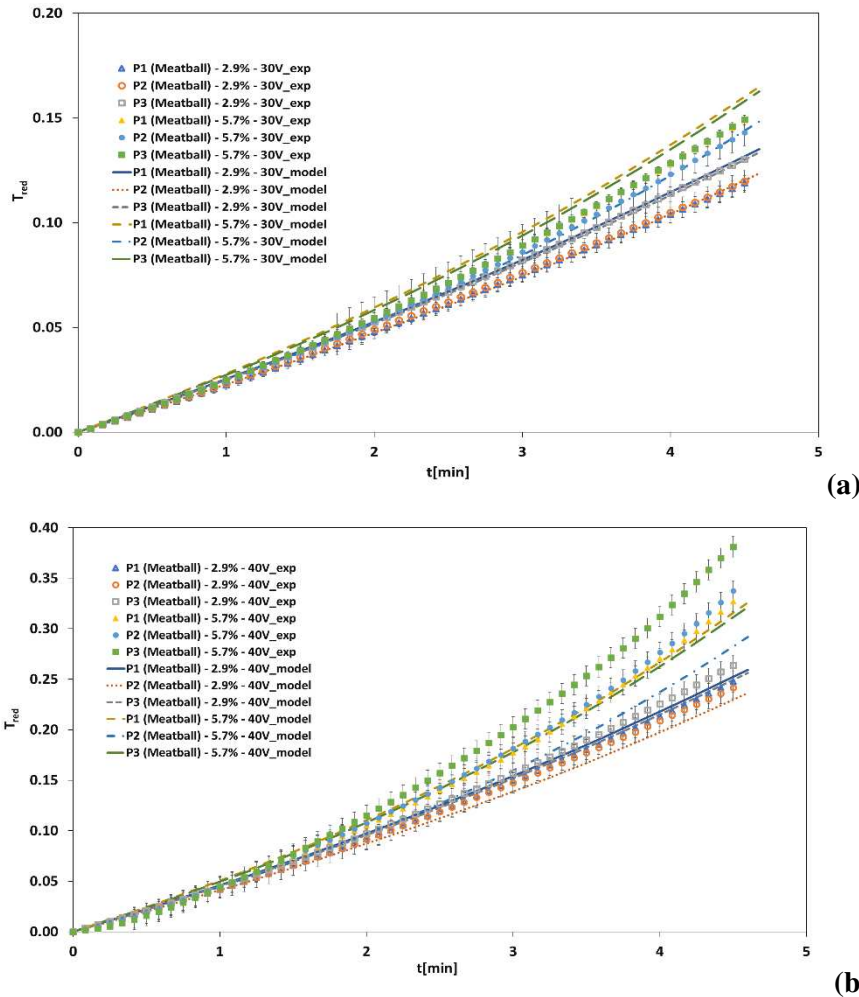


Figure 7.5 Comparison between experimentally measured and model predicted temperature evolution for an applied voltage of 30 V (a) and 40 V (b), mashed potato salt concentration A (2.9%) and B (5.7%). A concentration model profiles are solid blue for P1, dotted dark red for P2, short-dashed grey for T3. B concentration model profiles are dashed brown for T1, point&dash blue for T2, long dashed green for T3.

7.3 Summary

The implemented model for the simulation of a static MEF heating cell delivers good results, providing satisfactory correlation between predicted and experimental data. The model simulation shows as some heat losses especially on the top surface could be reduced but they not crucially affect the experiment.

An optimal set of electric conductance of the mashed potato/steel and mashed potato/meatballs interfaces was estimated by an overall analysis of all experimental tests.

Furthermore, the model shows a thermal boundary layer in the proximity of the junctions of electrodes with lateral sample surface. With the proposed cell configuration, colder external shells are the critical areas to be monitored and limited with additional insulations.

Conclusions

This research work was conducted to assess the suitability of MEF heating to heterogeneous food systems.

Different experimental tests were carried out on heterogeneous food systems to better understand the influence of different parameters such as composition, system configuration, applied voltage, shape of the foodstuff and applied field strength.

First of all, experimental tests were carried out on a homogeneous food system constituted by reconstituted potato flakes (RPF) at two different ionic content (5.7% and 10.9%). Results showed, at a given salt content, a good heating uniformity in the points investigated. Reconstituted potato flakes at higher ionic content (10.9%) were heated faster than the ones at lower ionic content (5.7%): thus, having the potatoes the same electrical and thermo-physical properties, the salt content, influenced the heating.

Further experimental tests were carried out on a heterogeneous system composed by reconstituted potato flakes (RPF), at different ionic content (5.7% and 10.9%) and chicken meatballs. Meatballs were dispersed in reconstituted potato flakes considering different system configurations (2PSiRP, 2PAiRP, 3PiRP). Results showed that the heating of the meatballs was not influenced by meatball position, but by the number of meatballs in the system and by the salt content of the surrounding reconstituted potato flakes. The temperature- time evolutions of meatballs, especially at 5.7% ionic content, mapped closely that one of reconstituted potato flakes. Having meatballs electrical conductivity lower than RPF, this means that the spherical shape of the meatballs gives to them a higher local potential variation respect to reconstituted potato flakes, that affects strongly the heating.

Further experimental studies were performed on two homogeneous food system, composed by reconstituted potato flakes (one having butter in its composition (RPF_B) and one not (RPF_{NB})) at different salt compositions (RPF_B at 0%, 2.9% and 5.7% salt content; RPF_{NB} at 0.37%, 0.74%, 1.39% and 2.75% salt content). In both considered homogeneous systems, results showed a good heating uniformity. Heating was affected by the amount of salt in reconstituted potato flakes: higher the salt content, higher the temperature reached by the system at the same target time. Homogeneous system RPF_B was compared with homogeneous system RPF. The two considered homogeneous system (RPF_B and RPF) had the same salt content, but different applied electrical field strength. In particular, RPF_B was subjected to a higher field strength than RPF and heats faster than the last one. Thus, the heating was affected by the applied field strength.

Conclusions

Another set of experimental tests was carried out on a heterogeneous food system composed by reconstituted potato flakes (RPFB) at different salt contents (0%, 2.9% and 5.7%) and meatballs. Chicken meatballs were heated in RPFB using different configurations (2PSiRP, 2PAiRP, 3PiRP). For symmetric configuration (2PSiRP) meatballs, also if they had lower electrical conductivity than potatoes, reach, at the target time, a higher temperature than RPFB. This was due to the applied field strength and to the proximity of meatballs to the electrodes. For the other two analyzed configurations (2PAiRP, 3PiRP) obtained experimental results showed discrepancies respect to 2PSiRP analyzed system. In this regard, a mathematical model for the system 3PiRP was developed. Model confirmed the influence of the local potential variation and of the proximity of the electrodes on the heating.

For each analyzed system, the effect of varying the applied voltage was investigated. Results showed that, higher the applied voltage and the quicker the heating.

Overall, this study has demonstrated the potential of MEF heating in heterogeneous food systems, also if the food macro components exhibit quite different electrical conductivity values

Bibliography

- Achir, N., Dhuique-Mayer, C., Hadjal, T., Madani, K., Pain, J. P., & Dornier, M. (2016). Pasteurization of citrus juices with ohmic heating to preserve the carotenoid profile. *Innovative Food Science and Emerging Technologies*, *33*, 397–404.
<https://doi.org/10.1016/j.ifset.2015.11.002>
- Allali, H., Marchal, L., & Vorobiev, E. (2010). Blanching of strawberries by ohmic heating: Effects on the kinetics of mass transfer during osmotic dehydration. *Food and Bioprocess Technology*, *3*(3), 406–414.
<https://doi.org/10.1007/s11947-008-0115-5>
- Amatore, C., Berthou, M., & Hébert, S. (1998). Fundamental principles of electrochemical ohmic heating of solutions. *Journal of Electroanalytical Chemistry*, *457*, 191–203.
[https://doi.org/10.1016/S0022-0728\(98\)00306-4](https://doi.org/10.1016/S0022-0728(98)00306-4)
- Assiry, A. M., Gaily, M. H., Alsamee, M., & Sarifudin, A. (2010). Electrical conductivity of seawater during ohmic heating. *Desalination*, *260*(1–3), 9–17. <https://doi.org/10.1016/j.desal.2010.05.015>
- Assiry, A., Sastry, S. K., & Samaranyake, C. (2003). Degradation kinetics of ascorbic acid during ohmic heating with stainless steel electrodes. *Journal of Applied Electrochemistry*, *33*, 187–196.
<https://doi.org/10.1023/A:1024076721332>
- Bansal, V., Sharma, A., Ghanshyam, C., & Singla, M. L. (2014). Coupling of chromatographic analyses with pretreatment for the determination of bioactive compounds in *Embllica officinalis* juice. *Analytical Methods*, *6*(2), 410–418. <https://doi.org/10.1039/c3ay41375f>
- Barron, D., & Nordh, E. (2020). *Microwave oven safety. Development of Packaging and Products for Use in Microwave Ovens*. Elsevier Ltd.
<https://doi.org/10.1016/b978-0-08-102713-4.00017-7>
- Baysal, A. H., & İcier, F. (2010). Inactivation kinetics of *alicyclobacillus acidoterrestris* spores in orange juice by ohmic heating: Effects of voltage gradient and temperature on inactivation. *Journal of Food Protection*, *73*, 299–304. <https://doi.org/10.4315/0362-028X-73.2.299>
- Bozkurt, H., & İcier, F. (2012). Ohmic thawing of frozen beef cuts. *Journal of Food Process Engineering*, *35*, 16–36.
<https://doi.org/10.1111/j.1745-4530.2009.00569.x>
- Carson, J. K., Willix, J., & North, M. F. (2006). Measurements of heat

Bibliography

- transfer coefficients within convection ovens. *Journal of Food Engineering*, 72(3), 293–301.
<https://doi.org/10.1016/j.jfoodeng.2004.12.010>
- Castro, I., Teixeira, J. A., Salengke, S., Sastry, S. K., & Vicente, A. A. (2003). The influence of field strength, sugar and solid content on electrical conductivity of strawberry products. *Journal of Food Process Engineering*, 26, 17–29. <https://doi.org/10.1111/j.1745-4530.2003.tb00587.x>
- Chaiwanichsiri, S., Ohnishi, S., Suzuki, T., Takai, R., & Miyawaki, O. (2001). Measurement of electrical conductivity, differential scanning calorimetry and viscosity of starch and flour suspensions during gelatinisation process. *Journal of the Science of Food and Agriculture*, 81, 1586–1591. <https://doi.org/10.1002/jsfa.983>
- Chassagne, C., Dubois, E., Jiménez, M. L., van der Ploeg, J. P. M., & Turnhout, J. van. (2016). Compensating for electrode polarization in dielectric spectroscopy studies of colloidal suspensions: Theoretical assessment of existing methods. *Frontiers in Chemistry*, 4, 1–19. <https://doi.org/10.3389/fchem.2016.00030>
- Cho, H. Y., Yousef, A. E., & Sastry, S. K. (1999). Kinetics of inactivation of *Bacillus subtilis* spores by continuous or intermittent ohmic and conventional heating. *Biotechnology and Bioengineering*, 62, 368–372. [https://doi.org/10.1002/\(SICI\)1097-0290\(19990205\)62:3<368::AID-BIT14>3.0.CO;2-0](https://doi.org/10.1002/(SICI)1097-0290(19990205)62:3<368::AID-BIT14>3.0.CO;2-0)
- Choi, W., Kim, S. S., Park, S. H., Ahn, J. B., & Kang, D. H. (2020). Numerical analysis of rectangular type batch ohmic heater to identify the cold point. *Food Science and Nutrition*, 8(1), 648–658. <https://doi.org/10.1002/fsn3.1353>
- Dai, Y., Zhang, Q. na, Wang, L., Liu, Y., Li, X. min, & Dai, R. tong. (2014). Changes in Shear Parameters, Protein Degradation and Ultrastructure of Pork Following Water Bath and Ohmic Cooking. *Food and Bioprocess Technology*, 7, 1393–1403. <https://doi.org/10.1007/s11947-013-1145-1>
- Darvishi, H., Khostaghaza, M. H., & Najafi, G. (2013). Ohmic heating of pomegranate juice: Electrical conductivity and pH change. *Journal of the Saudi Society of Agricultural Sciences*, 12, 101–108. <https://doi.org/10.1016/j.jssas.2012.08.003>
- Davies, L. J., Kemp, M. R., & Fryer, P. J. (1999). The geometry of shadows: Effects of inhomogeneities in electrical field processing. *Journal of Food Engineering*, 40(4), 245–258. [https://doi.org/10.1016/S0260-8774\(99\)00061-8](https://doi.org/10.1016/S0260-8774(99)00061-8)
- De Alwis, A., Halden, K., Fryer P., J. (1989). Shape and conductivity effects in the ohmic heating of foods. *Chemical Engineering Research and Design*, 67(2), 159–168.
- De Alwis, A. A. P., & Fryer, P. J. (1990). A finite-element analysis of heat

- generation and transfer during ohmic heating of food. *Chemical Engineering Science*, 45(6), 1547–1559. [https://doi.org/10.1016/0009-2509\(90\)80006-Z](https://doi.org/10.1016/0009-2509(90)80006-Z)
- De Halleux, D., Piette, G., Buteau, M. L., & Dostie, M. (2005). Ohmic cooking of processed meats: Energy evaluation and food safety considerations. *Canadian Biosystems Engineering / Le Genie Des Biosystems Au Canada*, 47, 41–47.
- De Oliveira, C. F., Giordani, D., Gurak, P. D., Cladera-Olivera, F., & Marczak, L. D. F. (2015). Extraction of pectin from passion fruit peel using moderate electric field and conventional heating extraction methods. *Innovative Food Science and Emerging Technologies*, 29, 201–208. <https://doi.org/10.1016/j.ifset.2015.02.005>
- Dey, A., & Neogi, S. (2019). Oxygen scavengers for food packaging applications: A review. *Trends in Food Science and Technology*, 90, 26–34. <https://doi.org/10.1016/j.tifs.2019.05.013>
- Engchuan, W., Jittanit, W., & Garnjanagoonchorn, W. (2014). The ohmic heating of meat ball: Modeling and quality determination. *Innovative Food Science and Emerging Technologies*, 23, 121–130. <https://doi.org/10.1016/j.ifset.2014.02.014>
- Fabiano, B., Perego, P., Pastorino, R., & Del Borghi, M. (2000). The extension of the shelf-life of “pesto” sauce by a combination of modified atmosphere packaging and refrigeration. *International Journal of Food Science and Technology*, 35, 293–303. <https://doi.org/10.1046/j.1365-2621.2000.00336.x>
- Farag, K. W., Lyng, J. G., Morgan, D. J., & Cronin, D. A. (2011). A Comparison of Conventional and Radio Frequency Thawing of Beef Meats: Effects on Product Temperature Distribution. *Food and Bioprocess Technology*, 4(7), 1128–1136. <https://doi.org/10.1007/s11947-009-0205-z>
- Fardet, A. (2016). Minimally processed foods are more satiating and less hyperglycemic than ultra-processed foods: A preliminary study with 98 ready-to-eat foods. *Food and Function*, 7(5), 2338–2346. <https://doi.org/10.1039/c6fo00107f>
- Fryer, P. J., de Alwis, A. A. P., Koury, E., Stapley, A. G. F., & Zhang, L. (1993). Ohmic processing of solid-liquid mixtures: Heat generation and convection effects. *Journal of Food Engineering*, 18, 101–125. [https://doi.org/10.1016/0260-8774\(93\)90031-E](https://doi.org/10.1016/0260-8774(93)90031-E)
- Galanakis, C. M. (2012). Recovery of high added-value components from food wastes: Conventional, emerging technologies and commercialized applications. *Trends in Food Science and Technology*, 26(2), 68–87. <https://doi.org/10.1016/j.tifs.2012.03.003>
- Gavahian, M., Chu, Y. H., & Sastry, S. K. (2018). Extraction from Food and Natural Products by Moderate Electric Field: Mechanisms, Benefits, and Potential Industrial Applications. *Comprehensive Reviews in Food*

Bibliography

- Science and Food Safety*, 17(4), 1040–1052.
<https://doi.org/10.1111/1541-4337.12362>
- Halden, K., De Alwis, A. A. P., & Fryer, P. J. (1990). Changes in the electrical conductivity of foods during ohmic heating. *International Journal of Food Science & Technology*, 25(1), 9–25.
<https://doi.org/10.1111/j.1365-2621.1990.tb01055.x>
- Icier, F. (2009). Influence of ohmic heating on rheological and electrical properties of reconstituted whey solutions. *Food and Bioprocess Technology*, 87(4), 308–316. <https://doi.org/10.1016/j.fbp.2009.01.002>
- Icier, F. (2012). *Ohmic Heating of Fluid Foods. Novel Thermal And Non-Thermal Technologies For Fluid Foods*. Elsevier Inc.
<https://doi.org/10.1016/B978-0-12-381470-8.00011-6>
- Icier, F., & Ilicali, C. (2005a). Temperature dependent electrical conductivities of fruit purees during ohmic heating. *Food Research International*, 38(10), 1135–1142.
<https://doi.org/10.1016/j.foodres.2005.04.003>
- Icier, F., & Ilicali, C. (2005b). The use of tylose as a food analog in ohmic heating studies. *Journal of Food Engineering*, 69(1), 67–77.
<https://doi.org/10.1016/j.jfoodeng.2004.07.011>
- Icier, F., & Tavman, S. (2006). Ohmic heating behaviour and rheological properties of ice cream mixes. *International Journal of Food Properties*, 9(4), 679–689.
<https://doi.org/10.1080/10942910600547467>
- Imai, T., Uemura, K., Ishida, N., Yoshizaki, S., Noguchi, A. (1995). Ohmic heating of Japanese white radish. *International Journal of Food Science & Technology*, 30, 461–472.
- Jaeger, H., Roth, A., Toepfl, S., Holzhauser, T., Engel, K. H., Knorr, D., ... Steinberg, P. (2016). Opinion on the use of ohmic heating for the treatment of foods. *Trends in Food Science and Technology*, 55, 84–97.
<https://doi.org/10.1016/j.tifs.2016.07.007>
- Jojo, S., & Mahendran, R. (2013). Radio frequency heating and its application in food processing: A Review. *International Journal of Current Agricultural Research*, 1(9), 042–046.
- Jun, S., & Sastry, S. (2007). Reusable pouch development for long term space missions: A 3D ohmic model for verification of sterilization efficacy. *Journal of Food Engineering*, 80(4), 1199–1205.
<https://doi.org/10.1016/j.jfoodeng.2006.09.018>
- Kanjanapongkul, K. (2017). Rice cooking using ohmic heating: Determination of electrical conductivity, water diffusion and cooking energy. *Journal of Food Engineering*, 192, 1–10.
<https://doi.org/10.1016/j.jfoodeng.2016.07.014>
- Kim, S. S., & Kang, D. H. (2015). Effect of milk fat content on the performance of ohmic heating for inactivation of Escherichia coli O157:H7, Salmonella enterica Serovar Typhimurium and Listeria

- monocytogenes. *Journal of Applied Microbiology*, 119, 475–486.
<https://doi.org/10.1111/jam.12867>
- Kumar, T. (2018). A Review on Ohmic Heating Technology: Principle, Applications and Scope. *International Journal of Agriculture, Environment and Biotechnology*, 11(4). <https://doi.org/10.30954/0974-1712.08.2018.10>
- Lakkakula, N. R., Lima, M., & Walker, T. (2004). Rice bran stabilization and rice bran oil extraction using ohmic heating. *Bioresource Technology*, 92, 157–161.
<https://doi.org/10.1016/j.biortech.2003.08.010>
- Lascorz, D., Torella, E., Lyng, J. G., & Arroyo, C. (2016). The potential of ohmic heating as an alternative to steam for heat processing shrimps. *Innovative Food Science and Emerging Technologies*, 37, 329–335.
<https://doi.org/10.1016/j.ifset.2016.06.014>
- Lee, S. Y., Sagong, H. G., Ryu, S., & Kang, D. H. (2012). Effect of continuous ohmic heating to inactivate Escherichia coli O157: H7, Salmonella Typhimurium and Listeria monocytogenes in orange juice and tomato juice. *Journal of Applied Microbiology*, 112, 723–731.
<https://doi.org/10.1111/j.1365-2672.2012.05247.x>
- Lee, Su Yeon, Ryu, S., & Kang, D. H. (2013). Effect of frequency and waveform on inactivation of Escherichia coli O157:H7 and Salmonella enterica serovar typhimurium in salsa by ohmic heating. *Applied and Environmental Microbiology*, 79(1), 10–17.
<https://doi.org/10.1128/AEM.01802-12>
- Leizerson, S., & Shimoni, E. (2005). Stability and sensory shelf life of orange juice pasteurized by continuous ohmic heating. *Journal of Agricultural and Food Chemistry*, 53(10), 4012–4018.
<https://doi.org/10.1021/jf047857q>
- Lima, M., Heskitt, B. F., & Sastry, S. K. (1999). Effect of frequency and wave form on the electrical conductivity-temperature profiles of turnip tissue. *Journal of Food Process Engineering*, 22(1), 41–54.
<https://doi.org/10.1111/j.1745-4530.1999.tb00470.x>
- Ling, B., Tang, J., Kong, F., Mitcham, E. J., & Wang, S. (2015). Kinetics of Food Quality Changes During Thermal Processing: a Review. *Food and Bioprocess Technology*, 8, 343–358.
<https://doi.org/10.1007/s11947-014-1398-3>
- Liu, L., Llave, Y., Jin, Y., Zheng, D. yu, Fukuoka, M., & Sakai, N. (2017). Electrical conductivity and ohmic thawing of frozen tuna at high frequencies. *Journal of Food Engineering*, 197, 68–77.
<https://doi.org/10.1016/j.jfoodeng.2016.11.002>
- Loypimai, P., Moongngarm, A., Chottanom, P., & Moontree, T. (2015). Ohmic heating-assisted extraction of anthocyanins from black rice bran to prepare a natural food colourant. *Innovative Food Science and Emerging Technologies*, 27, 102–110.

Bibliography

- <https://doi.org/10.1016/j.ifset.2014.12.009>
- Lyng, J. G., Arimi, J. M., Scully, M., & Marra, F. (2014). The influence of compositional changes in reconstituted potato flakes on thermal and dielectric properties and temperatures following microwave heating. *Journal of Food Engineering*, *124*, 133–142. <https://doi.org/10.1016/j.jfoodeng.2013.09.032>
- Marcotte, M., Trigui, M., Ramaswamy, H. S. (2000). Effect of salt and citric acid on electrical conductivities and ohmic heating of viscous liquids. *Journal of Food Processing and Preservation*, *24*, 389–406.
- Marcotte, M., Piette, J. P. G., & Ramaswamy, H. S. (1998). Electrical conductivities of hydrocolloid solutions. *Journal of Food Process Engineering*, *21*(6), 503–520. <https://doi.org/10.1111/j.1745-4530.1998.tb00466.x>
- Marra, F., Zell, M., Lyng, J.G., Morgan, D.J. Cronin, D. A. (2009). Analysis of heat transfer during ohmic processing of a solid food. *Journal of Food Engineering*, *91*, 56–63. <https://doi.org/10.1016/j.jfoodeng.2008.08.015>
- Marra, F., Zhang, L., & Lyng, J. G. (2009). Radio frequency treatment of foods: Review of recent advances. *Journal of Food Engineering*, *91*(4), 497–508. <https://doi.org/10.1016/j.jfoodeng.2008.10.015>
- Masino, F., Ulrici, A., & Antonelli, A. (2008). Extraction and quantification of main pigments in pesto sauces. *European Food Research and Technology*, *226*(3), 569–575. <https://doi.org/10.1007/s00217-007-0572-5>
- McKenna, B. M., Lyng, J., Brunton, N., & Shirsat, N. (2006). Advances in radio frequency and ohmic heating of meats. *Journal of Food Engineering*, *77*(2), 215–229. <https://doi.org/10.1016/j.jfoodeng.2005.06.052>
- Mizrahi, S., Kopelman, I. J., & Perlman, J. (1975). Blanching by electro-conductive heating. *Journal of Food Technology*, *10*, 281–288.
- Monteiro, C. A., Cannon, G., Levy, R., Moubarac, J.-C., Jaime, P., Martins, A. P., ... Parra, D. (2016). NOVA. The Star Shines Bright (Food Classification. Public Health). *World Nutrition*, *7*(1–3), 28–38. Retrieved from <https://worldnutritionjournal.org/index.php/wn/article/view/5>
- Moses, D. B. (1938). Electrical pasteurization of milk. *Agricultural Engineering*, *19*, 525–526.
- Murphy, A. B., Powell, K. J., & Morrow, R. (1991). Thermal treatment of sewage sludge by ohmic heating. *IEE Proceedings: Science, Measurement and Technology*, *138*(4), 242–248. <https://doi.org/10.1049/ip-a-3.1991.0033>
- Nair, G. R., Divya, V. R., Prasannan, L., Habeeba, V., Prince, M. V., & Raghavan, G. S. V. (2014). Ohmic heating as a pre-treatment in solvent extraction of rice bran. *Journal of Food Science and Technology*,

- 51(10), 2692–2698. <https://doi.org/10.1007/s13197-012-0764-2>
- Palaniappan, S., Sastry, S., K. (1991a). Electrical conductivity of selected juices: influences of temperature, solids content, applied voltage, and particle size. *Journal of Food Process Engineering*, 14(4), 247–260. <https://doi.org/10.1111/j.1745-4530.1991.tb00135.x>
- Palaniappan, S., & Sastry, S. K. (1991b). Electrical conductivities of selected solid foods during ohmic heating. *Journal of Food Process Engineering*, 14(3), 221–236. <https://doi.org/10.1111/j.1745-4530.1991.tb00093.x>
- Palaniappan, S., Sastry, S. K., & Richter, E. R. (1992). Effects of electroconductive heat treatment and electrical pretreatment on thermal death kinetics of selected microorganisms. *Biotechnology and Bioengineering*, 39, 225–232. <https://doi.org/10.1002/bit.260390215>
- Park, I. K., & Kang, D. H. (2013). Effect of electroporation by ohmic heating for inactivation of escherichia coli O157: H7, Salmonella enterica serovar typhimurium, and listeria monocytogenes in buffered peptone water and apple juice. *Applied and Environmental Microbiology*, 79(23), 7122–7129. <https://doi.org/10.1128/AEM.01818-13>
- Park, S. H., Balasubramaniam, V. M., Sastry, S. K., & Lee, J. (2013). Pressure-ohmic-thermal sterilization: A feasible approach for the inactivation of Bacillus amyloliquefaciens and Geobacillus stearothermophilus spores. *Innovative Food Science and Emerging Technologies*, 19, 115–123. <https://doi.org/10.1016/j.ifset.2013.03.005>
- Pathare, P. B., & Roskilly, A. P. (2016). Quality and Energy Evaluation in Meat Cooking. *Food Engineering Reviews*, 8(4), 435–447. <https://doi.org/10.1007/s12393-016-9143-5>
- Pereira, R., Martins, J., Mateus, C., Teixeira, J., & Vicente, A. A. (2007). Death kinetics of Escherichia coli in goat milk and Bacillus licheniformis in cloudberry jam treated by ohmic heating. *Chemical Papers*, 61, 121–126. <https://doi.org/10.2478/s11696-007-0008-5>
- Pereira, R. N., Rodrigues, R. M., Genisheva, Z., Oliveira, H., de Freitas, V., Teixeira, J. A., & Vicente, A. A. (2016). Effects of ohmic heating on extraction of food-grade phytochemicals from colored potato. *LWT - Food Science and Technology*, 74, 493–503. <https://doi.org/10.1016/j.lwt.2016.07.074>
- Piette, G., Dostie, M., Ramaswamy, H. (2001). Ohmic cooking of processed meats—state of the art and prospects. *47th International Congress of Meat Science and Technology*, 62_67.
- Pittia, P., & Paparella, A. (2016). *Safety by Control of Water Activity: Drying, Smoking, and Salt or Sugar Addition. Regulating Safety of Traditional and Ethnic Foods*. Elsevier Inc. <https://doi.org/10.1016/B978-0-12-800605-4.00002-5>
- Poisson, A. (1980). Conductivity/salinity/temperature relationships of

Bibliography

- diluted and concentrated standard seawater. *IEEE Journal of Oceanic Engineering*, 5(1). <https://doi.org/10.1080/15210608209379433>
- Rao, M., A., Rizvi, S., S., H., & Datta, K. A. (2014). *Engineering properties of foods*. (U. CRC Press, Boca Raton, Florida, Ed.), *Engineering Properties of Foods, Fourth Edition* (Third Edit). <https://doi.org/10.1201/b16897>
- Roberts, J. S., Balaban, M. O., Zimmerman, R., & Luzuriaga, D. (1998). Design and testing of a prototype ohmic thawing unit. *Computers and Electronics in Agriculture*, 19, 211–222. [https://doi.org/10.1016/S0168-1699\(97\)00044-6](https://doi.org/10.1016/S0168-1699(97)00044-6)
- Ruan, R., Chen, P., Chen, X., Y., Doona, C., Yang, T. (2004). *Developments in ohmic heating. Improving the thermal processing of foods*. Woodhead Publishing Ltd.
- Sagong, H. G., Park, S. H., Choi, Y. J., Ryu, S., & Kang, D. H. (2011). Inactivation of escherichia coli O157:H7, salmonella typhimurium, and listeria monocytogenes in orange and tomato juice using ohmic heating. *Journal of Food Protection*, 74(6), 899–904. <https://doi.org/10.4315/0362-028X.JFP-10-552>
- Sakr, M., & Liu, S. (2014). A comprehensive review on applications of ohmic heating (OH). *Renewable and Sustainable Energy Reviews*, 39, 262–269. <https://doi.org/10.1016/j.rser.2014.07.061>
- Samaranayake, C. P., & Sastry, S. K. (2005). Electrode and pH effects on electrochemical reactions during ohmic heating. *Journal of Electroanalytical Chemistry*, 577, 125–135. <https://doi.org/10.1016/j.jelechem.2004.11.026>
- Sarang, S., Sastry, S. K., & Knipe, L. (2008). Electrical conductivity of fruits and meats during ohmic heating. *Journal of Food Engineering*, 87(3), 351–356. <https://doi.org/10.1016/j.jfoodeng.2007.12.012>
- Sastry, S. (2008). Ohmic heating and moderate electric field processing. *Food Science and Technology International*, 14(5), 419–422. <https://doi.org/10.1177/1082013208098813>
- Sastry, S. K. (2014). Overview of ohmic heating. In CRC Press, Boca Raton, FL (Ed.), *Ohmic heating in food processing* (pp. 10–13).
- Sastry, Sudhir K., & Palaniappan, S. (1992). Influence of particle orientation on the effective electrical resistance and ohmic heating rate of a liquid- particle mixture. *Journal of Food Process Engineering*, 15(3), 213–227. <https://doi.org/10.1111/j.1745-4530.1992.tb00153.x>
- Sensoy, I., & Sastry, S. K. (2004). Extraction Using Moderate Electric Fields. *Journal of Food Science*, 69(1), 7–13. <https://doi.org/10.1111/j.1365-2621.2004.tb17861.x>
- Shirsat, N., Lyng, J. G., Brunton, N. P., & McKenna, B. (2004). Ohmic processing: Electrical conductivities of pork cuts. *Meat Science*, 67(3), 507–514. <https://doi.org/10.1016/j.meatsci.2003.12.003>
- Shrestha, A. K., Basnet, N., Bohora, C. ., & Khadka, P. (2017). Variation of

- Electrical Conductivity of the Different Sources of Water with Temperature and Concentration of Electrolyte Solution NaCl. *International Journal of Recent Research and Review*, 10(3), 24–26.
- Silva, V. L. M., Santos, L. M. N. B. F., & Silva, A. M. S. (2017). Ohmic Heating: An Emerging Concept in Organic Synthesis. *Chemistry - A European Journal*, 23, 7853–7865.
<https://doi.org/10.1002/chem.201700307>
- Ushie, P., Osang, J., Ojar, J., Ohakwere-eze, M., Alozie, S. (2014). Investigation of the efficiency of olive oil as dielectric material and its economic value on the environment using its dielectric properties. *International Journal of Advance Research*, 2(1), 1–7.
- Vanýsek, P. (1998). Equivalent Conductivity of Electrolytes in Aqueous Solution. In B. R. CRC Press (Ed.), *CRC Handbook of Chemistry and Physics, 79th edn.* (pp. 5–76). Retrieved from [https://sites.chem.colostate.edu/diverdi/all_courses/CRC reference data/equivalent conductivity of electrolytes.pdf](https://sites.chem.colostate.edu/diverdi/all_courses/CRC%20reference%20data/equivalent%20conductivity%20of%20electrolytes.pdf)
- Varghese, K. S., Pandey, M. C., Radhakrishna, K., & Bawa, A. S. (2012). Technology, applications and modelling of ohmic heating: a review. *Journal of Food Science and Technology*, 51(10), 2304–2317.
<https://doi.org/10.1007/s13197-012-0710-3>
- Wang, W.-C., & Sastry, S. K. (1997). Starch Gelatinization in Ohmic Heating. *Journal of Food Engineering*, 34(3), 225–242.
<https://doi.org/10.1111/j.1745-4530.2003.tb00587.x>
- Wang, W. C., & Sastry, S. K. (1993a). Salt diffusion into vegetable tissue as a pretreatment for ohmic heating: determination of parameters and mathematical model verification. *Journal of Food Engineering*, 20, 311–323. [https://doi.org/10.1016/0260-8774\(93\)90081-T](https://doi.org/10.1016/0260-8774(93)90081-T)
- Wang, W. C., & Sastry, S. K. (1993b). Salt diffusion into vegetable tissue as a pretreatment for ohmic heating: Electrical conductivity profiles and vacuum infusion studies. *Journal of Food Engineering*, 20, 299–309.
[https://doi.org/10.1016/0260-8774\(93\)90080-4](https://doi.org/10.1016/0260-8774(93)90080-4)
- Wang, W. C., & Sastry, S. K. (1997). Changes in electrical conductivity of selected vegetables during multiple thermal treatments. *Journal of Food Process Engineering*, 20(6), 499–516.
<https://doi.org/10.1111/j.1745-4530.1997.tb00435.x>
- Więckowski, A., Korpas, P., Krysicki, M., Dughiero, F., Bullo, M., Bressan, F., & Fager, C. (2014). Efficiency optimization for phase controlled multi-source microwave oven. *International Journal of Applied Electromagnetics and Mechanics*, 44(2), 235–241.
<https://doi.org/10.3233/JAE-141764>
- Wongsa-Ngasri, P., & Sastry, S. K. (2015). Effect of ohmic heating on tomato peeling. *LWT - Food Science and Technology*, 61(2), 269–274.
<https://doi.org/10.1016/j.lwt.2014.12.053>
- Yang, T. C. S., Cohen, J. S., Kluter, R. A., Tempest, P., Manvell, C.,

Bibliography

- Blackmore, S. J., & Adams, S. (1997). Microbiological and sensory evaluation of six ohmically heated stew type foods. *Journal of Food Quality*, 20, 303–313. <https://doi.org/10.1111/j.1745-4557.1997.tb00473.x>
- Yildiz-Turp, G., Sengun, I. Y., Kendirci, P., & Icier, F. (2013). Effect of ohmic treatment on quality characteristic of meat: A review. *Meat Science*, 93(3), 441–448. <https://doi.org/10.1016/j.meatsci.2012.10.013>
- Yin, Z., Hoffmann, M., & Jiang, S. (2018). Sludge disinfection using electrical thermal treatment: The role of ohmic heating. *Science of the Total Environment*, 615, 262–271. <https://doi.org/10.1016/j.scitotenv.2017.09.175>
- Yongsawatdigul, J., Park, J. W., & Kolbe, E. (1995). Electrical Conductivity of Pacific Whiting Surimi Paste during Ohmic Heating. *Journal of Food Science*, 60(5), 922–925. <https://doi.org/10.1111/j.1365-2621.1995.tb06262.x>
- Yoon, S. W., Lee, C. Y. J., Kim, K. M., & Lee, C. H. (2002). Leakage of cellular materials from *Saccharomyces cerevisiae* by ohmic heating. *Journal of Microbiology and Biotechnology*, 12(2), 183–188.
- Zardetto, S., & Barbanti, D. (2020). Shelf life assessment of fresh green pesto using an accelerated test approach. *Food Packaging and Shelf Life*, 25, 100524. <https://doi.org/10.1016/j.foodpack.2020.100524>
- Zareifard, M. R., Ramaswamy, H. S., Trigui, M., & Marcotte, M. (2003). Ohmic heating behaviour and electrical conductivity of two-phase food systems. *Innovative Food Science and Emerging Technologies*, 4, 45–55. [https://doi.org/10.1016/S1466-8564\(02\)00088-7](https://doi.org/10.1016/S1466-8564(02)00088-7)
- Zell, M., Lyng, J. G., Morgan, D. J., & Cronin, D. A. (2009). Development of rapid response thermocouple probes for use in a batch ohmic heating system. *Journal of Food Engineering*, 93(3), 344–347. <https://doi.org/10.1016/j.jfoodeng.2009.01.039>
- Zell, Markus, Lyng, J. G., Cronin, D. A., & Morgan, D. J. (2009a). Ohmic cooking of whole beef muscle - Optimisation of meat preparation. *Meat Science*, 81(4), 693–698. <https://doi.org/10.1016/j.meatsci.2008.11.012>
- Zell, Markus, Lyng, J. G., Cronin, D. A., & Morgan, D. J. (2009b). Ohmic heating of meats: Electrical conductivities of whole meats and processed meat ingredients. *Meat Science*, 83(3), 563–570. <https://doi.org/10.1016/j.meatsci.2009.07.005>
- Zell, Markus, Lyng, J. G., Cronin, D. A., & Morgan, D. J. (2010a). Ohmic cooking of whole beef muscle - Evaluation of the impact of a novel rapid ohmic cooking method on product quality. *Meat Science*, 86(2), 258–263. <https://doi.org/10.1016/j.meatsci.2010.04.007>
- Zell, Markus, Lyng, J. G., Cronin, D. A., & Morgan, D. J. (2010b). Ohmic cooking of whole turkey meat - Effect of rapid ohmic heating on selected product parameters. *Food Chemistry*, 120, 724–729. <https://doi.org/10.1016/j.foodchem.2009.10.069>

- Zeppa, G., & Turon, C. (2014). Application of the central composite design approach to define chlorophyll degradation during pesto sauce pasteurization. *Industria Alimentari*, *53*, 5–11.
- Zhao, Y., Kolbe, E., & Flugstad, B. (1999). A method to characterize electrode corrosion during ohmic heating. *Journal of Food Process Engineering*, *22*, 81–89. <https://doi.org/10.1111/j.1745-4530.1999.tb00472.x>
- Zhong, T., & Lima, M. (2003). The effect of ohmic heating on vacuum drying rate of sweet potato tissue. *Bioresource Technology*, *87*, 215–220. [https://doi.org/10.1016/S0960-8524\(02\)00253-5](https://doi.org/10.1016/S0960-8524(02)00253-5)
- Zhu, S. M., Zareifard, M. R., Chen, C. R., Marcotte, M., & Grabowski, S. (2010). Electrical conductivity of particle-fluid mixtures in ohmic heating: Measurement and simulation. *Food Research International*, *43*, 1666–1672. <https://doi.org/10.1016/j.foodres.2010.05.009>

Nomenclature

I	Current (A)
V	Voltage (V)
R	Resistance (Ω)
t	Time (s)
ρ	Density (kg/m^3)
C _p	Heat capacity (J/kg K)
T	Temperature (K)
λ	Thermal conductivity (W/m K)
Q _{GEN}	Specific power source term (W/m^3)
σ	Electrical conductivity (S/m)
V _s	Total volume of solids (m^3)
r	Average radius of solids in suspension (m)
A _s	Cross- sectional area of solids exposed to electric current (m^2)
n	Number of solid particles in suspension
c	Concentration (mol/m^3)
K _T	Temperature coefficient (S/m °C)
K _{TC}	Temperature and concentration coefficient (S/m °C%)
K _{σT}	Temperature coefficient (S/m °C)
σ_{25}	Electrical conductivity at 25°C (S/m)
K	Cell constant (1/m)
M _s	Solid concentration (%)
L	Distance between the electrodes (m)
A	Cross- section of the material in the treatment cell
W	Width of the treatment cell (m)
H _{filling}	Height of the filling in treatment cell
G	Conductance (S)
T _{red}	Reduced temperature
T ₀	Initial temperature (°C)
T _{sat}	Fictitious saturated temperature (K)
H _p	Volumetric heat capacity ($\text{MJ/m}^3 \text{ K}$)

h	Heat transfer coefficient ($\text{W}/\text{m}^2 \text{K}$)
q_{eq}	Heat flux (W/m^2)
T_{air}	Air temperature (K)
j	Current density (A/m^2)
h_c	Electric conductance

Appendix A

Modeling Aspects in Simulation of MEF Processing of Solid Behaving Foods

Oriana Casaburi, Francesco Petrosino, Francesco Marra

*Dipartimento di Ingegneria Industriale, Università degli Studi di Salerno,
Via Giovanni Paolo II 132, 84084, Fisciano, Salerno, Italy*

frpetrosino@unisa.it



Modeling Aspects in Simulation of MEF Processing of Solid Behaving Foods

Oriana Casaburi, Francesco Petrosino*, Francesco Marra

Department of Industrial Engineering, University of Salerno, Via Giovanni Paolo II 132, Fisciano SA 84084 Italy
frpetrosino@unisa.it

Moderate Electric Field (MEF) processes involve electric fields less than or equal to 1000 V/cm (Sastry, 2008) and found applications in food heating processes. Industrially, systems based on MEF at 50 Hz (traditionally addressed as ohmic) are employed for heating of liquid food products (sauces, fruit juices) or particulate-dispersed-in-liquid food products (soups).

Solid-behaving heterogeneous systems have been less studied, especially due to the not easy coupling between the physical and electrical characteristics of the materials that constitute the food system subjected to MEF assisted heating. The set-up of a virtual lab able to simulate the MEF assisted heating of a heterogeneous food system allows to investigate on the role played by main process parameters (applied electrical potential, MEF cell geometry and electrode configuration) as well as on materials' electrical conductivity and thermos-physical properties, and also on geometric characteristic of the food system itself. On the other hand, the set-up of such virtual tool is not trivial because it requires the coupling of phenomena of different nature (the passage of electric current in the MEF circuit, including the food loading system; the heat transfer within the food system and its coupling with the local gradient of the electrical potential).

In this work, the modeling aspects related to the simulation of MEF processing applied to a heterogeneous food system are presented. Particularly, the study was devoted to analyzing the MEF heating performances in a food system made by 3 meatballs dispersed in 145 g of reconstituted potatoes. The food system was put in a experimental MEF cell 100 mm long, 51 mm wide, with electrodes made in stainless steel.

The model set-up has been built following the work presented by Marra et al. (2009). Comparison of experimental results with heating trends provided by simulations in different operating conditions (applied potential gradient of 3 and 4 V/cm) have shown a good agreement when dissipative effects were considered on applied potential. Discrepancies may be due to electrolysis happening near the electrodes.

1. Introduction

MEF processing has reemerging in different industrial food processes fields only the last 10 to 15 years, the scientific and technical developments achieved having finally allowed its safe application at the industrial scale. The heating consists by a passage of electric currents in the food matrix. Throughout the joule heating phenomena, the treated electroconductive material could be heated (Sastry, 2008). Comparing the Ohmic heating processes to other electrical methods such as induction, microwave, and radio frequency heating, it has flexibility on the frequency and waveforms of the electric field (Samaranayake and Sastry, 2016). Popular frequencies of ohmic heating tend to be those of power supplies (50 or 60 Hz); However no limitation are present for the use of different voltages and frequencies different from the popular ones and this technology has becoming widely used because it's remarkably rapid and relatively spatially uniform in comparison with other electrical methods (Sastry, 2008). MEF could involve electric fields up to 1000 V/cm depending on the specific desired heating rate and compatibly with the analyzed sample. The MEF processing could be used in many and many applications specially in food industry. Initially, it was adopted to heat liquid-like foods such as fruit juices, soups, sauces, milk etc. (Sepulveda et al. 2005) However, the wide improvements of MEF became attractive for many more types of foods and it started to be adopted in solid foods processing. In spite of the increasing use of MEF in solid foods processing, the MEF heating of heterogeneous systems still represents a challenging problem that has received a limited coverage in the scientific literature, both for the different coupling problems between the physical and electrical characteristics of the materials and for the interfacial

transfer phenomena that could play a key role and could represent the bottleneck of the overall process performance. Modeling and simulation approaches are receiving more and more interest in different scientific and technological areas and could be quoted as the enabling technology of science and engineering that could describe various scales of complex systems (Jinghai and Kwauk, 2003). Many engineering modelling applications have demonstrated the potential of these tools in a wide variety of fields from bioengineering (Petrosino et al., 2020) to fluid dynamics (Turek et al. 2016).

Modelling and simulation also play a key role in the MEF processes area. Different works are present in the literature. Sastry and Salengke (1998) proposed a comparison among mathematical models for ohmic heating of solid-liquid mixtures; Soojin and Sastry (2005) proposed a modeling and optimization study of a pulsed ohmic heating system of a flexible package for food reheating and sterilization for long-duration space missions food supplies; Shim, Seung, and Soojin (2010) proposed the modeling of the thermal behavior of multiphase food products with various electrical conductivities under ohmic heating; a comprehensive 3D, transient-free convection, and multiphase model was developed by Hashemi et al. (2019) to determine the performance of ohmic heating. In the present work, a modeling and simulation tool of MEF processing applied to a heterogeneous food system is proposed. In particular, an experimental MEF heating cell was used to investigate the performances of a food system made by 3 meat balls (MB) dispersed in 145 g of reconstituted potatoes. The MEF cell was 100 mm long, 51 mm wide, with electrodes made in stainless steel.

The model set-up was built following the work presented by Marra et al. (2009). Comparison of experimental results with modelling in different operating conditions shows a good agreement.

2. MEF heating setup

2.1 Food sample preparation

Mashed potato (MP) samples were prepared by mixing flakes (potato flakes, Crastan, Italy), pure dried salt (Conad Soc. Coop., Italy), unsalted butter (Conad Soc. Coop., Italy), and distilled water. Two different salt concentration were investigated equal to 2.9% w/w (MP29) and 5.7% w/w (MP57) following the preparation and mixing procedure published by Lyng et al. (2014). The prepared samples were allowed to cool overnight at 5°C in a refrigerator where they were stored until use in the experimental runs.

Pre-cooked and frozen chicken MB (Ikea Italia, Italy) were composed of chicken meat (61%), onion, potato starch, salt (1.6%) and spices. The chicken balls were stored in freezer at -20 °C and, before the use for the experiments, they were transferred to a refrigerator where they thawed naturally overnight at 5 °C.

2.2 MEF equipment and meatball configuration

The MEF heating system was configured with an AC variable power supply unit (VAM20F-1N, K-Factor, Italy), three T-type thermocouples to monitor the temperature of the sample at three different selected points of the system (T1, T2 and T3 corresponding to the linear equally spaced MB core points) and a treatment cell, in which the samples were placed (Figure 1). The cooking glass cell (height 60 mm, length 100 mm and width 51 mm) was equipped with two AISI304 stainless steel electrodes (height 60 mm, width 43 mm and thickness 2 mm). The cooking system was installed inside a commercial oven (Whirlpool Europe, Biandronno, Italy) and an ad-hoc wiring was realized with a power supply panel consisting of a residual current device, current circuit breaker and self-interlock dispositive. A PicoLog data logger (KA028 TC 08 USB, Pico Technology Ltd, St. Neots, UK) was used to record temperatures and a Hold-Peak meter (Yongtian Road, Zhuhai, China) was used to record currents and voltages (Figure 1)

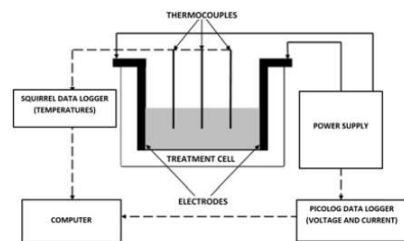


Figure 1. MEF heating equipment

2.3 MEF heating procedure

For each heating experiment the cell was filled carefully to avoid air presence by 3 MB dispersed in 145 g of MP (resulting in an average height up to 36 mm) and placed into positions T1, T2 and T3, according to the configuration illustrated in section 2.2. Once the cell was filled, electrically insulated thermocouples were inserted in each meat ball, taking care to locate each probe tip at the meat ball center. Thermocouples were fixed with a home-made stand to avoid possible movements during the experiment.

Two different applied potential gradients (APG) were investigated, respectively 3 and 4 V/cm, for both MP29 and MP57, compatibly with any thermal degradation of the samples. Every heating experiment was performed in triplicate for 4.5 minutes. Considering the cell length of 10cm, the applied potentials resulted of 30 and 40 V.

2.4 Measurement of physical properties

Physical properties were evaluated according to published procedures (Lyng et al. 2014; Marra et al. 2009). MP and MB electrical conductivity was investigated by using the same cell equipment filled with MP and minced MB only, respectively. Conductivity was so calculated according to the Eq.1 of Marra et al. (2009). Thermal conductivity and volumetric heat capacity were measured with a portable handheld device for thermal properties (KD2 Pro, Decagon, WA, USA). The measurements were performed on sets of 50 single tests on MP and MB at different temperatures. Finally, density measurements were performed on samples at a single temperature (298.15 K) using analytic balance and the volume of the MEF cell.

Table 1a: physical properties as function of temperature of MP29

Property	Description	Units	Function (T in °C)
σ	Elec. cond.	S/m	$0.0644 T + 1.9898$
K	Therm. cond.	W/(m K)	$0.0005 T + 0.4554$
Hp	Vol. heat cap.	MJ/(m ³ K)	$0.0024 T + 3.1624$
ρ	Density	kg/m ³	946.72

Table 1b: physical properties as function of temperature of MP57

Property	Description	Units	Function (T in °C)
σ	Elec. cond.	S/m	$0.1093 T + 3.6994$
K	Therm. cond.	W/(m K)	$0.0026 T + 0.4262$
Hp	Vol. heat cap.	MJ/(m ³ K)	$0.0092 T + 2.9604$
ρ	Density	kg/m ³	991.80

Table 1c: physical properties as function of temperature of meatball (MB)

Property	Description	Units	Function (T in °C)
σ	Elec. cond.	S/m	$0.0708 T + 1.5675$
K	Therm. cond.	W/(m K)	$0.0044 T + 0.2985$
Hp	Vol. heat cap.	MJ/(m ³ K)	$0.0082 T + 2.977$
ρ	Density	kg/m ³	1131.77

3. Model implementation

A mathematical model of MEF heating was developed for the ohmic cell described in Section 2.2.

3.1 Transport equations and modeling tools

The heat transfer phenomena that take places during ohmic heating of a solid-like food-domain such as the analyzed heterogenous system, are described by the classical unsteady state heat transfer equation by conduction considering a heat generation term (Marra et al. 2009).

$$\rho C_p \frac{\partial T}{\partial t} = \nabla \cdot k \nabla T + \sigma |\nabla V|^2 \quad (1)$$

where T is the temperature within the sample, t is the process time, k is the thermal conductivity, ρ is the density, C_p is the mass heat capacity and the last term represent the ohmic heat generation source where σ is the electric conductivity and $|\nabla V|$ the modulus of the gradient of electrical potential. The product ρC_p is equal to the measured volumetric heat capacity.

The electrical potential distribution within the sample can be computed using the following Laplace equation:

$$\nabla \cdot \sigma \nabla V = 0 \quad (2)$$

While the electrical conductivity depends on temperature, Eqs. (1) and (2) are dependent on each other and the problem must be solved in a coupled form. The complete MEF cell geometry was designed using Solidworks software (Solidworks corp., Dessault Systems, Paris, France) and a final assembled design was imported into Comsol Multiphysics software (Comsol AB, Sweden) to define the model builder structure.

Custom materials were created for MP and MB according to their measured physical properties. Silica glass and AISI 304 stainless steel Comsol library materials were used respectively for ohmic cell and electrodes. In order to model the overall MEF equipment behaviour, the appropriate coupling with multi-physics-correlated electromagnetic heating module were computed. A reduced temperature variable was defined as:

$$T_{red} = \frac{T - T_0}{T_{sat} - T_0} \quad (3)$$

where T denotes the instantaneous temperature, T_0 the starting temperature of the measured position, and T_{sat} the upper limit temperature imposed equal to 373.15 K.

3.2 Initial and boundary conditions

It is assumed that the entire sample is at a uniform initial voltage, $V_0=0$ and temperature T_0 (301.15 K, as it was the average value of the sample temperature measured after the cell filling manual operations).

As boundary conditions for the heat transfer equation, continuous domains were considered assuming ideal conductive transport between MP, electrodes, and glass interfaces domains. For the external surfaces, different considerations were made. The external lower face of the glass cell was considered adiabatic due to the oven insulation. All others glass and steel surfaces in contact with external surrounding air were considered as convective heat walls with external natural convection. The upper MP face is in free air and the moisture loss heat transfer was assimilated to an overall convective heat flux as:

$$q_{eq} = h (T_{air} - T) \quad (4)$$

where h was considered ranging from 5 to 100 W/m^2K and different simulation tests were preliminary performed in accordance with the literature (Carson, Willix, and North 2006).

The electric equation boundary conditions were considered as perfect insulation surfaces for all boundaries except of the hereafter considered ones. A fixed voltage drop over the cell electrodes was imposed. The interfacial surfaces between MP and electrodes and between MP and MB were considered as surfaces in electric contact where current flux J is described by:

$$J = h_c (V_1 - V_2) \quad (5)$$

h_c was the electric conductance in S/m^2 and after different parameter optimization runs, its values were estimated and reported in table 2 for every interface type. Finally, half body symmetry boundary condition was considered also to reduce the simulation computational efforts. See section 4 figures for details.

3.3 Numerical solution solver implementation

The implemented model was solved by the Comsol Multiphysics software. A multi-sweep study respectively for APG (3 and 4 V/cm) and materials (MP29 and MP57) was implemented.

Numerical tests were performed with different mesh parameters to evaluate the simulation results and to find the best mesh settings. The set providing the best spatial resolution for the considered domain and for which the solution was found to be independent of the grid size, was composed of 125311 tetrahedrons, 16634 triangles boundary elements, 988 edge elements, 58 vertex elements with 367894 of degrees of freedom. The numerical solution was attained on a workstation equipped with a motherboard MSI X79A-GD65 (8D), CPU Intel I7-3820 @ 3600 GHz FSB (front side bus): 1.600 MHz Socket: Socket R (LGA 2011) 4 cores; equipped with a RAM of 64 Gb DDR3 1600 MHz. The workstation runs under Windows 7 Professional operating system at Dipartimento di Ingegneria Industriale, Università degli studi di Salerno, Italy.

4. Results and discussions

The numerical solution of the proposed model allows to acquire the transient spatial (3D) distribution of temperature and intensity of the electric field, thus following also the local distribution of the heat source (given by the interaction of the electric field with the food undergoing heating). The analysis of such model output is presented below and discussed in terms of heating uniformity.

4.1 Spatial representation of the Model outputs

Figure 2 shows four examples of a temperature distribution (as slices on XZ planes) plot after 4 minutes of MEF heating for MP29, assuming for the heat transfer coefficient h the values 5, 25, 50 and 100 $W/(m^2 K)$, for APG the value 3 V/cm, and for h_c the values reported in Table 2. The MEF heating of the considered system, heaven if non-homogeneous, reveals a uniform temperature distribution in a large portion of the investigated domain. Whatever the heat transfer coefficient h , the less heated zones remain confined at the outer shells. Ad-hoc test experiments run on the same system discussed in this work revealed a different temperature between the core and surface of the food system of 3°C, which is the value obtained by numerical solution when a heat transfer coefficient of 5 $W/(m^2 K)$ was used. For this reason, all other numerical solutions discussed in this work were obtained considering this value.

Figure 3 shows three examples of electric field slice plot after 4 minutes of ohmic heating for MP29 and MP57, considering a value of $5 \text{ W}/(\text{m}^2 \text{ K})$ for the heat transfer coefficient h , an APG of 3 and 4 V/cm, and the values reported in Table 2 for h_c . The larger APG, the higher is the resulting electric field as expected. Moreover, a considerable reduced electric field homogenization could be observed for a higher salt concentration of MP.

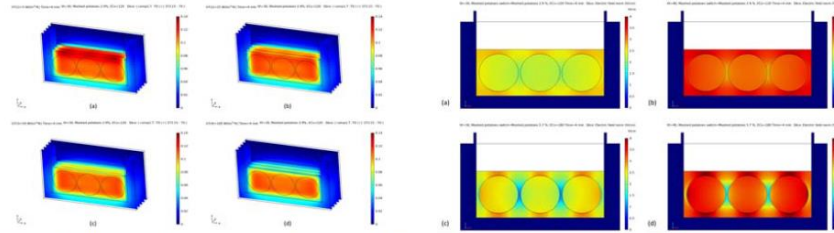


Figure 2. Slice plot of temperature after 4min, APG = 3 V/cm, MP29, (a) $5 \text{ W}/(\text{m}^2 \text{ K})$, (b) $25 \text{ W}/(\text{m}^2 \text{ K})$, (c) $50 \text{ W}/(\text{m}^2 \text{ K})$ and (d) $100 \text{ W}/(\text{m}^2 \text{ K})$

Figure 3. Electric field at 4min. APG=3 V/cm (a, c) and 4 V/cm (b, d), MP29 (a, b) MP57 (c, d), $h=5 \text{ W}/(\text{m}^2 \text{ K})$

Table 2: electric conductance, h_c , for MP - steel and MP -MB interfaces

Property	interface	El. Cond. [S/m^2]
h_c	MP29-steel	120
h_c	MP57-steel	180
h_c	MP29-MB	800
h_c	MP57-MB	800

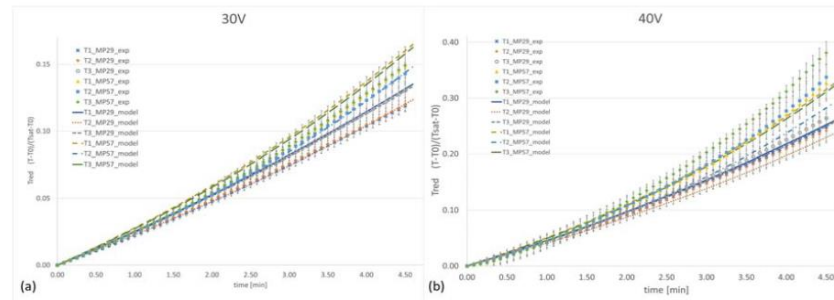


Figure 4. Comparison between experimentally measured and model predicted temperature evolution for an APG of 3 V/cm (a) and 4 V/cm (b), MP29 and MP57 compositions. MP29 concentration model profiles are solid blue for T1, dotted dark red for T2, short-dashed grey for T3. MP57 concentration model profiles are dashed brown for T1, point&dash blue for T2, long dashed green for T3.

4.2 MEF profiles experimental comparison

Hereafter an experimental MEF heating of the investigated heterogeneous system, respectively for APG of 3 and 4 V/cm, for both MP29 and MP57 are reported and compared with the model predictions. Every experimental test is performed at least in triplicate. Average and standard deviation are also reported. In Figure 4a, the comparison of temperature evolution (model predicted and experimentally measured at the chosen points) for an APG of 3 V/cm, is reported. The model prediction shows a good agreement with the experimental results and drives the heating curve within the maximum of experimental standard deviation of 5%. It is worthwhile remarking that the model predicts temperature at external locations to be higher than at the central one as expected for the electrode proximity. For higher APG (Figure 4b), the experimentally measured temperature evolution in position 3 for MP57 shows a deviation from the model prediction for longer times probably due to the rising of other phenomena not considered by the model. The agreement between the model and experimental set is satisfactory.

5. Conclusions

The implemented model for the simulation of a static ohmic heating cell delivers good results, providing satisfactory correlation between predicted and experimental data. An optimal set of electric conductance, h_c , of the MP/steel and MP/MB interfaces was estimated by an overall analysis of all experimental tests and it was applied in all the simulations. With the proposed cell configuration, when MEF heating is used for sterilization of solid foods, colder external shells are the critical areas to be monitored and limited with additional insulations. Future developments will deal with a microscopic modeling of the crucial interfaces where current conductance plays a key role and a multiscale model implementation reducing the number of parameter optimization. Moreover, higher applied potential gradients (5 V/cm and more) will be investigated to better describe the rising deviation already observed at 4 V/cm.

Acknowledgements

This study has been supported by the ERA-NET SusFood2 project, "Improving Sustainability in Food Processing using Moderate Electric Field (MEF) for Process Intensification and Smart Processing (MEFPROC).

References

- Aymeric, P. Pierrat, B., Gorges, S., Albertini, J., and Avril, S. 2020. "Finite-Element Based Image Registration for Endovascular Aortic Aneurysm Repair". *Modelling* 1(1):22–38.
- Carson, J. K., Willix J., and North, M. F. 2006. "Measurements of Heat Transfer Coefficients within Convection Ovens." *Journal of Food Engineering* 72(3):293–301.
- Chaminda P. and Sastry, S. 2016. "Effect of Moderate Electric Fields on Inactivation Kinetics of Pectin Methyltransferase in Tomatoes: The Roles of Electric Field Strength and Temperature". *Journal of Food Engineering* 186:17–26.
- Hashemi, S., Bagher, M. and Roohi, R.. 2019. "Ohmic Heating of Blended Citrus Juice: Numerical Modeling of Process and Bacterial Inactivation Kinetics". *Innovative Food Science and Emerging Technologies* 52:313–24.
- Jinghai, L. and Kwauk M. 2003. "Exploring Complex Systems in Chemical Engineering - The Multi-Scale Methodology" *Chemical Engineering Science* 58(3–6):521–35.
- Lyng, J. G., Arimi, J. M., Scully, M. and Marra, F. 2014. "The Influence of Compositional Changes in Reconstituted Potato Flakes on Thermal and Dielectric Properties and Temperatures Following Microwave Heating". *Journal of Food Engineering* 58:220–28.
- Marra, F., Zell, M. Lyng, J. G., Morgan, D. J., and Cronin, D. A. 2009. "Analysis of Heat Transfer during Ohmic Processing of a Solid Food". *Journal of Food Engineering* 35:187–36.
- Marra, F., Lyng, J., Romano, V. and McKenna, B.. 2007. "Radio-Frequency Heating of Foodstuff: Solution and Validation of a Mathematical Model". *Journal of Food Engineering* 56:345–34.
- Petrosino, F., Hallez, Y., De Luca, G. and Curcio, S. 2020. "Osmotic Pressure and Transport Coefficient in Ultrafiltration: A Monte Carlo Study Using Quantum Surface Charges" *Chemical Engineering Science* 224:115762.
- Sastry, S. 2008. "Ohmic Heating and Moderate Electric Field Processing". *Food Science and Technology International* 14(5):419–22.
- Sastry, S. and Salengke, S. 1998. "Ohmic heating of solid-liquid mixtures: a comparison of mathematical models under worst-case heating conditions". *Journal of Food Process Engineering* 21(6):441–58.
- Sepulveda, D. R., Góngora-Nieto, M. M., Guerrero, J. A., and Barbosa-Cánovas, G. V. 2005. "Production of Extended-Shelf Life Milk by Processing Pasteurized Milk with Pulsed Electric Fields". *Journal of Food Engineering* 62:450–29.
- Shim, J. Y., Seung Hyun L., and Soojin J. 2010. "Modeling of Ohmic Heating Patterns of Multiphase Food Products Using Computational Fluid Dynamics Codes". *Journal of Food Engineering* 99(2):136–41.
- Soojin, J. and Sastry, S. 2005. "Modeling and Optimization of Ohmic Heating of Foods inside a Flexible Package". *Journal of Food Process Engineering* 45:217–54.
- Stijn W., Van Hulle, H., Boeckx, P., Volcke, E., Van Cleemput, O., Vanrolleghem, P. A., and Verstraete, W. 2004. "Modeling and Simulation of Oxygen-Limited Partial Nitritation in a Membrane-Assisted Bioreactor (MBR)". *Biotechnology and Bioengineering* 86(5):531–42.
- Turek, V., Fialová, D., Jegla, Z. 2016. "Efficient Flow Modelling in Equipment Containing Porous Elements" *Chem. Eng. Trans.*, 52, 42-6.
- Zhi, H. Zhang, B. Marra, F. and Wang, S. 2016. "Computational Modelling of the Impact of Polystyrene Containers on Radio Frequency Heating Uniformity Improvement for Dried Soybeans". *Innovative Food Science and Emerging Technologies* 35:215-13.

Appendix B

Ohmic Heating of Basil-Based Sauces: Influence of the Electric Field Strength on the Electrical Conductivity

Oriana Casaburi, Cosimo Brondi*, Aldo Romano, Francesco Marra

*Dipartimento di Ingegneria Industriale, Università degli Studi di Salerno,
Via Giovanni Paolo II 132, 84084, Fisciano, Salerno, Italy*

cbrondi@unisa.it



Ohmic Heating of Basil-Based Sauces: Influence of the Electric Field Strength on the Electrical Conductivity

Oriana Casaburi, Cosimo Brondi*, Aldo Romano, Francesco Marra

Dipartimento di Ingegneria Industriale, Università degli Studi di Salerno, Via Giovanni Paolo II 132, 84084, Fisciano, Salerno, Italy
cbrondi@unisa.it

The Moderate Electric Field (MEF) processing of foods consists in the application of an electric potential gradient ($\Delta V/L$) ranging from 1 to 1000 V/cm on a food item (homogeneous or heterogeneous) placed between two electrodes, its main effect being the food heating due to the dissipation of a part of the electric energy into heat within the food item. The heating performances of such a system depend on several process and system parameters, including the applied $\Delta V/L$, the food electrical conductivity, and its thermo-physical properties. In this study, the effects due to the salt composition and to the applied $\Delta V/L$ to a heterogeneous food (constituted by a basil-based sauce, mainly fibers dispersed in a slightly salted water-oil emulsion) treated in a custom MEF system on the food heating rate are investigated. The samples were prepared at different salinities (3.25, 1.63, 0.86 and 0.43% w/w respectively). In the explored range of compositions, the heating rate increased linearly with the square power of applied $\Delta V/L$. A slight linearity deviation above 55°C was observed for the basil-based sauce at 1.63% and 5.20 V/cm, associated with bubble formation within the ohmic system and the electrolytic reactions occurring at the electrode-solution interface during the MEF heating process.

The salt content as well as the ratio between water and oil in the sample formulation played a crucial role in determining the thermo-electrical behavior of the basil-based sauce samples. Samples with salinity of 1.63%, compared to samples at 3.25%, exhibited a higher electrical conductivity, being due to a minor concentration of the non-conductive phase (namely the oil phase as well as the dispersed vegetable fibers into the solution) that exerts a major degree of electrical insulation. As the salinity decreases from 1.63% to 0.43%, samples were characterized by lower electrical conductivities, being due to a reduced ionic mobility when the salt contained into the sample is drastically reduced.

1. Introduction

According to the definition given by Sensoy and Sastry (2004), MEF is a thermal-electrical technique in which a food material is subjected to the passage of an alternating electric current. The food product acts as an electrical resistance and the electrical energy is converted into thermal energy. However, MEF may be characterized or not by thermal effects due to the heating process. In this way, MEF might comprise both heating processes at high temperatures, that is, ohmic heating, or controlled low temperatures to minimize the thermal effects (Sensoy and Sastry, 2004). MEF applications include blanching, evaporation, drying, thawing extraction, peeling and fermentation. Moreover, several food systems such as fruits, vegetables, milk, meat, poultry, and fish products have been processed by means of batch ohmic heating (Sastry, 2014). MEF heating process is an emerging technology with considerable potential for the food industry, its main advantages being the rapid and relatively uniform heating together with the lower capital cost compared to other heating methods such as microwave and radio frequency heating (Marra et al., 2009). However, the performance of this method depends on various factors, such as shape, size, and composition of the food item as well as the physical configuration of the MEF equipment.

Basil-based sauce is made from fresh basil leaves, extra virgin olive oil, garlic, pine nuts, cheese (Parmigiano and Pecorino cheese), pine nuts, garlic, and extra virgin olive oil. Whatever the blending process applied to its ingredients, pesto is a heterogeneous system, seen as a water-oil emulsion in which food particulates are

Paper Received: 19 October 2020; Revised: 16 March 2021; Accepted: 15 April 2021

Please cite this article as: Casaburi O., Brondi C., Romano A., Marra F., 2021, Ohmic Heating of Basil-based Sauces: Influence of the Electric Field Strength on the Electrical Conductivity, Chemical Engineering Transactions, 87, 343-348 DOI:10.3303/CET2187058

dispersed. Demand of pesto has progressively increased worldwide, being considered second as pasta sauce to tomato sauce only (Masino et al., 2007). However, fresh basil pesto usually needs to be processed to improve its microbiological safety and shelf-life. There is very little information about the preservation of basil pesto sauce (Zardetto and Barbanti, 2020) even if outbreaks involving sauces made by fresh herbs clearly show that the global marketing of such products should not be underestimated as a vehicle of foodborne illness (Eckner et al., 2015). Food preservation techniques -including pasteurization (Franceschini et al., 2011) and aseptic packaging, vacuum packaging, modified atmosphere packaging and refrigeration (Fabiano et al., 2000), are employed to prevent pesto from spoiling and, therefore, to enhance its shelf-life. However, these processes may affect the organoleptic properties of pesto sauces, the most evident being the pesto colour which could vary from the pale green to a dark brownish green. The texture degradation and the colour change are due to the variation in the content of the fresh basil pigments, i.e., chlorophylls and carotenoids (Zeppa and Turon, 2014). The fresh green pesto is highly appreciated for its characteristic colour, taste, and texture, and losing these attributes may lead to a lower demand from the consumers.

Conventional heating is the most common processing technology in the food industry (Ling et al., 2015). Classic convective methods comprise plate heat exchangers, still the most popular methods in the heating of foodstuff. The major drawbacks of conventional heating are the low energy efficiency and long drying times (Gavahian et al., 2018). MEF heating is an efficient technique used to extend the shelf-life of prepared vegetables. To our knowledge, no data are available in the literature on heating behaviour of fresh basil pesto under a MEF heating process. Before considering experiments devoted to studying how MEF heating can impact the shelf life of a product like pesto there is the need of feeling the lack of knowledge on the behaviour of pesto undergoing this process. In fact, during the heating process, it is necessary to understand the different phenomena taking place inside the MEF cell, such as the temperature distribution and the heating rate in the food sample that also affect, consequently, its electrical conductivity. It is also important to consider the balance between the heating time, safety of the food and the energy usage to select proper processing parameters. Therefore, in this present work, we studied the effect of the $\Delta V/L$ on the thermo-physical properties of several pesto sauce samples. Different temperature-time histories and heating rates were compared, and electrical conductivity behavior was also evaluated.

2. Materials and methods

2.1 Sample preparation

Basil pesto sauce was purchased from a local market in Fisciano (Italy) and stored at room temperature (25 °C) prior to experiments. Pesto composition and relative properties at room temperature before the MEF heating are indicated in Table 1. The sauce was diluted with deionized water to obtain samples at different salinities (evaluated as salt mass on total solution mass) and content of macronutrients (see Table 2), and they were mixed until a homogeneous mixture was obtained. In this way, it was possible to appreciate the effect of salinity on the electrical conductivity during the heating process. A total mass of 190 g was poured into the MEF cell and heated at 3.12, 4.16 and 5.20 V/cm.

Table 1: Pesto sauce composition and its thermal properties.

	Fats	Carbohydrates	Water	Fibers	Proteins	Salt*
Mass [g]	46	9.8	31.25	5	4.7	3.25

Thermal conductivity was 0.31 (± 0.01) W/(m °C) (at 25 °C) and volumetric heat capacity was 2.86 (± 0.07) MJ/(m³ °C) (at 25 °C).

*Salt is already contained in pesto sauce. Reported amounts are average values on a basis of 100 g of pesto, according to the nutritional values datasheet.

Table 2: Diluted sample compositions.

Pesto [g]	Salt [g]	Water [g]	Total mass [g]	Salinity % [(w/w)×100]
190	6.18	0	190	3.25
95	3.09	95	190	1.63
50	1.63	140	190	0.86
25	0.81	165	190	0.43

2.2 MEF heating system and process

The scheme of the MEF system used in this work is shown in Figures 1a and 1c. The MEF system is mainly composed by: a variable transformer (VAM20F-1N, Input, 230V AC, 50/60Hz, K-FACTOR Castellano, Italy);

an insulated chamber to contain the heating system; a MEF cell made of glass with internal dimensions of 10 cm × 6 cm × 5.1 cm (length × height × width respectively) and two removable steel electrodes (Figure 1b) with a thickness of 0.19 cm each, resulting in a distance between the electrodes of 9.62 cm. A Teflon cap was designed with a central opening for the insertion of a T-type thermocouple (TC Misure e Controlli srl, Torino, Italy) at the sample centre, wired to a data logger system (TC-08 Thermocouple data logger, Pico Technology Ltd, St. Neots, UK).

For each $\Delta V/L$, the reported values of temperature versus heating time refer to the average over three replicates.

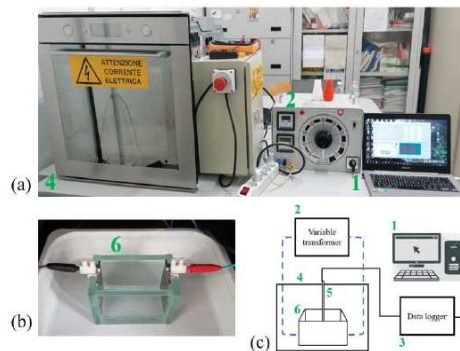


Figure 1: Pictures of the adopted instrumentation: (a) assembly of the MEF heating equipment, showing the (1) data acquisition system, (2) the variable transformer and (4) the insulated chamber. (b) Detail of the (6) MEF cell with the electrodes. (c) Schematic diagram of the experimental setup representing the insertion of (5) the thermocouple into the cell.

2.3 Electrical conductivity

The electrical conductivity (σ) was evaluated from temperature, voltage and current data recorded at 30 s intervals. Voltage and current readings were acquired by using a digital multimeter (model Bt-90EPC, Holdpeak, Zhuhai, China) and a data acquisition software, Pc-link-v1.1 (Holdpeak, Zhuhai, China). Electrical conductivity was calculated according to the following equation:

$$\sigma = \frac{I L}{V A} \quad (1)$$

where I is the current passing through the food item, V is the applied voltage, L is the length between the electrodes and A is the area of the electrodes occupied by the sample. The ratio L/A is known as the cell constant of the MEF heating unit. The cell constant of the MEF heater was 60.1 m^{-1} when filled with a mass of 190 g. The cell was calibrated by using several aqueous solutions of NaCl in deionized water (concentrations were 1%, 2.5% and 5% w/w respectively). Measured values were compared to corresponding published values (Weast, 1989). The calibration results revealed that there was a difference between standard electrical conductivity of the NaCl solutions and the experimental data of maximum 5%. The electrodes were thoroughly rinsed using a brush and dematerialized with twice-distilled water after each run. The reported values of electrical conductivity refer to the average over three replicates.

3. Results and discussion

3.1. Heating rate

Figure 2 reports the temperature evolution of the tested samples (error bars represent 2x the standard deviation).

Experimental data comparison shows the two significant effects of the salt composition (3.25, 1.63, 0.86 and 0.43% w/w) and of the applied $\Delta V/L$ (3.12 V/cm, 4.16 V/cm and 5.20 V/cm) on the heating rates. When samples with salinity up to 1.63% are considered, an increase in the applied potential gradient corresponds to an evident increase in heating rate. The value of the applied $\Delta V/L$ has a limited effect on the heating of the pure pesto, due to its composition in fat, which acts as an insulator. Also a higher concentration (and

dispersion) of vegetable solid particles exerts a higher electrical resistance to the passage of the electrical current leading, consequently, to a lower heat rate, also reported in (Zhu et al., 2010). As the salinity decreases to 1.63%, the temperature rise was higher and shorter heating time was required to reach higher temperature values in comparison with values observed at 3.25%.

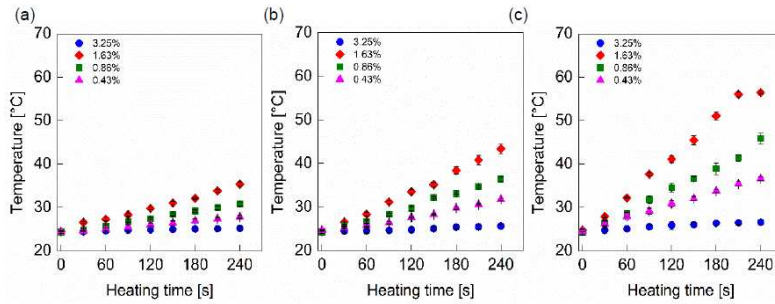


Figure 2: Heating rates of the basil-based sauce samples at the different $\Delta V/L$: (a) 3.12 V/cm, (b) 4.16 V/cm and (c) 5.20 V/cm.

As the salinity gradually decreases to 0.43%, temperature evolutions are characterized by a slower rise. This effect may be ascribed to a lower salt concentration within the liquid medium that exerts a minor ionic mobility when the electrical current passes through the food item. When higher $\Delta V/L$ were applied, the same behavior was observed. Overall, whatever the applied potential gradient, the temperature at the sample core increases linearly with the heating time. A slightly nonlinear deviation for temperature-time profile of sample at 1.63% and 5.20 V/cm (Figure 2c) can be observed at temperature above 55 °C. This nonlinear behavior may be related to air bubble formation, a phenomenon which was observed during MEF heating. These bubbles do not conduct electrical current and, therefore, may disable electrical conductivity rise. The formation of gas bubbles may be attributed to several mechanisms such as (i) hydrogen bubbles as byproduct of electrochemical reactions occurring at the interface between the foodstuff and the surface of the electrode (Palaniappan and Sastry, 1991); (ii) formation of bubbles due to the temperature gradients occurring through the MEF cell in which hotter spots promote water boiling while part of the cell is still a temperature below the boiling point (Zhao and Kolbe, 1999), these temperature gradients may be due to distortions of the electric field caused by the solely present solid fraction within the liquid phase of the food system (Fryer et al., 1993); (iii) cell lysis, in which the breakdown of cell wall components, due to the stress applied by the electrical field, can lead to an efflux of cytoplasm components and to the release of non-conductive gas bubbles from the structure of the food material (Halden et al., 1990). Table 3 reports the heating rates (HR) obtained by the linear fitting of the experimental data. R^2 values indicate a good agreement between the measured values and the linear fitting. The listed HR s strengthen the observations made for the temperature evolutions. On one hand, the effect of the applied voltage is readily evident, as expected, higher $\Delta V/L$ induced a higher passage of the electrical current through the sample (Sastry, 2014). On the other hand, the salinity also influenced the ionic mobility throughout the food item. At 3.12 V/cm, it can be observed that HR goes from 3.60×10^{-3} °C/s to 4.34×10^{-2} °C/s (at 3.25 and 1.63% w/w). Therefore, as the salinity further decreases, the HR reaches lower values first at 2.51×10^{-2} °C/s and then at 1.41×10^{-2} °C/s (at 0.86 and 0.43% w/w respectively). Moreover, the same trend is observed at 4.16 V/cm and 5.20 V/cm as well.

Table 3: Heating rates of basil-based sauce samples at the applied $\Delta V/L$.

Salinity % [w/w]	3.12 V/cm		4.16 V/cm		5.20 V/cm	
	HR [°C/s]	R^2	HR [°C/s]	R^2	HR [°C/s]	R^2
3.25	3.60×10^{-3}	0.974	4.71×10^{-3}	0.968	6.97×10^{-3}	0.978
1.63	4.34×10^{-2}	0.995	7.58×10^{-2}	0.996	1.54×10^{-1}	0.999
0.86	2.51×10^{-2}	0.999	4.75×10^{-2}	0.999	8.15×10^{-2}	0.999
0.43	1.41×10^{-2}	0.977	2.85×10^{-2}	0.981	5.07×10^{-2}	0.999

3.2 Electrical conductivity

The change in σ with the temperature and the salinity is shown in Figure 3 (error bars represent 2x the standard deviation). As the change in the electrical conductivity is independent of the applied $\Delta V/L$, the set of data obtained at the several applied voltages (3.12 V/cm, 4.16 V/cm and 5.20 V/cm) are reported together at each specific salinity. For all the considered samples, the electrical conductivity shows a positive linear dependence on temperature, which is a typical effect attributed to a reduced drag for the ions' movement within the medium (Darvishi et al., 2013).

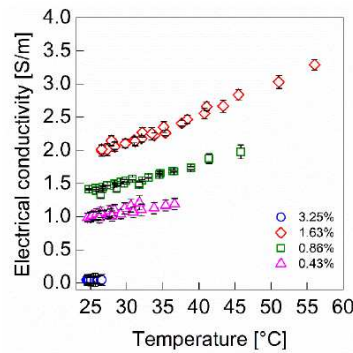


Figure 3: Electrical conductivities of the basil-based sauce samples.

Experimental data were linearly fitted by the following equation:

$$\sigma = \sigma_0 + mT \quad (2)$$

where σ_0 and m respectively represent the intercept and the slope of the linear model. Results of the fitting procedure are reported in Table 4. R^2 values indicate a good agreement between the measured values and the linear fitting procedure. Also, in this case, data are consistent with the analysis. Indeed, it can be observed that m goes from 2.68×10^{-4} S/(m °C) to 4.28×10^{-2} S/(m °C) (at 3.25% and 1.63% respectively). In practice, the fat content and the vegetable solid particles are characterized by a lower electrical conductivity than liquids for particulate foods. For this reason, samples at 1.36% of salinity are characterized by higher values of electrical conductivity, as a lower fat concentration leads to a minor degree of resistance to the electrical current. After that, the m lowers to 2.39×10^{-2} S/(m °C) and then to 1.68×10^{-2} S/(m °C) (at 0.86% and 0.43% respectively). This gradual reduction in the slope is attributed to a decreasing salinity that induces a minor passage of the electric current.

Table 4: Electrical conductivities of basil-based sauce samples.

Salinity % [w/w]	σ_0 [S/m]	m [S/(m °C)]	R^2
3.25	0.041	2.68×10^{-4}	0.963
1.63	0.828	4.28×10^{-2}	0.984
0.86	0.808	2.39×10^{-2}	0.977
0.43	0.585	1.68×10^{-2}	0.972

4. Conclusions

This work discussed the heating process of a heterogeneous food system (basil-based sauce) assisted by moderate electric field, in a custom equipment calibrated on purpose. First, in the investigated range of $\Delta V/L$, the different temperature-time evolutions were characterized by a linear behavior, except for the sample with a salinity of 1.63% and treated at 5.20 V/cm. A slight deviation from linearity with respect to the temperature was observed above 55°C. This deviation was associated with bubble formation during the MEF heating process. The heating rates of the samples at different salinities, undergoing different applied $\Delta V/L$, were characterized

in terms of electrical conductivity. The pure pesto exhibited a scarce response to MEF heating, due to the high fat concentration and its effect on the electrical conductivity of the sample. The sample with salinity of 1.63% exhibited the higher electrical conductivity. This occurrence is due to a minor concentration of the oil phase as well as the dispersed vegetable fibers into the solution that are responsible for a major degree of electrical insulation. As the salinity decreases to 0.86% and to 0.43%, samples were characterized by lower electrical conductivities, resulting from slower heating rates. This depletion may be ascribed to the reduced salinity that usually enhances the ionic mobility when a food item is subjected to the passage of the electrical current.

Acknowledgments

This study has been supported by the ERA-NET SusFood2 project, "Improving Sustainability in Food Processing using Moderate Electric Field (MEF) for Process Intensification and Smart Processing (MEFPROC).

References

- Darvishi H., Khostaghaza M.H., Najafi G., 2013, Ohmic heating of pomegranate juice: Electrical conductivity and pH change, *Journal of the Saudi Society of Agricultural Sciences*, 12, 101-108.
- Eckner K.F., Høgåsen H.R., Begum M., Økland M., Cudojoe K.S., Johannessen G.S., 2015, Survival of Salmonella on Basil Plants and in Pesto, *Journal of Food Protection*, 78 (2), 402-406.
- Fabiano B., Perego P., Pastorino R., Del Borghi M., 2000, The extension of the shelf-life of 'pesto' sauce by a combination of modified atmosphere packaging and refrigeration, *International Journal of Food Science and Technology*, 35, 293-303.
- Franceschini B., Guerra G.L., Previdi M.P., 2011, Influence of chemical-physical parameters on the stability of heat treated Pesto alla Genovese, *Industria Conserve*, 86, 143-147.
- Fryer P.J., de Alwis A.A.P., Koury E., Stapley A.G.F., Zhang L., 1993, Ohmic processing of solid-liquid mixtures: Heat generation and convection effects, *Journal of Food Engineering*, 18, 101-125.
- Gavahian M., Chu Y., Sastry S.K., 2018, Extraction from Food and Natural Products by Moderate Electric Field: Mechanisms, Benefits, and Potential Industrial Applications, *Comprehensive Reviews in Food Science and Food Safety*, 17, 1040-1052.
- Halden K., De Alwis A.A.P., Fryer P.J., 1990, Changes in the electrical conductivity of foods during ohmic heating, *International Journal of Food Science and Technology*, 25, 9-25.
- Ling B., Tang J., Kong F., 2015, Kinetics of Food Quality Changes During Thermal Processing: a Review, *Food Bioprocesses Technology*, 8, 343-358.
- Marra F., Zell M., Lyng J.G., Morgan D.J., Cronin D.A., 2009, Analysis of heat transfer during ohmic processing of a solid food, *Journal of Food Engineering*, 91, 56-63.
- Masino F., Ulrici A., Antonelli A., 2007, Extraction and quantification of main pigments in pesto sauces, *European Food Research Technology*, 226, 569-575.
- Palaniappan S., Sastry S.K., 1991, Electrical conductivities of selected solid foods during ohmic heating, *Journal of Food Process Engineering*, 14, 221-236.
- Sastry S.K., 2014, Overview of Ohmic Heating, Chapter in: *Ohmic Heating in Food Processing*, CRC Press, Boca Raton, FL, 10-13.
- Sensoy I., Sastry S.K., 2004, Extraction Using Moderate Electric Fields, *Journal of Food Science*, 69, 7-13.
- Weast R.C. (Ed.), 1989, *Handbook of Chemistry, and Physics*, CRC Press, Boca Raton, FL, 221.
- Zardetto S., Barbanti D., 2020, Shelf life assessment of fresh green pesto using an accelerated test approach, *Food Packaging and Shelf Life*, 25, 100524.
- Zeppa G., Turon C., 2014, Application of the central composite design approach to define chlorophyll degradation during pesto sauce pasteurization, *Industrie Alimentari*, 53, 5-11.
- Zhao Y., Kolbe E., 1999, A method to characterize electrode corrosion during ohmic heating, *Journal of Food Process Engineering*, 22, 81-89.
- Zhu S.M., Zareifard M.R., Chen C.R., Marcotte M., Grabowski S., 2010, Electrical conductivity of particle-fluid mixtures in ohmic heating: Measurement and simulation, *Food Research International*, 43, 1666-1672.

Appendix C

Poster and oral contributions

Poster contribution - Convegno GRICU 2019 “Il contributo dell’Ingegneria italiana alla sostenibilità globale” – Palermo, Italy.



Riscaldamento mediante Campi Elettrici Moderati (MEF) applicato a sistemi eterogenei

O. Casaburi^a, D. Orrico^a, F. Marra^a, T. F. Bedane^b e J. G. Lyng^b

^a Dipartimento di Ingegneria Industriale - Università degli Studi di Salerno, via Giovanni Paolo II, 132 - 84084 - Fisciano, SA, Italy

^b School of Agriculture and Food Science - University College Dublin, Belfield, Dublin 4, Ireland

Introduzione

Il riscaldamento assistito da MEF è un processo nel quale viene generato calore all'interno di un materiale grazie al passaggio di corrente elettrica alternata, nel range 50-10000 Hz e intensità di campo elettrico tra 1 e 1000 V/cm. Nell'applicazione dei MEF l'energia elettrica dissipata in energia termica è proporzionale alla conducibilità elettrica del materiale processato e al quadrato dell'intensità di campo elettrico locale [Eq. 2]. La maggior parte degli alimenti possiede conducibilità compresa tra 10⁻¹ S/m e 10 S/m e, quindi, possono essere sottoposti a tale tipo di processo. I MEF presentano un ampio range di applicazioni tra cui pastorizzazione e sterilizzazione [1], blanching [2], estrazione [3] e decongelamento. L'applicazione dei MEF a sistemi alimentari omogenei favorisce un riscaldamento rapido e uniforme dell'alimento trattato garantendone, rispetto ai metodi convenzionali, una buona sicurezza microbiologica e un minore deterioramento delle proprietà organolettiche. Ad oggi, tale tecnologia trova applicazione nel caso di alimenti liquidi e di sistemi liquido- solido quanto più possibili omogenei. Mancano, invece, studi approfonditi sull'applicazione dei MEF per alimenti solidi e sistemi eterogenei.

Scopo del lavoro

Il lavoro mira a valutare la fattibilità del riscaldamento assistito da MEF per un sistema eterogeneo, costituito da polpette di pollo, aventi concentrazione di cloruro di sodio pari a 1.6%, e da pure di patate con due diverse composizioni, aventi rispettivamente concentrazioni di cloruro di sodio al 5,7% e 10,9%, studiando anche la distribuzione delle temperature in funzione della conformazione di sistema.

La valutazione è basata sulla applicazione di un voltaggio di 30 V ed una frequenza di 50 Hz. L'uniformità di riscaldamento del sistema eterogeneo, caratterizzato dai due sotto-domini, è stata valutata lungo l'asse principale tra i due elettrodi.

MEF: Fenomeni di trasporto

Equazione di trasferimento del calore per la distribuzione di temperatura [4]:

$$\rho c_p \frac{\partial T}{\partial t} = \nabla \cdot \lambda \nabla T + Q_{GEN} \quad (1)$$

T: temperatura del materiale;
t: tempo di processo;
c_p: calore specifico;
ρ: densità;
λ: conducibilità termica;
Q_{GEN}: potenza generata

$$Q_{GEN} = \sigma |\nabla V|^2 \quad (2)$$

Equazione di Laplace per la distribuzione del potenziale elettrico:

$$\nabla \cdot \sigma \nabla V = 0 \quad (3)$$

Materiali e Metodi

Sample compositions- MEF heating (University College Dublin, Belfield, Ireland)

Formulazione	Acqua [%]	Sale [%]	Burro [%]	Patate [%]
1	65,60	5,70	5,00	23,70
2	64,40	10,90	4,90	19,80

Tab. 1: Formulazione dei campioni di pure di patate analizzati

Configurazioni del sistema eterogeneo studiato

Fig. 1: Sistema RP, costituito da solo pure di patate.
Fig. 2: Sistema 2PSRP, costituito da 2 polpette posizionate in maniera simmetrica in pure di patate.
Fig. 3: Sistema 2PAIRP, costituito da 2 polpette posizionate in maniera asimmetrica in pure di patate.
Fig. 4: Sistema 3PRIP, costituito da 3 polpette posizionate in pure di patate.

Risultati

Fig. 5: evoluzione della temperatura nel tempo per sistema RP

Fig. 6: evoluzione della temperatura nel tempo per sistema 2PSRP

Fig. 7: evoluzione della temperatura nel tempo per sistema 2PAIRP

Fig. 8: evoluzione della temperatura nel tempo per sistema 3PRIP

Configurazione	Composizione	
	[5,7%]	[10,9%]
	t [min]	t [min]
2PSRP	18,03	15,18
2PAIRP	18,00	15,39
3PRIP	20,35	16,65

Configurazione	Composizione	
	[5,7%]	[10,9%]
	Q _{GEN} · 10 ⁴ [W/m ²]	Q _{GEN} · 10 ⁴ [W/m ²]
2PSRP	2,94	4,19
2PAIRP	2,66	3,79
3PRIP	2,82	3,31

Configurazione	Composizione (5,7%)			
	Polpette	Patate	Polpette	Patate
	Q _{GEN} · 10 ⁴ [W/m ²]	Q _{GEN} · 10 ⁴ [W/m ²]	Q _{GEN} · 10 ⁴ [W/m ²]	Q _{GEN} · 10 ⁴ [W/m ²]
2PSRP	2,94	2,53	4,19	3,84
2PAIRP	2,66	2,26	3,79	3,31

Discussione e Conclusioni

Nonostante il pure di patate sia caratterizzato, in entrambi i casi considerati (5,7% e 10,9% di cloruro di sodio), da conducibilità elettrica ben superiore (rispettivamente 5,60 S/m e 9,74 S/m) a quella delle polpette (1,46 S/m), i due sotto-domini (pure di patate e polpetta di carne) si riscaldano mantenendo minime differenze di temperatura quando il pure di patate è al 5,7% di sale, grazie al diverso gradiente di potenziale elettrico che si sviluppa in entrambi. La differenza di temperatura misurata tra la patata e le polpette di carne diventa molto più evidente quando il pure di patate contiene il 10,9% di sale. La posizione delle polpette nel dominio influenza l'evoluzione di temperatura sia nelle polpette che nel pure di patate. Altre indagini fondamentali, includendo anche la forma dei sotto domini di un sistema eterogeneo, devono essere effettuate per caratterizzare il riscaldamento MEF.

Bibliografia

- [1] Achir, N., Dhuique-Mayer, C., Hadjal, T., Madani, K., Pain, J. P., Domier, M., Pasteurization of citrus juices with ohmic heating to preserve the carotenoid profile, *Innovative Food Science and Emerging Technologies*, 33, 397-404 (2016).
- [2] Allali, H., Marchal, L., Vorobiev, E., Blanching of strawberries by Ohmic Heating: Effects on the Kinetics of Mass Transfer during Osmotic Dehydration, *Food Bioprocess Technol.*, 3, 406-414 (2010).
- [3] Loyprapai, P., Moonngarm, A., Chottanom, P., Moortree, T., Ohmic heating-assisted extraction of anthocyanins from black rice bran to prepare a natural food colourant, *Innovative Food Science and Emerging Technologies*, 27, 102-110 (2015).
- [4] Gally, T., Stowand, O., Junk, V., Le-Saif, A., Bread baking using ohmic heating technology: a comprehensive study based on experiments and modelling, *Journal of Food Engineering*, 190, 176-184 (2018).

Oral contribution - 3rd World Congress on Electroporation (Toulouse, France), 3 -6 September 2019: Analysis of Moderate Electric Field processing in a heterogeneous system.

Oral contribution - Perfectly matching- 100 years Confindustria Salerno (Salerno, Italia), 14 June 2019: Applicazione di processi basati su Campi Elettrici Moderati (MEF) nella produzione industriale.